SCHOOL OF DOCTORAL STUDIES
University of Milano-Bicocca

Department of Economics, Management and Statistics (DEMS)
PhD program in Economics and Statistics (ECOSTAT), XXXVI Cycle
Economics Curriculum

Silent Killers: Delving into the Health Effects of Short-term PM2.5 Exposure

-Essay on Air Pollution and Public Health: Evidence from Italy and Europe-

Lorena Popescu

876430

Research Mentors:

Supervisor: Elena Cottini, Catholic University of Sacred Heart - Milan (Italy)

Tutor: Luca Salmasi, Catholic University of Sacred Heart - Rome (Italy)

Co-tutor: Gilberto Turati, Catholic University of Sacred Heart - Rome (Italy)

Coordinator: Matteo Manera, University of Milano-Bicocca (Italy)

Academic year 2024-2025

Overview

This thesis examines the causal impact of air pollution on public health in Southern Europe through two interconnected studies.

The first study: *"Poisoned Air, Shortened Lives: $PM_{2.5}$ Exposure in Southern European cities"* investigates the causal impact of air pollution exposure on premature mortality in Southern European cities from 2010 to 2018. To address endogeneity, we leverage local variations in rainfall as a source of random variation in $PM_{2.5}$ air pollution exposure, integrating it with the Two-Sample Two-Stage Least Squares (TS2SLS) estimator. Our findings reveal a positive and statistically significant effect of $PM_{2.5}$ on premature mortality indicators. A one-unit μg/m^3 increase in $PM_{2.5}$, equivalent to 7.5% of the average $PM_{2.5}$ level, leads to an increase in the cardio-respiratory mortality rate for individuals under 65 by 0.2887 per 100,000 population, representing 8.49% of the average mortality rate, and a rise in the infant mortality rate by 0.3134 per 1,000 live births, corresponding to 10.57% of the average. The most affected populations are those residing in urban areas and individuals living below the median poverty rate.

The second study: *"Chilly Temperatures, Polluted Air: the health impacts of residential heating emissions"* investigates the causal effects of air pollutants from residential heating systems on urgent hospitalisations and in-hospital mortality for cardiovascular and pulmonary diseases during the period 2015-2019. Our findings indicate that the activation of heating systems implies a significant increase in $PM_{2.5}$, PM_{10}, and NO_2 levels, which in turn is associated with increased hospitalisations for most of the diseases considered. We also find heterogeneous effects for what concerns in-hospital mortality, where AMI, STEMI, NSTEMI and hemorrhagic stroke show heightened sensitivity to pollution exposure, particularly during periods associated with the largest variation in pollutant concentrations. The most affected groups of the population include elderly individuals, those with lower educational attainment, free-comorbidity individuals and residents of specific climatic zones, including the Po Valley.

Collectively, these findings reveal that both ambient and heating-derived pollution impose substantial health burdens, with stark heterogeneities across outcomes and populations. The results advocate for targeted policies to curb emissions, adopt more efficient heating systems and protect high-risk groups.

Contents

Chapter 1

Paper I: Poisoned Air, Shortened Lives: PM2.5 Exposure in Southern European cities

1.1 Introduction

Air pollution constitutes a serious public health concern, contributing to premature mortality and a broad spectrum of critical illnesses, including cardiovascular and respiratory diseases, lung cancer, and heightened vulnerability to infections (Pope & Dockery (2012)). Its presence is particularly pronounced in urban environments (Graff Zivin & Neidell (2013); He et al. (2019); Giaccherini et al. (2021)). Both short- and long-term exposure to air pollutants have been associated with a range of adverse health outcomes. These effects are especially pronounced among vulnerable populations, such as individuals with pre-existing health conditions, children, the elderly, and socioeconomically disadvantaged groups (Neidell (2004); Deryugina et al. (2019); DeCicca & Malak (2020); Giaccherini et al. (2021); Palma et al. (2022), among others).

Lately, efforts to mitigate emissions (e.g., European Parliament and Council (2008); European Parliament and Council (2010); European Parliament and Council (2016)) have resulted in measurable improvements in air quality, as reported by the European Environment Agency (2023). However, substantial challenges remain, particularly in urban areas, where pollution levels continue to exceed recommended thresholds[1]. In 2022, 96% of the EU's urban population was exposed to $PM_{2.5}$ concentrations surpassing the World Health Organization (WHO) guidelines, with limits being breached in more than 100 cities across the continent (European Commission 2022). Despite occupying merely 4% of the EU's total land area, urban zones accommodate 75% of its population, significantly amplifying pollution exposure risks. According to European Environment Agency (2022), in 2020, air pollution contributed to a substantial number of premature deaths across EU-27 Member States[2]. According to Khomenko et al. (2021), adherence to WHO air quality standards could prevent approximately 30 deaths per 100,000 urban residents annually[3], underscoring the urgent need for further policy interventions.

Particulate matter (PM) is recognized as a leading environmental health risk due to its ability to penetrate deep into the lungs and bloodstream (Chay & Greenstone (2003); World Health Organization - WHO (2013)). In particular, fine particulate matter with

[1]The recommended thresholds as defined by World Health Organization - WHO (2021) are: **$PM_{2.5}$**: 5 µg/m^3 (annual), 15 µg/m^3 (24-hour); **PM_{10}**: 15 µg/m^3 (annual), 45 µg/m^3 (24-hour); **Nitrogen dioxide (NO_2)**: 10 µg/m^3 (annual), 25 µg/m^3 (24-hour); **Sulfur dioxide (SO_2)**: 40 µg/m^3 (24-hour); **Carbon monoxide (CO)**: 4µg/m^3 (24-hour); **Ozone (O_3)**: 100µg/m^3 (8-hour), 60µg/m^3 (peak season).

[2]Ambient $PM_{2.5}$ concentrations exceeding WHO (2021) guidelines accounted for 238,000 premature deaths, with NO_2 and acute O_3 exposure linked to 49,000 and 24,000 additional fatalities, respectively.

[3]This translates to 51,213 avoidable deaths in a population of 168,180,047.

aerodynamic diameters less than 2.5 μm ($PM_{2.5}$) is a major contributor to air pollution and has attracted global concern (Pui et al. (2014), Fan et al. (2020)). $PM_{2.5}$ concentrations are especially high in urban areas[4], where the widespread use of private vehicles and localized fuel combustion (e.g, such as for heating, industrial activities, and wood burning) are among the main contributing sources (Dominici et al. (2014); EEA (2021)). According to the European Environmental Agency (EEA), over the past decade, a 22% reduction in $PM_{2.5}$ levels corresponded with a 45% decrease in mortality attributable to this pollutant.

The adverse health effects of air pollution are well-documented, with a robust literature establishing causal links between exposure and outcomes across demographic groups, regions, and periods. However, much of the existing literature has examined various health effects of pollutants other than fine particulate matter < 2.5, including PM_{10}, NO_2, SO_2, CO and O_3.

Early evidence from Chay et al. (2003) on the 1970 Clean Air Act shows reduced TSPs but no clear link to adult or elderly mortality. Subsequent studies, Chay & Greenstone (2003), Currie & Neidell (2005), Knittel et al. (2016), Cesur et al. (2017), find a link between infant mortality and pollutants such as TSPs, CO, and PM. Research then shifts to acute effects, with Neidell (2004) showing CO's impact on childhood asthma. Bauernschuster et al. (2017*a*) exploit transit strikes in Germany, finding 11-13% more traffic, 14% increases in PM_{10}/NO_2, and 11% higher respiratory hospitalizations, especially in children. Similarly, Bauernschuster et al. (2017*b*) and Schlenker & Walker (2016) link traffic and airport emissions to pediatric and asthma-related admissions. Instrumental variable methods improve causal inference: Deryugina et al. (2019) use wind shifts to show $PM_{2.5}$ raises mortality among 25% of the U.S. elderly. To our knowledge, is the only study that specifically analyzes the impact of fine particulate matter on mortality in the U.S. Palma et al. (2022) leverage strikes as exogenous shocks, finding that a one-standard-deviation increase in PM_{10} raises hospitalisations by 0.79 per 100,000, especially among vulnerable and younger groups. Emerging research reveals specific vulnerabilities: Fan et al. (2023) identifies SO_2 as a cardiovascular mortality driver, especially in children under 5 years, whereas Cakaj et al. (2023) quantify growing ozone threats through a $1.3/10^6$ inhabitant rise in annual premature deaths.

In this paper, we investigate the causal effect of exposure to fine particulate matter $<$

[4]In urban areas, common pollutants also include PM_{10}, nitrogen dioxide (NO_2), sulfur dioxide (SO_2), carbon monoxide (CO), ozone (O_3), and volatile organic compounds (VOCs), originating from sources like vehicles, industry, and heating.

2.5 μm in European cities for the period 2010-2018 on premature mortality, measured as mortality rate under 65 due to diseases of the circulatory or respiratory systems and infant mortality rate. We focus on these mortality indicators because there is a widespread consensus about their direct connection with air pollution, particularly with exposure to $PM_{2.5}$, see for example Loomis et al. (1999), Pope et al. (2009), Brook et al. (2010*a*), Yixing et al. (2016), Heft-Neal et al. (2020), Ortigoza et al. (2021), just to cite a few.

Cities, as previously mentioned, represent a critical setting for examining the health impacts of air pollution. Our analysis focuses on cities in Italy, Spain, Greece, Croatia, and Portugal - regions identified by the European Environment Agency (EEA) as experiencing some of the most severe air pollution in Europe, particularly with regard to $PM_{2.5}$ concentrations.[5] We combine satellite-based measures of air pollution with statistics on premature mortality and we focus on fine particulate matter, namely $PM_{2.5}$. To identify the causal effect of exposure to particulate matter, we leverage local variations in rainfall as a source of random variation in air pollution exposure, integrating it with the Two-Sample Two-Stage Least Squares (TS2SLS) estimator. Stable weather conditions, coupled with intense local economic activity, can sustain concentration levels above permissible limits for several days. In contrast, windy days or rainfall can disperse air pollution far from its source. For these reasons, changes in wind direction have been employed as an instrument for SO_2 concentrations (Yang et al. 2017), while local weather conditions have been utilized for PM_{10} and CO (Knittel et al. 2016). Thermal inversions, likely to cause a temporary accumulation of certain pollutants, have also served as instruments for PM_{10}, CO, SO_2, and O_3 (Arceo et al. 2016). More recently, total rainfall has been used as an instrument for PM_{10} exposure during the prenatal period (see Palma et al. (2022)). Following this literature, we employ precipitation as an instrumental variable for air pollution. Our identification strategy exploits yearly within-city variations in precipitation, assuming they are randomly distributed across cities and relies on the fact that, according to the literature (Shukla et al. (2008), Sundar et al. (2020), Tripathi et al. (2021) - just to cite a few), rain can effectively *clear* the air of pollution. We conduct further robustness checks to rule out potential violations of the exclusion restrictions. In order

[5]The highest $PM_{2.5}$ levels in Europe are recorded in Eastern Europe and Northern Italy. In many Central and Eastern European countries, this stems from the widespread use of solid fuels (e.g., coal for residential heating, industrial processes, and power generation. The Po Valley (Northern Italy) represents a critical hotspot due to its dense industrialization, high population density, and meteorological conditions that trap pollutants. This region consistently exceeds the EU $PM_{2.5}$ limit ($15\mu g/m^3$, 24-hour) EEA (2021). Due to insufficient mortality data for Eastern European cities, we prioritize Southern Europe in this study.

to avoid measurement error issues deriving by aggregating at the city level information about weather conditions and air pollution collected by monitoring stations we employ the TS2SLS estimator proposed by Angrist & Krueger (1992) that allows us to obtain consistent instrumental variables estimation when only the outcome and the instrument (but not the endogenous variable) are observed in one sample and the endogenous and the instrument (but not the outcome) are observed in a second different sample. In our case, we can observe the instrument, the endogenous and the outcome in the sample at the city level. Still, we can observe only the instrument and the endogenous in the station-level sample.

Our results show a positive and statistically significant effect of $PM_{2.5}$ on both premature mortality indicators. We find that a one-unit increase in $PM_{2.5}$, corresponding to 7.5% of the average level of $PM_{2.5}$, implies an increase in the mortality rate under 65 and in the infant mortality rate of 0.2887 and 0.3134, corresponding to 8.49% and 10.57% of the corresponding average values. Strong effects are also observed for PM_{10} and NO_2 exposure (4.9-6.0% increases). Robustness checks using multiple weather-based instruments confirm these results, particularly for working-age populations. Spatial heterogeneity reveals urban areas face sever mortality impacts, while a paradoxical socioeconomic gradient emerges: lower-poverty-risk cities exhibit higher pollution vulnerability, likely due to concentrated exposure.

We contribute to the existing literature in several ways. First, we focus on the finest measure of particulate matter, namely $PM_{2.5}$, which is the air pollutant driving the most significant health problems and premature mortality, being able to travel deeply into the respiratory tract and reaching the lungs. So far, the literature, especially in the case of European countries, mostly focused on PM_{10} (see for example Palma et al. (2022), Bauernschuster et al. (2017*a*) or Giaccherini et al. (2021)), in the case of US evidence on $PM_{2.5}$ is concentrated among the elderly Deryugina et al. (2019).

A second contribution is that we focus on individuals under 65 and infants aged 0-1. This represents a relevant contribution to the literature, as our estimates are not affected by "mortality displacement" or "harvesting" - a common limitation in previous studies. A key concern in assessing the mortality impact of pollution is whether those who die from exposure would have died soon regardless, particularly if effects are concentrated among the elderly or those already in poor health. In such cases, the estimated number of life-years lost may be overstated. By contrast, focusing on younger populations allows for a more accurate assessment of long-term mortality impacts.

Third, our analysis focuses on cities as the primary unit of analysis, which provides a more policy-relevant framework for evaluating interventions. Urban areas are particularly critical in this context, as they often serve as hotspots for air pollution and its associated health burdens. This is underscored by our data: In all cities sampled, 84% of the population was exposed to $PM_{2.5}$ concentrations that exceeded the WHO-recommended guidelines (World Health Organization - WHO (2021)).

The remainder of the paper is organized as follows. In the next Section 1.2, we describe the data, the main variables used, and the sample. Section 1.3 presents our empirical methodology, including the identification strategy. The main results of our analysis, some robustness checks and effect heterogeneity are discussed in Section 1.4. Section 1.5 summarises the main findings and concludes.

1.2 Data and sample

1.2.1 Data

We build a geospatial data set by combining data on infant and premature mortality for cities in Italy, Spain, Greece, Portugal and Croatia (2010-2018) from Urban Audit (UA) with pollution and weather data from the Airbase and Climate Data Records (CDR) of the European Environmental Agency, respectively. Weather data consist of annual precipitation averages, computed by aggregating daily records from monitoring stations, while pollution levels are provided as pre-aggregated annual concentrations, both georeferenced by latitude and longitude. Mortality outcomes are restricted to cities with no missing records, though some years exhibit gaps due to intermittent reporting. Using a maximum matching radius of 12.5 km, we first pair the nearest weather and pollution monitoring stations and then link the resulting station pairs to the closest cities, allowing a maximum of 10 station pairs restricted by the radius. This yields a final sample of 80 cities and 202 station pairs. The dataset includes 536 city-year observations and 1,305 station-year for infant mortality rate, with smaller samples for mortality rate among individuals under 65 due to circulatory and respiratory diseases (472 city-level and 1,019 station-level). We then add some useful covariates that lead to some negligible attrition. Our primary infant mortality sample comprises 482 city-year and 1,030 station-year observations and premature mortality 429 city-level and 915 station-level, covering 75 cities and 180 monitoring

stations in total.[6]

1.2.1.1 City data

The UA database provides information on the quality of life in cities, considered as a local administrative unit where the majority of the population lives in an urban centre of at least 50,000 inhabitants. The dataset includes information on cities and their commuting zones (the so-called Functional Urban Areas). The information collected includes demography, housing, health, labour market, education, environment, transport and tourism. Data availability differs among variables and years, as the statistics are provided voluntarily. As of 2020, this dataset contains 980 cities and 49 greater cities[7] in 31 European countries. From these data, we gather two measures of premature mortality available at the city level: (i) infant mortality rate, defined as the number of infant deaths per 1,000 live births, and (ii) mortality rate among individuals under 65 due to circulatory and respiratory diseases, measured as deaths in this category per 100,000 of the total population.

1.2.1.2 Monitoring station data

The Airbase database of the European Environmental Agency (EEA) includes validated concentration measures from monitoring stations in the majority of cities all over Europe. Our primary measure of pollution is fine particulate matter ($PM_{2.5}$). In addition, for robustness reasons, we will also use other pollutants such as PM_{10}, NO_2, SO_2, CO and O_3.

We employ data from the Climate Data Records (CDR), which are systematically collected and maintained by the National Centers for Environmental Information[8]. Specifically, we employ annual averages of temperature, wind speed at a 10-meter elevation, and total precipitation.

1.2.1.3 Additional data

We supplement our analysis with regional socioeconomic indicators from Eurostat: GDP per capita (NUTS3, PPS-adjusted to EU27 averages), unemployment rates, and poverty risk (NUTS2). These variables account for disparities in pollution exposure and health

[6]The dataset is an unbalanced panel due to non-continuous mortality reporting by cities and intermittent station operation. Thus, observed city-years (482 for infant mortality) and station-years (1,030) fall below the theoretical maximum (675 and 1,620, respectively).

[7]The 49 greater cities correspond to 160 cities and represent a city with a larger area or a combination of several cities.

[8]For more details on the data refer to https://www.ncei.noaa.gov/products/climate-data-records

vulnerability. Lower-SES populations face elevated risks due to both greater pollutant exposure and increased susceptibility from behavioral factors (e.g., smoking, limited health knowledge; Novi (2010)) and reduced capacity to mitigate environmental harms (Sexton (1997)). While Wang et al. (2022) find higher $PM_{2.5}/NO_2$ exposure among high-SES individuals in China, this likely reflects urban density effects rather than reduced low-SES vulnerability. Controlling for these factors isolates pollution effects while addressing structural inequities.

1.2.2 Sample

Our primary dataset combines data collected at two distinct levels: city-level, containing outcome variables and economic indicators, and station-level, capturing detailed measurements of pollution and meteorological conditions.

The city-level dataset contains information on premature mortality outcomes and economic indicators. Data collected from monitoring stations, instead, integrates information about air quality and weather conditions, respectively. However, monitoring stations may be located in different areas of the city, potentially failing to represent the same territorial cluster and leading to weather measurements that are not fully representative of $PM_{2.5}$ levels. Additionally, some stations may be located far from urban centres, making $PM_{2.5}$ measurements less representative of the city's premature mortality indicators. To address these issues, we employ a two-step approach: (i) we identify the weather monitoring station closest to each air quality monitoring station, ensuring a maximum (average) Euclidean distance of 12.5 km (5 km); (ii) we select station pairs located within a maximum (average) radius of 12.5 km (5 km) from the city centroid. This methodology enhances the spatial representativeness of our dataset in relation to both air pollution and meteorological conditions. Notice that the selected maximum distance of 12.5 km is associated with a smaller average distance between stations and couples of stations and cities.

Our final dataset collects relevant information relative to 75 cities in Southern European Countries (Croatia, Greece, Italy, Portugal, Spain) on mortality rates [9], pollution[10], and weather conditions[11] collected by 180 monitoring stations. Table A1.1 shows descriptive

[9]The spatial distribution, along with the average corresponding values and variability of the two outcomes, are presented in Figures A1.1 and A1.2 in the Appendix.

[10]The spatial distribution, along with the average corresponding values and variability of the $PM_{2.5}$ levels, are presented in Figure A1.3 in the Appendix.

[11]The spatial distribution, along with the average corresponding values and variability of the Mean precipitations, are presented in Figures A1.4 in the Appendix.

statistics about our main sample. Notably, the number of observations collected at the monitoring station level is higher than the number of observations at the city level, as a single city may have multiple pairs of monitoring stations for pollution and meteorological conditions. The air monitoring stations in our dataset report information about their location: urban, suburban or rural[12]. Our sample consists of 57% of Spanish cities, 35% of Italian cities, 5.6% of Portuguese cities, 1.7% of Greek cities, and 0.7% of Croatian cities. The sample comprises 79% of stations classified as urban, 20% as suburban, and the remaining 1% as rural, based on their territorial location. For a visual representation of both urban and suburban monitoring stations, refer to the figure A1.5 provided in the appendix. Considering our outcome measures, infant mortality is on average 2.97 every 1,000 live births. The mortality rate under the age of 65 due to circulatory or respiratory diseases is equal to 3.4 every 100,000 individuals. Regarding meteorological conditions, the average wind speed is 6.4 m/s, the mean temperature is 15.5°C, and the average precipitation level is 0.05 mm/day. Annual average air pollution levels in the sample reveal an average $PM_{2.5}$ concentration of 13.3 $\mu g/m^3$, PM_{10} at 24.5 $\mu g/m^3$, NO_2 at 27.2 $\mu g/m^3$, SO_2 at 4.5 $\mu g/m^3$, CO at 4.4 $\mu g/m^3$, and O_3 at 52.19 $\mu g/m^3$. For comparison, the 2021 WHO Air Quality Guidelines recommend the following limits: an annual average of 5 $\mu g/m^3$ for $PM_{2.5}$, 15 $\mu g/m^3$ for PM_{10}, and 10 $\mu g/m^3$ for NO_2; a 24-hour limit of 4 $\mu g/m^3$ for CO; a 24-hour limit of 40 $\mu g/m^3$ for SO_2 and a maximum of 60 $\mu g/m^3$ for O_3. These statistics indicate that, on average, the levels of $PM_{2.5}$, PM_{10}, and NO_2 exceed the WHO-recommended thresholds, suggesting potential adverse health effects associated with air pollution exposure in the sampled cities. In contrast, the average concentrations of SO_2, CO, and O_3 remain within or close to the recommended limits.

1.3 Empirical strategy

We aim to estimate the causal effect of air pollution on mortality in Southern European cities. We start by considering a standard OLS regression:

[12]Urban areas are defined as continuously built-up regions where streets are predominantly lined with buildings, each having at least two floors, or large detached buildings with similar characteristics. These areas are mostly free of non-urbanised spaces, except for city parks. In contrast, suburban areas consist mainly of detached buildings, with a lower building density than urban areas. It's important to note that, in this context, suburban areas can exist independently of an urban centre, which differs from the common definition of a suburb as an outlying part of a city or town.

$$Y_{ct} = \alpha + \beta PM2.5_{ct} + \sum_{k=1}^{N_K} \iota_k X_{kct} + \sum_{j=1}^{N_J} \gamma_j X_{jrt} + \theta_c + \psi trend_t + \xi trend_t^2 + \epsilon_{ct}, \qquad (1.1)$$

Y_{ct} describes the outcomes of interest: (i) the mortality rate under 65 due to diseases of the circulatory or respiratory systems per 100,000 individuals recorded in city c and year t and (ii) the infant mortality rate per 1,000 live births recorded in city c and year t. Air pollution is measured using the level of $PM2.5$ in micrograms per cubic meter ($\mu g/m^3$) in city c and year t. X_{ct} represents a matrix of covariates at the city-year level. X_{rt} represents a matrix of covariates at the region-year level. θ_c are city fixed effects and $trend_t^i$, with $i = 1, 2$ is a quadratic time trend. ϵ_{ct} indicates the error term.

However, within the present context, the coefficient of interest, β, which quantifies the effect of air pollution on health, is biased if pollution levels are correlated with unobservable characteristics that also exert an influence on individuals' health status. As pointed out by Neidell (2004), individuals may adopt avoidance behaviours by responding to smog alerts, implying attenuation bias on OLS estimates[13] that would, in turn, seriously underestimate the causal effect of air pollution on health. A possible solution is to adopt an IV strategy that leverages random variations in weather conditions as an instrument for air pollution. In this paper, we use yearly precipitations recorded in city c during year t as an instrumental variable. A valid instrument should satisfy two conditions: (i) relevance: rainfall should correlate with air pollution; (ii) exclusion restriction: rainfall should only affect mortality through its impact on pollution. For what concerns relevance, it can be pointed out that rainfall facilitates the transportation of suspended particles from the earth's atmosphere to the ground, which occurs via dry and wet deposition. As a raindrop falls through the atmosphere, it can attract tiny aerosol particles to its surface before hitting the ground[14]. Concerning the exclusion restriction, it must be noted that our identification, by including city-specific fixed effects, relies on within-city yearly variations in precipitation levels, which we assume to be randomly distributed across cities and years. A possible threat to identification in our model is represented by healthy individuals deciding to move towards cities with larger yearly variations in precipitation levels. However, it seems implausible for at least two reasons: (i) migration decisions

[13]For a discussion, see also Deryugina et al. (2019)

[14]The process by which droplets and aerosols attract particles is called coagulation, a natural phenomenon that can clear the air of particle pollutants such as $PM_{2.5}$ (Ardon-Dryer et al. 2015). The effect of rainfall on pollution is broadly referred to as the *washing effect* (Guo et al. 2016) or *removal effect* (Zhao et al. 2020).

are driven by income or labour market opportunities Borjas (1999); (ii) even admitting a possible role for weather conditions, it would not be rational to decide to move towards cities with more rain (and thus worse weather conditions). However, this mechanism may also arise spuriously if rain is positively correlated with income or if healthy individuals decide to move away from cities with high pollution levels and smaller yearly variations in precipitation levels. In order to explore this potential threat to identification, we perform some checks in the robustness section 1.4.2.

If the above-mentioned conditions hold, we can estimate an IV model, using the 2SLS estimator, where the first stage regression is:

$$PM2.5_{ct} = \alpha^1 + \lambda^1 Rain_{ct} + \sum_{k=1}^{N_K} \iota_k^1 X_{kct} + \sum_{j=1}^{N_J} \gamma_j^1 X_{jrt} + \theta_c^1 + \psi^1 trend_t + \xi^1 trend_t^2 + \epsilon_{ct}^1 \quad (1.2)$$

Where $Rain_{ct}$ represents annual mean daily precipitation recorded in city c during year t and all other covariates remain as previously defined and discussed in Equation 1.3. Whereas the second stage regression is:

$$Y_{ct} = \alpha^2 + \beta_{2SLS}^2 PM2.5_{ct} + \sum_{k=1}^{N_K} \iota_k^2 X_{kct} + \sum_{j=1}^{N_J} \gamma_j^2 X_{jrt} + \theta_c^2 + \psi^2 trend_t + \xi^2 trend_t^2 + \epsilon_{ct}^2, \quad (1.3)$$

Now, β_{2SLS}^2 captures the causal effect of $PM2.5$ on mortality. It must be noted that both the first and second-stage equations report variables measured at the city-year level. However, both pollution and other information about meteorological conditions, including our instrument about precipitation, are recorded by monitoring stations located in different parts of the city. Ideally, one would like to exploit the station-year variability when estimating the first stage and the city-year variability for the second stage. This has two main advantages: (i) first-stage estimates rely on a larger sample size and, consequently, are more precise, (ii) by not aggregating pollution and weather data at the city level we avoid the risk of incurring in measurement error due to estimating the correlation between precipitation and pollution measured by monitoring stations located in very distant areas, but close to the same city, or to relying on opposite measurements by different stations located close to the same city, that after aggregation could potentially lead to null variations. Nevertheless, in the latter scenario, we may observe an increase in pollution-related mortality at the city level, stemming from an area with lower variations

in annual precipitation - and consequently higher pollution levels - if that area is more densely populated by individuals facing elevated health risks. In this paper, we use the TS2SLS estimator proposed by Angrist & Krueger (1992) according to which consistent instrumental variables estimation is possible when only the outcome and the instrument (but not the endogenous variable) are observed in one sample and the endogenous and the instrument (but not the outcome) are observed in a second different sample. In our case, we can observe the instrument, the endogenous and the outcome in the sample at the city level. Still, we can observe only the instrument and the endogenous in the station-level sample. In the case of exact identification, the conventional TS2SLS estimator is:

$$\hat{\beta}^2_{TS2SLS} = \left(\widehat{PM2.5}'_c \widehat{PM2.5}_c\right)^{-1} \widehat{PM2.5}'_c Y_c \tag{1.4}$$

Where $\widehat{PM2.5}_c = Rain_c \left(Rain'_s Rain_s\right)^{-1} Rain'_s PM2.5_s$. As demonstrated by Inoue & Solon (2005), the TS2SLS estimator is preferred to the TSIV version. The first stage equation then becomes:

$$PM2.5_{st} = \alpha^1 + \gamma^1 Rain_{st} + \sum_{k=1}^{N_K} \iota^1_k X_{kst} + \sum_{j=1}^{N_J} \gamma^1_j X_{jrt} + \theta^1_s + \psi^1 trend_t + \xi^1 trend^2_t + \epsilon^1_{st} \tag{1.5}$$

Lastly, to validate the consistency of our estimates, we consider four different specifications of the TS2SLS version of the model presented in Equations 1.3 and 1.5: specification (1), which includes in the first (second) stage equation station- (city-) specific fixed effects plus a quadratic time trend, in order to account for time invariant unobservable characteristics at the station (city) level, and non linear long-term mortality trends; specification (2), which introduces city-specific linear trends, in place of the basic linear trend included in specification 1, and maintains the common quadratic trend component, in order to account for heterogeneous temporal dynamics across cities; specification (3), which adds, with respect to specification (1), station-level covariates (i.e., the share of days with valid measurements along the year, the average wind speed and temperature measured by station s in city c during year t) and two spatial economic covariates (Gross domestic product GDP at current market prices measured at the provincial level $p - NUTS3$, and unemployment rates measured at the regional level $r - NUTS2$, during year t); specification (4), which refines specification (3) by including city-specific linear trend while excluding the common linear time trend, allowing to account for flexible city-level

temporal dynamics in mortality rates and pollution. Standard errors are clustered at the station (city) level in the first (second) stage equation.

1.4 Results

1.4.1 Baseline results

Table 1.1 presents our baseline estimates of the effect of $PM_{2.5}$ on the mortality rate under 65, specifically for circulatory and respiratory diseases measured per 100,000 individuals in city c at time t, for all 4 specifications described in Section 2.4. Panel A shows the OLS estimates, while Panel B displays the TS2SLS estimates. OLS estimates (see Panel A of Table 1.1) show positive but not always statistically significant effects. TS2SLS estimates (see Panel B) are always positive and highly statistically significant across all specifications. Coefficients range from 0.2660 (column 4) to 0.3346 (column 2). Our preferred specification is that shown in column (3), which includes a linear time trend instead of a city-specific linear trend to prevent excessive absorption of $PM_{2.5}$ variation, thereby preserving the identification of its effect on premature mortality.[15] According to our estimates, an increase of one unit of $\mu g/m^3$ in $PM_{2.5}$ (corresponding to 7.5% of the average level) is associated with 0.2887 additional deaths per 100,000 inhabitants due to circulatory and respiratory diseases among individuals under 65. This corresponds to an 8.49% increase relative to the average mortality rate. Notably, this estimate is 20 times larger than the OLS estimate of 0.0139, suggesting a substantial downward bias in the latter.

Table 1.2 shows estimates for the effect of $PM_{2.5}$ on the infant mortality rate per 1,000 live births recorded in city c at time t. OLS estimates, also in this case, show coefficients that are not statistically significant (see Panel A). Coefficients estimated by TS2SLS are positive, but statistically significant only in some specifications at the 5 and 10% levels. In column (4), we do not find a statistically significant effect of $PM_{2.5}$ on the infant mortality rate per 1,000 live births. The magnitude of the coefficient associated with our preferred specification is of considerable size because, in this case, a one $\mu g/m^3$ increase in $PM_{2.5}$ (corresponding to 7.5% of the average) implies an increase in the infant mortality rate of

[15] While a city-specific trend, model (4), would account for unobserved local factors, it could also reduce the valuable variation in $PM_{2.5}$, compromising the precision of the estimates. Since the model already incorporates station fixed effects, quadratic time trends, meteorological variables, monitoring station characteristics and economic factors, the linear time trend provides an optimal balance, capturing common temporal trends without over-controlling for local differences already accounted for.

0.3134 points, corresponding to 10.57% of the average infant mortality rate per 1,000 live births.

First stage estimates (see Tables A1.2 and A1.3), show that rainfall is a strong predictor of $PM_{2.5}$ levels for both outcomes. The estimated coefficients are similar since the information at the station level differs for only 3 stations (3 more for the infant mortality rate). This is confirmed by the first-stage F-statistics shown in the table, which varies from 29.6 (column 1) to 62.3 (column 2) and is well above 10 in every specification considered. According to our preferred estimates in column (3), each 1 unit of rain/day (e.g. 100 mm/day) increase in average rainfall is associated with a 0.1737-unit reduction in $PM_{2.5}$, suggesting atmospheric washing-out effects.

Table A1.4 shows reduced form estimates. The upper (lower) panel prove that rain significantly affects our outcome variables plausibly through the effect generated by $PM_{2.5}$.

Table 1.1: <65 Cardio-Respiratory MR $\times$ 100,000 population - OLS and TS2SLS

	(1)	(2)	(3)	(4)
Panel A: OLS				
$PM_{2.5}$	0.0129	0.0394*	0.0139	0.0337
	(0.0233)	(0.0227)	(0.0241)	(0.0230)
Panel B: TS2SLS				
$PM_{2.5}$	0.3171***	0.3346**	0.2887***	0.2660**
	(0.1065)	(0.1331)	(0.1060)	(0.1149)
Mean of Y	3.4012	3.4012	3.4012	3.4012
SD of Y	1.1711	1.1711	1.1711	1.1711
F-stat	29.6	62.6	31.1	53.4
p-value F-stat	8.968e-8	3.595e-14	4.58e-8	1.955e-12
Number of cities	75	75	75	75
Number of stations	180	180	180	180
Observations cities	429	429	429	429
Observations stations	915	915	915	915
Station FE	Yes	Yes	Yes	Yes
Linear trend	Yes	No	Yes	No
Quadratic trend	Yes	Yes	Yes	Yes
Station control variable	No	No	Yes	Yes
Weather control variables	No	No	Yes	Yes
City linear trend	No	Yes	No	Yes
GDP and Unemployment	No	No	Yes	Yes

Notes: Standard errors are clustered at the city level. Significant levels: *** p<0.01, ** p<0.05, * p<0.1.

Table 1.2: Infant MR × 1,000 population - OLS and TS2SLS

	(1)	(2)	(3)	(4)
Panel A: OLS				
$PM_{2.5}$	-0.0193	0.0392	-0.0205	0.02332
	(0.0415)	(0.0481)	(0.0429)	(0.0492)
Panel B: TS2SLS				
$PM_{2.5}$	0.3787**	0.4038*	0.3134*	0.2985
	(0.1803)	(0.2224)	(0.1795)	(0.1951)
Mean of Y	2.9665	2.9665	2.9665	2.9665
SD of Y	1.6519	1.6519	1.6519	1.6519
F-stat	29.6	62.6	31.1	53.4
p-value F-stat	8.968e-8	3.595e-14	4.58e-8	1.955e-12
Number of cities	75	75	75	75
Number of stations	177	177	177	177
Observations cities	482	482	482	482
Observations stations	1,030	1,030	1,030	1,030
Station FE	Yes	Yes	Yes	Yes
Linear trend	Yes	No	Yes	No
Quadratic trend	Yes	Yes	Yes	Yes
Station control variable	No	No	Yes	Yes
Weather control variables	No	No	Yes	Yes
City linear trend	No	Yes	No	Yes
GDP and Unemployment	No	No	Yes	Yes

Notes: Standard errors are clustered at the city level. Significant levels: *** p<0.01, ** p<0.05, * p<0.1.

1.4.2 Robustness

In this section, we present a series of robustness analyses conducted using specification (3).

First, we test whether rainfall is correlated with income, a potential confounder in the relationship between pollution and mortality. As shown in Table A1.7 column(1), we find no significant correlation between GDP and rainfall, suggesting that rainfall does not operate through income to affect mortality. Furthermore, as shown in Column (2) of the table, current rainfall is not significantly predicted by precipitation levels in the two preceding years. This supports the assumption that rainfall is not systematically influenced by persistent local factors, thereby strengthening the evidence for the instrument's exogeneity.

Second, we examine whether healthier individuals are more likely to relocate from cities with higher pollution levels and lower variability in annual precipitation. We estimate an OLS regression model that includes city-specific time trends, as well as city and year fixed

effects. Table A1.8 shows no significant correlation between lagged $PM_{2.5}$ levels and migration outcomes (immigration, emigration, or net inflow), even controlling for one-year lagged values of GDP, wind speed, and precipitation.

Third, while our primary focus remains on $PM_{2.5}$, we assess the robustness of our findings by extending the analysis to other pollutants - PM_{10}, NO_2, SO_2, CO and O_3 - whose concentrations are often correlated with particulate matter. This approach helps isolate whether observed health effects are uniquely attributable to $PM_{2.5}$ or driven by co-exposure to a broader pollutant mixture. According to previous studies, PM_{10}, which counts coarse (bigger) particles, gas pollutants such as nitrogen dioxide[16] (NO_2), sulfur dioxide[17] (SO_2), ozone (O_3)[18], and carbon monoxide (CO)[19] particularly widespread in urban areas, are important contributors to the incidence of pediatric asthma globally (see Pandey et al. (2005), Giaccherini et al. (2021), Orellano et al. (2021), Anenberg (2022)) and represent serious health risks, especially in terms of infant mortality Currie & Neidell (2005). This extended analysis serves two key purposes: (1) it tests whether the observed scavenging effect of rainfall is consistent across pollutants with differing chemical compositions and atmospheric lifetimes, and (2) it helps identify potential heterogeneity in precipitation-driven pollution dynamics. While maintaining $PM_{2.5}$ as our primary exposure of interest, we evaluate these additional pollutants to disentangle their potential confounding effects, as they typically exhibit strong spatial and temporal correlations in urban environments.

We report results using these additional pollutants in Table 1.3. We estimate significant causal effects of PM_{10} and NO_2 on mortality. We do not find evidence of any significant effect when considering the other pollutants. Results show that a one-unit increase in PM_{10} implies an increase in the mortality rate under 65 due to diseases of the circulatory or respiratory systems per 100,000 individuals of 0.1659 points (a 4.88% increase of the average mortality rate). In comparison, a one-unit increase in NO_2 implies an increase in mortality under 65 of 0.1525 points (equal to a 4.48% increase in the mortality rate). In

[16]Major NO_2 sources include on-road and non-road transportation tailpipe emissions (including heavy, medium, and light duty vehicles, shipping, and aviation), power plants, industrial manufacturing, and agriculture. Previous studies have linked NO_2 with approximately 13% of the global paediatric asthma burden, and up to approximately 50% in the most populated 250 cities worldwide (see for example Achakulwisut P (2019)).

[17]Major sources include fossil fuel combustion from power plants and industry, with additional emissions from metal extraction, volcanic activity, and high-sulfur fuel use in transport and heavy machinery.

[18]O_3 is a secondary pollutant formed when volatile organic compounds (VOCs) and nitrogen oxides react in sunlight.

[19]CO is a direct byproduct of combustion, primarily released by vehicles, industrial processes, and household appliances such as gas stoves and heaters.

the lower panel of Table 1.3, we show the effect of air pollution on the infant mortality rate per 1,000 live births. Coefficients are positive and marginally statistically significant. A one-unit increase in PM_{10} (NO_2) is associated with a 6.04% (5.58%) increase in the average infant mortality rate per 1,000 live births. First-stage estimates, available upon request, confirm that rainfall is a strong predictor of air pollution levels. In Table 1.3 the F-statistic is always above 10 when considering PM_{10} and NO_2 (thumb rule > 10).

Lastly, we extend our IV strategy to include, alongside precipitations, wind speed (used, among others, by Deryugina et al. (2019), Di Porto et al. (2021)) (2IV) and average temperature (implemented, among other, by Sager (2019), Filomena et al. (2023)) (3IV) as instrumental variables. This approach leverages exogenous weather-driven variation in $PM_{2.5}$ through distinct pathways: (1) precipitation's aerosol scavenging - as discussed, (2) wind speed's dual role in dispersion/resuspension, and (3) temperature's effects on emissions (e.g., heating demand) and atmospheric chemistry. Together, these instruments better isolate $PM_{2.5}$'s causal effect while addressing unobserved confounding. To validate our multi-instrument IV strategy, we implement the Sargan test of overidentifying restrictions. Table A1.6 shows results for both premature outcomes considered. In the upper section of the table, we observe a significant effect of air pollution on cardio-respiratory mortality among individuals under 65, while no effect is detected for infant mortality, both in the 2IV and in the 3IV specifications, respectively. The estimated effect ranges from 8.2% (2IV) to 8.9% (3IV), closely aligning with the results obtained using the baseline specification with one instrumental variable and other weather conditions as control variables. The Sargan test fails to reject the null hypothesis of valid overidentifying restrictions, confirming instruments' validity. This aligns with atmospheric mechanisms where precipitation scavenges aerosols, while wind/temperature influence dispersion and chemical formation. The differential findings across age groups - with consistent mortality effects for <65 but null results for infant mortality under 2IV/3IV specifications - likely reflect distinct exposure-response mechanisms. For working-age populations, the enhanced precision of multiple instruments (rain, wind, temperature) better isolates $PM_{2.5}$'s causal effect by addressing confounding from occupational/outdoor exposure pathways. In contrast, infants' limited outdoor exposure and higher indoor air pollution buffering may attenuate measurable effects.

Table 1.3: Effect of PM_{10} , NO_2 , SO_2 , CO and O_3 concentration on < 65 Cardio-Respiratory MR × 100,000 and Infant MR × 1,000 - TS2SLS

	PM_{10}	NO_2	SO_2	CO	O_3
	(1)	(2)	(3)	(4)	(5)
Panel A: < 65 Cardio-Respiratory MR × 100,000					
Pollutant	0.1659**	0.1525***	-1.2305	-2.0942	-0.4929
	(0.0666)	(0.0574)	(0.9042)	(35.5495)	(0.3568)
Mean of Y	3.4012	3.4012	3.4012	3.4012	3.4012
SD of Y	1.1711	1.1711	1.1711	1.1711	1.1711
F-stat	15.3	11.6	1.2662	3.9064	0.5407
p-value F stat	1.05e-4	7.286e-4	0.2613	0.0488	0.4626
Number of cities	75	75	75	75	75
Number of pollution stations	180	180	166	180	178
Observations cities	429	429	429	429	429
Observations stations	914	915	818	913	890
Panel B: Infant MR × 1,000					
Pollutant	0.1791*	0.1655*	-1.2172	-2.2733	-0.4712
	(0.1074)	(0.0958)	(1.1138)	(38.6009)	(0.4256)
Mean of Y	2.9664	2.9664	2.9664	2.9664	2.9664
SD of Y	1.6519	1.6519	1.6519	1.6519	1.6519
F-stat	15.3	11.6	1.2662	3.9064	0.5407
p-value F stat	1.05e-4	7.286e-4	0.2613	0.0488	0.4626
Number of cities	75	75	75	75	75
Number of pollution stations	177	177	130	177	175
Observations cities	482	482	482	482	482
Observations stations	1,029	1,030	935	1,028	1,004

Notes: The specification used is that of tables 1.1 and 1.2, column (3). Notice that the number of observation varies on the kind of pollutant explored. This is because not all the air-monitoring stations have registered pollutants continuously over the considered period. Standard errors are clustered at the city level. Significant levels: *** p<0.01, ** p<0.05, * p<0.1.

1.4.3 Heterogeneity

This section investigates whether our baseline results are heterogeneous across several dimensions. First, we test whether the effect of $PM_{2.5}$ differs by metropolitan area. Second, we consider cities located in regions above or below the median of the distribution of the rate of individuals at risk of poverty within a given country.

Table 1.4 presents estimates of the heterogeneous effects of pollution on mortality across urban - column (1) - and suburban - column (2) - areas, exploiting information about monitoring stations' location. In the upper panel A, we can see that the effect of $PM_{2.5}$

on the mortality rate under 65 due to diseases of the circulatory or respiratory systems per 100,000 individuals is significant only when considering monitoring stations located in urban, rather than suburban areas. This result suggests heightened vulnerability or exposure intensity in urban parts of the cities subject to higher concentrations of traffic-related pollutants or to the effect of heating systems. However, the lack of significance in non-urban areas could stem from lower pollution levels, different emission sources, or less precise exposure measurement. Whereas, in columns (3) and (4), we conduct the analysis splitting our sample according to whether cities are located in regions where the proportion of individuals at risk of poverty is above or below the national median. This approach enables us to assess the effects of $PM_{2.5}$ exposure in relation to economic conditions, offering a comparative perspective within the broader socioeconomic context. From this analysis we can see that $PM_{2.5}$ has a significant effect on the mortality rate under 65 due to diseases of the circulatory or respiratory systems per 100,000 individuals in cities located in regions below the median of the distribution of the rate of individuals at risk of poverty within a given country. Individuals living in these regions have a lower risk of poverty at the cost of being exposed to higher levels of air pollution. Looking at Panel B, refereed to infant mortality rate per 1,000 live birth, we find no statistically significant effects either splitting our sample of cities according to metropolitan area, columns (1) and (2), or according to the rate of individuals at risk of poverty in the country, columns (3) and (4).

Table 1.4: Effect of $PM_{2.5}$ concentration on < 65 Cardio-Respiratory MR × 100,000 and Infant MR × 1,000 - TS2SLS estimates by metropolitan areas type and risk of poverty rate

	Metropolitan areas		**Risk of Poverty rate**	
	Urban	Suburban	Above	Below
	(1)	(2)	(3)	(4)
Panel A: < 65 Cardio-Respiratory MR × 100,000				
$PM_{2.5}$	0.3112***	0.2456	0.1249	0.2352***
	(0.1124)	(0.2133)	(0.9397)	(0.0736)
Mean of Y	3.4674	3.2797	3.7119	3.1373
SD of Y	1.1649	1.0134	1.1233	1.1481
F-stat	30.8	2.7732	6.1475	24.3
p-value F-stat	5.788e-8	0.0981	0.0141	1.662e-6
Number of cities	67	27	46	44
Number of pollution stations	102	38	98	96
Observations cities	359	148	197	232
Observations stations	714	195	433	459
Panel B: Infant MR × 1,000				
$PM_{2.5}$	0.2473	0.3165	1.5334	0.2047
	(0.1843)	(0.3724)	(2.6447)	(0.1319)
Mean of Y	2.9739	2.7638	3.1643	2.7719
SD of Y	1.6209	1.5632	1.6464	1.6373
F-stat	30.8	2.7732	6.1475	24.3
p-value F-stat	5.788e-8	0.0981	0.0141	1.662e-6
Number of cities	67	27	47	44
Number of pollution stations	138	38	99	93
Observations cities	404	169	239	243
Observations stations	798	226	512	490

Notes: The specification used is that of tables 1.1 and 1.2, column (3). Urban and Suburban Areas: Urban areas are characterized by continuous built-up development, while suburban areas consist of largely built-up regions on the outskirts of urban centers. Cities are further categorized based on their economic status, with distinctions made between those above and below the poverty line (median). Standard errors are clustered at the city level. Significant levels: *** p<0.01, ** p<0.05, * p<0.1.

1.5 Conclusions

This paper provides causal estimates of the impact of air pollution on mortality in Southern European cities, focusing on two critical outcomes: (1) the under-65 mortality rate due to circulatory and respiratory diseases, and (2) the infant mortality rate. To address endogeneity concerns in pollution exposure, we employ the Two-Sample Two-Stage Least Squares (TS2SLS) estimator with an instrumental variable (IV) strategy, using yearly average total millimeters of daily rainfall as our instrument. Rainfall acts as a plausibly exogenous source of variation in pollution levels, as it influences atmospheric dispersion while being uncorrelated with unobserved determinants of mortality. We concentrate on fine particulate matter ($PM_{2.5}$) as our primary pollution measure due to its well-documented role as a leading environmental risk factor for premature mortality and severe health conditions. Our findings contribute to the growing body of evidence on the adverse health effects of $PM_{2.5}$, particularly in urban settings where pollution concentrations are elevated due to traffic, heating systems, industrial activity, and other anthropogenic sources. We find a positive and statistically significant effect of $PM_{2.5}$ on both mortality indicators. According to our estimates, a one-unit increase in $PM_{2.5}$, corresponding to 7.5% of the average level of $PM_{2.5}$, implies an increase in the mortality rate under 65 and in the infant mortality rate of 0.2887 and 0.3134, corresponding to 8.49% and 10.57% of the corresponding average values.

Our empirical analysis further quantifies the adverse health effects of additional urban air pollutants beyond $PM_{2.5}$, specifically examining particulate matter with a diameter $\leq 10\mu m$ (PM_{10}) and nitrogen dioxide (NO_2). The results demonstrate statistically significant increases in both mortality outcomes studied: exposure to these pollutants is associated with a 4.88% (PM_{10}) and 4.48% (NO_2) rise in under-65 mortality from circulatory and respiratory diseases per 100,000 population. More alarmingly, we observe even greater impacts on infant mortality, with both PM_{10} and NO_2 exposure corresponding to a 6.04% and 5.58% increases, respectively, in deaths per 1,000 live births. The particularly strong effects on infant mortality highlight the heightened vulnerability of this demographic to air quality degradation, warranting special policy consideration for maternal and child health protection in urban environmental planning.

As part of our robustness checks, we employ an expanded instrumental variables approach incorporating multiple weather-based instruments, including wind direction patterns, temperature variations, and precipitation levels, to validate our core findings. This compre-

hensive analysis yields estimates for the under-65 mortality rate that remain consistent with our primary specification using rainfall as the sole instrument. The convergence of results across these alternative specifications strengthens the credibility of our causal identification strategy, suggesting that our estimated pollution-mortality relationship is not sensitive to the particular choice of weather instrument. Notably, the robustness of these effects persists most strongly for working-age mortality outcomes, reinforcing our central findings regarding the vulnerability of this demographic group to air pollution exposure.

Our analysis reveals significant spatial and socioeconomic heterogeneity in the health impacts of $PM_{2.5}$ exposure. We find substantially stronger effects on under-65 mortality from circulatory and respiratory diseases in urban areas compared to suburban settings (a one-unit increase in $PM_{2.5}$, corresponding to 7.5% of the average level of $PM_{2.5}$, implies an increase in the mortality rate under 65 of 8.96% in urban areas), likely reflecting higher pollution concentrations and greater population exposure in dense urban environments. Notably, the mortality impacts are particularly pronounced in cities located in regions with lower poverty risk (below the national median), suggesting an unexpected socioeconomic gradient in vulnerability because individuals living in these regions have a lower risk of poverty at the cost of being exposed to higher levels of air pollution. This pattern may stem from several factors: more accurate mortality reporting in wealthier areas, differences in population age structures, varying compositions of pollution sources with differential toxicity, or distinct exposure patterns related to occupational and leisure activities. These findings highlight the complex interplay between environmental and socioeconomic factors in determining pollution-related health outcomes, emphasizing the need for spatially and demographically targeted policy interventions to mitigate the public health burden of air pollution. The results underscore the importance of considering both geographic context and local socioeconomic conditions when assessing the mortality impacts of $PM_{2.5}$ exposure and designing effective regulatory responses.

Overall, our results suggest that air pollution is an important determinant of health. In contrast to Deryugina et al. (2019), that focus on over-65 mortality rates, we use two measures associated with premature mortality, the mortality rate under 65 and the infant mortality rate. The policy implications of this work point in the direction of implementing policies aimed at decreasing $PM_{2.5}$ levels across cities, especially in those areas where air pollution is more prevalent.

Chapter 2

Paper II: Chilly Temperatures, Polluted Air: the health impacts of residential heating emissions

2.1 Introduction

Air pollution remains a critical public health challenge, with fine particulate matter ($PM_{2.5}$) identified as the most harmful pollutant by the World Health Organization (WHO). Due to its microscopic size, $PM_{2.5}$ can penetrate deeply into the lungs, enter the bloodstream, and affect multiple organs. While efforts to reduce emissions have led to improvements[1], significant challenges persist. Urban areas remain hotspots for pollution, with 96% of the EU's urban population still exposed to $PM_{2.5}$ levels exceeding WHO guideline thresholds in 2022.

The sources of $PM_{2.5}$ pollution are diverse, encompassing both anthropogenic and natural contributors. According to IQAir, human-related emissions primarily stem from motor vehicles, power plants, industrial activities, residential wood burning, and agricultural practices. Natural sources include dust, soot, windborne salt, plant spores, pollen, and wildfire smoke. The dominant sources of $PM_{2.5}$ vary by season, weather conditions, and urbanization levels, further complicating mitigation strategies.

Among anthropogenic sources, residential heating plays a particularly significant role. The European Union Emission Inventory Report 1990-2022 EEA (2024) highlights that Italy registered a 29% reduction in $PM_{2.5}$ emissions between 2000 and 2022. Notably, residential heating emerged as the largest contributor, accounting for 62% of total $PM_{2.5}$ emissions in 2022. Alarmingly, emissions from this sector increased by 35% between 2005 and 2022, offsetting reductions achieved in other sectors, i.e. transport. While European emission standards have successfully curbed pollution from road transport and industrial activities, these efforts have not been sufficient to counterbalance the rise in emissions from residential heating.

The impact of heating systems on air quality is particularly pronounced in Italy. In 2012, ISPRA reported that while overall emissions had declined, $PM_{2.5}$ emissions from residential heating, responsible for the largest share of emissions (54%), surged by 171% due to the increasing reliance on biomass for heating. Zauli-Sajani et al. (2024) also emphasize that nearly all anthropogenic $PM_{2.5}$ emissions from the residential sector originate from biomass combustion.

While the link between biomass heating and pollutant emissions is well-established, the

[1] According to the European Environment Agency (EEA), the number of premature deaths in the EU attributable to $PM_{2.5}$ declined by 45% between 2005 and 2022, driven by lower pollutant concentrations and reduced population exposure.

associated health effects remain less thoroughly explored. Recent studies highlight the direct impact of heating emissions on air quality and health. Salva et al. (2023) find that individual heating systems release significantly higher NO_2 and CO concentrations in residential areas compared to district heating systems. Similarly, Fan et al. (2020) report that winter heating leads to a 36% increase in the weekly Air Quality Index and a 14% rise in mortality rates. The consequences extend beyond health risks; Curci et al. (2023) shows that elevated levels of PM_{10} related to heating emissions in Italy contribute to work-related accidents and disabilities.

A growing body of literature underscores the severe and varied health consequences of exposure to air pollutants, affecting populations in different geographic and demographic contexts. Although efforts to reduce emissions have made some progress, certain regions continue to experience elevated levels of pollution, often exacerbated by factors such as residential heating systems and vehicular traffic. To fully grasp the complex dynamics of air pollution and its health-related effects, this study draws on insights from existing research.

The emission of harmful pollutants into the atmosphere plays a critical role in exacerbating numerous health issues, including an elevated risk of respiratory infections, cardiovascular diseases, lung cancer, and premature mortality Pope & Dockery (2012). Various studies provide evidence of these effects. For instance, Giaccherini et al. (2021) estimate an increase in hospital admissions linked to exposure to PM_{10}, while Bauernschuster et al. (2017*b*) document higher hospitalization rates among young children due to NO_2 and PM_{10} emissions from traffic. Similarly, Schlenker & Walker (2016) report an increase in emergency room visits for asthma and respiratory and cardiac conditions due to CO emissions from airport congestion. Interestingly, He et al. (2020) find that straw burning increases particulate matter pollution and causes people to die from cardiorespiratory diseases. Additional research highlights mortality risks associated with air pollutants: Neidell (2004) and Chay & Greenstone (2003) link exposure to CO and total suspended particulates to increased health-related mortality, respectively. Cheung et al. (2020) analyses show that a 10-unit increase in the Air Pollution Index leads to a 1.77% rise in the monthly cardio-respiratory mortality rate, with the elderly being particularly vulnerable to air pollution. Similarly, Deryugina et al. (2019) find that mortality effects are concentrated in approximately 25% of this population, highlighting the increased risks faced by older individuals exposed to fine particulate matter. Moreover, Fan et al. (2020) observe that the activation of heating systems contributes to overall mortality through air

quality deterioration, and Fan et al. (2023) link SO2 exposure to cardiovascular deaths, particularly among individuals aged 60 and above and children under 5.

Adverse effects extend to neonatal and child health, as evidenced by studies such as DeCicca & Malak (2020), Fan et al. (2023), and Palma et al. (2022), which associate air pollution with premature births and compromised neonatal health.

Our study aims to estimate the causal effect of short-term exposure to pollutants from the activation of the residential heating system on urgent hospital admissions and in-hospital deaths related to specific cardiovascular and pulmonary diseases. The targeted conditions include Acute Myocardial Infarction (AMI) encompassing ST-segment Elevation Myocardial Infarction (STEMI) and Non-ST-segment Elevation Myocardial Infarction (NSTEMI), as well Ischemic and Hemorrhagic Stroke and Chronic Obstructive Pulmonary Disease (COPD). These particular cardiovascular diseases have been chosen due to their well-established association with $PM_{2.5}$, as documented in the medical literature. Among others, Yixing et al. (2016) and Ortigoza et al. (2021) provide compelling evidence linking $PM_{2.5}$ exposure to adverse health outcomes, particularly for the cardiovascular conditions examined in our study.

Our identification strategy is based on a staggered difference-in-differences (DiD) design (Callaway & Sant'Anna (2021)) comparing municipalities with above-median versus below-median biomass consumption (treatment vs. control groups), where biomass use is measured as appliance-adjusted adoption per municipal area. We define treatment timing using observed heating activation, namely, when the temperature threshold where Google searches for "Turning on the heating system" significantly increases. This approach captures actual heating behaviour while avoiding biases from non-compliance with official heating regulations.

This paper provides four main findings. First, the activation of biomass-fueled heating systems significantly elevates ambient levels of $PM_{2.5}$, PM_{10} (which includes $PM_{2.5}$), and NO_2. Second, increased pollution exposure raises hospitalisation rates for AMI, STEMI, NSTEMI, hemorrhagic stroke and COPD, though it has no detectable effect on ischemic strokes. The effect on mortality is most pronounced for AMI, STEMI and hemorrhagic stroke during 2015-2016, a period characterised by peak pollution fluctuations, and during 2018-2019 for NSTEMI. Third, the effects on health exhibit substantial heterogeneity. According to our estimates pollution exposure disproportionately affects middle-aged (45-64 years) and older adults (65+), individuals with low educational attainment and residents of specific climatic zones (D/E). Fourth, contrary to classic mortality displacement (which

accelerates deaths in vulnerable populations), we find that pollution harms individuals without comorbidities, implying novel biological pathways and higher societal costs from lost healthy life years. These results highlight the differential health and economic burdens imposed by pollution, with implications for targeted policy interventions.

Our paper contributes to the existing literature in several ways. First, we provide new evidence on the health effects of heating-generated $PM_{2.5}$, the finest and most harmful particulate matter (e.g. Xing et al. (2016), Feng et al. (2016)), and NO_2, associated to increase mortality for cardiovascular and respiratory disease according to Samoli et al. (2006), distinguishing between hospitalisations and in-hospital mortality for both cardiovascular and respiratory diseases. Unlike prior studies focusing on traffic-related PM_{10} and NO_2 emissions (e.g., Bauernschuster et al. (2017*b*); Giaccherini et al. (2021)), we highlight the role of decentralised heating systems, a critical pollution source in Italy. Second, we extend the analysis beyond respiratory outcomes, commonly examined in earlier work (e.g.,Neidell (2004), Schlenker & Walker (2016), Giaccherini et al. (2021)), to cardiovascular hospitalisations and mortality, offering a more comprehensive assessment of pollution-related health burdens. To our best knowledge, only Margaryan (2021) investigates the impact of PM_{10} and NO_2 on cardiovascular diseases, but her findings are limited to major German cities, raising concerns about external validity. In contrast, we analyse nationwide data on hospital admissions and in-hospital mortality across Italy, offering broader generalisation. Moreover, while Godzinski & Suarez Castillo (2021) find that carbon monoxide increases emergency cardiovascular admissions and particulate matter elevates mortality (using an IV approach), we demonstrate that $PM_{2.5}$ exposure affects both hospitalisations and in-hospital mortality - a novel contribution underscoring the wider health burden of fine particulate matter. Third, we refine the identification of vulnerable populations by employing the Charlson Comorbidity Index (CCI) to isolate healthy individuals, rather than relying solely on age-based classifications as in Deryugina et al. (2019) and Margaryan (2021), revealing adverse effects even among those without comorbidities. Fourth, we introduce a novel identification strategy that classifies municipalities by their reliance on biomass heating and leverages temperature-driven heating activation, addressing potential deviations from regulated heating dates (e.g., Fan et al. (2020); Curci et al. (2023)) and capturing household behavioural responses to cold weather. Together, these contributions advance understanding of the health impacts of heating-related air pollution while offering methodological and substantive innovations.

The remainder of the paper is organized as follows. In the next section 2.2, we describe the

background of heating system regulation in Italy. In section 2.3, we describe the data, the main variables used, how we link data from different sources and illustrate our sample. The empirical and identification strategies are discussed in section 2.4, respectively. The main results of our analysis, several robustness checks and effect heterogeneity are discussed in Section 2.5. Section 2.6 summarizes the main findings and concludes.

2.2 Heating system regulation in Italy

Italy is divided into six climatic zones. They are defined based on the categorization of temperature ranges established using the degree days (Deg_Days[2]). The degree days of a municipality are calculated by summing, for each day of the year, the positive differences between 20°C (Italy's conventionally and legally recognised threshold for comfortable indoor temperature below which heating is required, as established by Gazzetta Ufficiale della Repubblica Italiana - DPR 412/1993 (1993)) and the daily average outdoor temperature (T_e), as reported by the following formula:

$$Deg\_Days = \sum_{e=1}^{n}(20 - T_e) \tag{2.1}$$

In other words, for all days of the year when the outdoor temperature is lower than 20°C, the daily degree deficits to reach this threshold are summed. Once the annual sum is obtained, the municipality in question is placed within a climatic band, defined based on degree days intervals. The higher this number, the more the municipality will be in a cold temperature zone and consequently will demand more intensive building heating, see Table A2.1. Figure A2.1 illustrates the distribution of climatic zones across Italy and Table A2.2 provides a summary of the major Italian cities and their corresponding climatic zones.[3]

The regulation of the heating system in Italy is governed by a climate zone framework established by Gazzetta Ufficiale della Repubblica Italiana - DPR 412/1993 (1993) and then updated and improved by the Gazzetta Ufficiale della Repubblica Italiana - DPR 74/2013 (2013). The mandates fixed annual activation periods and daily operating hours calibrated to regional degree-day thresholds. This system, designed to optimise energy, presumes heating is unnecessary when outdoor temperatures exceed 18.3°C (65°F). How-

[2] *Deg_Days* stands for *"Gradi Giorno"*.

[3] For example, Milan and Turin are classified in climatic zone E, Rome in the milder zone D, and Naples in zone C.

ever, three critical nuances emerge: (i) binding schedules apply only to centralised systems, with autonomous heating often bypassing regulation[4]; (ii) the government, but even single municipalities, may override defaults and anticipate (posticipate) activation dates during periods of unusually cold (warm) temperatures or energy emergencies (e.g., 2022 gas crisis); and (iii) enforcement relies on ex-post inspections rather than real-time compliance monitoring. The divergence between de jure heating regulations and de facto practices, especially in biomass-reliant contexts with pervasive self-regulation, challenges the methodological reliance on official start dates, which may inadequately capture real-world heating initiation.

According to ISTAT (2021), 65.7% of Italian households primarily use autonomous heating systems, while 17.2% rely on single appliances (e.g., stoves, heat pumps) and 17.1% on centralised systems. Notably, 44.5% combine multiple systems, often blending centralised, autonomous, and auxiliary sources. Half of households own supplementary appliances, introducing significant variability in heating behaviour. This heterogeneity makes legal heating dates a poor proxy for actual pollution exposure, as private systems allow discretionary use, bypassing restrictions. Enforcement is further complicated by structural factors (insulation, building size) and socioeconomic disparities (vulnerable groups depend on heating for health, while wealthier households can sustain prolonged usage).

2.3 Data and sample

We construct a novel municipality-level dataset by merging multiple sources: (i) administrative data on Hospital Discharge Records (HDRs) from Italian Ministry of Health; (ii) pollution exposure measures from Copernicus Atmosphere Monitoring Service (CAMS) and European Environmental Agency monitoring stations (EEA); (iii) weather controls from Agri4Cast; and (iv) covariates including ISTAT population data, Terna biomass consumption, and Google searches indicators. Our analysis focuses on 2015-2019 to leverage the first available year of hospitalisation records while avoiding COVID-19 disruptions, which abruptly altered both pollution levels and healthcare utilisation patterns. Our sample covers about 479 municipalities containing 892 hospitals corresponding to the universe of hospitalisations in Italy[5].

[4] A study conducted by Idealista, the leading real estate portal in Italy for technological development, revealed that over 70% of homes for sale in the country have adopted independent heating systems in 2024.

[5] It pertains to municipalities that contain at least one hospital facility.

2.3.1 Hospital Discharge Records

The data offer information about hospitalisations across public and publicly funded private hospitals in Italy. The Italian National Health Service (NHS) is a national insurance scheme, tax-funded, covering a very broad set of constitutionally defined services. The dataset includes socio-demographic details about patients (age, gender, nationality, birthplace, region of residence, education), clinical information (diagnoses, procedures, transfers, discharges), and hospital-specific information (type, specialisation). In the analysis of HDRs, we focus on urgent, unplanned admissions to avoid self-selection of patients into more productive hospitals and we exclude patients who have been documented as transferred to a different admission regime (either day hospital or regular admission) or another type of care activity (acute care, rehabilitation, long-term care) within the same healthcare facility, to avoid duplicates of the same patient.

Our analysis is specifically centred on urgent hospitalisations related to cardiovascular and pulmonary diseases. The main outcome variables encompass AMI, STEMI, NSTEMI, ischemic stroke, hemorrhagic stroke and COPD. We sum the total number of hospital admissions per month and by municipality.

2.3.2 Pollution and Weather Data

CAMS data offer annual air quality reanalyses for Europe, based on both unvalidated and validated observations. CAMS [6] delivers yearly air quality reanalyses for Europe with a notably higher spatial resolution (0.1 degrees, approximately 10km) compared to global reanalyses. CAMS combines eleven European air quality models into a median ensemble, merging them with EEA monitoring data through data assimilation to produce consistent pollution estimates while quantifying uncertainty through model variation. In addition to in-situ data assimilation, satellite data and other observational sources can complement the dataset. Reanalyses are accessible at hourly intervals and various height levels. We opt for zero meters above the surface, coherent with our analysis purposes, and for the validated reanalysis type. CAMS represents the primary data source for $PM_{2.5}$.

While our primary pollution measures rely on CAMS gridded $PM_{2.5}$ data[7] (the only

[6] According to Wu et al. (2020) CAMS data are accurate and reliable, making them a valuable resource for monitoring air quality and pollution events.

[7] The decision to employ grid data, over air monitoring stations one, offers numerous advantages. Firstly, it provides full territorial coverage and detailed spatial resolution, ensuring that no area is overlooked and allowing for precise analysis at a granular level. Secondly, grid data ensures uniformity across space and time, facilitating consistency in comparisons and analyses. The continuous monitoring allows

pollutant available at our required resolution), we supplement these with station-level observations from the European Environmental Agency (EEA) Airbase database[8] for three key reasons: (i) CAMS lacked complete coverage for secondary pollutants (PM_{10}), Nitrogen Dioxide (NO_2), Sulfure Dioxide (SO_2), Carbon Monoxide (CO) and Ozone ($O3$) during our study period; (ii) monitoring stations provide validated ground measurements across European cities, enabling direct comparison with CAMS $PM_{2.5}$ estimates to assess potential bias; and (iii) multi-pollutant analysis helps isolate $PM_{2.5}$ effects from correlated emissions.

Agri4Cast[9] offers data for weather conditions. The JRC MARS Meteorological Database contains daily meteorological observations from weather stations, interpolated onto a 25×25 km grid, covering the European Union and neighboring countries. The variables considered in our analysis are mean air temperature °C, mean daily wind speed at 10m (m/s), and sum of precipitation (mm/day). Both pollution and weather variables have been mean-collapsed at the weekly and monthly municipality level, depending on the purpose of the analysis.

2.3.3 Supplementary data

Data on population were obtained from the ISTAT database (Italian National Institute of Statistics) for all municipalities and years considered. Additionally, the number of residential heating appliances for 2011 by municipality, as recorded in the Census of Population and Housing, was included, representing the only available year of data collection relevant to this study [10].Data on annual regional biomass consumption (GWh) were retrieved from Terna reports. Terna is a key player in the energy sector, providing essential data on energy consumption, production, and infrastructure at both regional and national levels.We obtained the absolute number of weekly Google searches for "Turning on the heating system" by climatic area.

for real-time or near-real-time tracking of changes and trends. Additionally, grid data help reduce assumptions about uniform pollutant concentrations, providing a more accurate representation of environmental conditions and identifying localized pollution hotspots.

[8]These point data are incorporated into the CAMS dataset.

[9]Mavromatis & Voulanas (2021) evaluate the suitability of Agri4Cast and E-OBS as the most appropriate datasets, over ERA-Interim, for climate and atmospheric research in Greece.

[10]The ISTAT census is conducted every ten years. However, since 2018, it has transitioned into a permanent, annual survey. Each year, it comprises two sample-based surveys: one relying on population registry data and the other on an area-based sample of addresses. This new approach involves only a representative sample of approximately 1.4 million households.

2.3.4 Data Linkage

In our main analysis, we employ geo-spatial analysis techniques to match the Italian municipalities to specific geographical grid points for air pollution and weather conditions. Each location in the dataset is identified by latitude and longitude coordinates, that allow us to identify the nearest grid point to each municipality location, considering as proximity threshold the first nearest neighbour. HDRs data are already provided with the municipality code. Hereafter, we link hospitalisations and in-hospital deaths using the municipality code.

In our robustness ($PM_{2.5}$ - EEA) and extended analysis for other pollutants (PM_{10}, NO_2, SO_2, CO, O_3), differently, we exploit air quality point data registered by monitoring stations. These stations are strategically positioned in various environments, capturing both urban and rural conditions, but they tend to register higher pollution levels due to their strategic points location, such as high-traffic roads. While we maintain the nearest-neighbour approach for pollution station assignment, we now impose a 12.5 km maximum distance threshold between the station and the municipality centroid. This refinement addresses cases where the geographically closest station was excessively distant (e.g., >12.5 km), potentially misrepresenting local exposure levels.

Overall, these drawbacks highlight the need for complementary approaches and data integration strategies to improve the comprehensiveness and accuracy of air quality assessments. Accordingly, the principal reference sample stems from the application of gridded-data. All the other variables considered as additional data have been linked using the municipality code.

2.3.5 Sample

Our main sample, including observations between 2015 and 2019, is further split into a biannual combination, consisting of data from April to December of the previous year (t) and from January to March of the following year ($t+1$). This approach ensures: (i) the irreversibility of the treatment as required in Callaway & Sant'Anna (2021)[11]; (ii)

[11]The irreversibility hypothesis, often termed the "absorbing state" assumption, states that once a unit receives treatment, it remains treated in all subsequent periods. This assumption simplifies staggered DiD designs by allowing potential outcomes to depend solely on the initial treatment timing, rather than the full treatment history. It extends the parallel trends assumption by requiring comparable outcome trends across groups defined by treatment timing, while the no-anticipation condition ensures pre-treatment outcomes are unaffected by future treatment. Although irreversibility enhances tractability, recent work (e.g. De Chaisemartin & D'Haultfœuille (2020)) explores its relaxation by allowing treatment reversal, but this requires generalisations of the parallel trends assumption and strong "no carryover" assumptions

clean separation of heating and non-heating seasons to identify treatment effects; (iii) comparable pre-treatment trends across groups (parallel trends). The considered biennia are 2015-16, 2016-17, 2017-18, and 2018-19.

Table A2.3 provides a detailed descriptive overview of health outcomes, air pollution, and weather conditions across Italian municipalities for our sample. For health outcomes, hospitalisation rates for AMI, STEMI, NSTEMI, stroke subtypes, and COPD exhibit modest but consistent declines. For instance, ischemic stroke hospitalizations fell from 4.65 cases (SD: 9.32) in 2015-16 to 3.83 (SD: 6.09) in 2018-19, while STEMI admissions decreased by 9.1% over the same period. Mortality rates remained stable for AMI, STEMI, NSTEMI and Hemorrhagic Stroke ($\sim$ 0.30, 0.14, 0.11 and 0.32 events/year, respectievly) but declined for ischemic stroke (-16.7%) and COPD (-5.4%).

Air pollution levels, particularly $PM_{2.5}$, decreased during the study period. Mean $PM_{2.5}$ concentrations (CAMS data) dropped from 16.40 μg/m^3 in 2015-16 to 13.35 μg/m^3 in 2018-19, with the number of days exceeding WHO thresholds (15 μg/m^3) declining by nearly half. Similar reductions were observed for PM_{10} and especially for NO_2. Notably, however, the levels for $PM_{2.5}$, PM_{10} and NO_2 still exceed the recommended threshold reported in Table A2.4. The observed discrepancies[12] between CAMS and EEA pollution metrics - particularly the 14% higher $PM_{2.5}$ levels in EEA monitoring data - underscore the importance of multi-source validation in exposure assessment. Weather conditions, including wind speed, temperature and precipitation, remained relatively stable, though minor fluctuations (e.g., higher wind speeds in 2017-18 and higher precipitations in 2016-17) may have contributed to pollution dispersion.

2.4 Empirical strategy

We aim to evaluate the impact of the activation of residential heating systems on pollutant emissions, in particular $PM_{2.5}$ and NO_2, and on urgent hospital admissions and in-hospital mortality associated with specific cardiovascular and pulmonary diseases, namely, AMI, STEMI, NSTEMI, Ichemic and Hemorrhagic Stroke, and COPD.

To estimate the causal effect of heating activation on pollution emissions and health outcomes, we employ a difference-in-differences framework. Our ideal specification would

that current outcomes depend only on present treatment status, not past exposure, hence not suitable for our study.

[12]The divergence stems from measurement approaches: EEA monitors target high-exposure urban areas, capturing localised peaks, while CAMS grids provide spatial averages that smooth extremes.

classify municipalities by biomass consumption, a major source of $PM_{2.5}$[13] and use official heating activation dates, which vary by climatic zone, as the treatment indicator for the post-period. However, as noted above, individuals may decide not to comply with the regulation if they are endowed with an autonomous heating system, or even municipalities may decide to anticipate or postpone official dates. Both decisions are driven by the outside temperature. In the following, we will describe how our empirical strategy addresses these issues.

First, we construct a measure of municipal exposure to biomass heating emissions through a three-stage spatial allocation procedure. Initially, we distribute regional biomass consumption obtained from Terna for the period 2015-2019 to municipalities using heating appliance penetration rates obtained from the 2011 ISTAT census. To identify heating systems fueled by biomasses we consider partial[14] residential heating appliances (RHA) and compute the regional share of such appliances as follows:

$$\text{Share\_Biomass\_heat}_{m,2011} = \frac{\text{Biomass\_heat}_{m,2011}}{\sum_{i=1}^{N_r^m} \text{Biomass\_heat}_{m,r,2011}} \tag{2.2}$$

Where the proportion of partial RHA in the municipality m during 2011 relative to its regional total is given by $\text{Share\_Biomass\_heat}_{m,2011}$. This represents the ratio between the numerator, $\text{Biomass\_heat}_{m,2011}$, which represents the number of partial RHAs in the municipality registered in 2011, and the denominator, $\sum_{i=1}^{N_r^m} \text{Biomass\_heat}_{m,r,2011}$, which represents the total number of partial RHAs in region r during 2011, with subscripts m, and r indexing municipalities, and regions respectively. Using these appliance shares, we distribute observed regional biomass consumption from Terna to municipalities through spatial disaggregation:

$$\text{Biomass}_{m,t} = \frac{(\text{Biomass}_{r,t} \times \text{Share\_Biomass\_heat}_{m,2011})}{\text{km}^2_{m,t}} \tag{2.3}$$

This transformation scales annual regional consumption $Biomass_{r,t}$ by each municipality's

[13]Virdis et al. (2015) explains that biomass is almost the entire source of $PM_{2.5}$ emissions in the civil sector (more than 99 percent), while other sources make a completely negligible contribution

[14]The term "partial" residential heating appliances refers to fixed single-point heating systems (including fireplaces, stoves, radiators, or heat pumps) that provide localised heating to specific sections of a dwelling, as opposed to whole-house central heating systems. These appliances are characterised by: spatially limited coverage (heating individual rooms or zones), independent operation from building-wide heating infrastructure, direct combustion (in biomass-based systems) or point-source heat generation. Partial RHAs are particularly relevant for $PM_{2.5}$ exposure studies as they: exhibit higher emission intensities per unit heat output, show greater variation in usage patterns, are more likely to use solid biomass fuels ISTAT (2011).

fixed appliance share, normalised by municipal area (km^2) to account for differences in municipality size. Next, we average these values across the years in our sample as follows:

$$\text{Biomass}_m = \frac{1}{\text{N}^T} \sum_{t=1}^{\text{N}^T} \text{Biomass}_{m,t} \tag{2.4}$$

Finally, we define as treated (controls) municipalities above (below) the median of such indicator[15].

$$\text{Treatment} = \begin{cases} 1 & \text{if Biomass}_m > 50^{\text{th}}\text{perc Biomass}_m \\ 0 & \text{otherwise} \end{cases} \tag{2.5}$$

Second, in order to identify the post-treatment period, we rely on behavioural responses to temperature-driven variations in heating demand. We consider that, according to equation 2.6, households will decide to turn on heating when the outdoor temperatures fall below a certain tipping point (an unknown, exogenous threshold at which heating becomes necessary). In order to identify this tipping point, we adopt a two-step approach. First, we estimate the temporal patterns of temperature and heating activation using the following specification:

$$\text{Y}_{r,w} = \gamma_0 + \gamma_r + \gamma_w + \nu_{r,w} \tag{2.6}$$

where r denotes regions and w indexes week-year observations. The dependent variable $\text{Y}_{r,w}$ captures two distinct measures: (i) regional average temperature, reflecting climatic conditions, and (ii) Google search frequencies for the phrase "Turning on the heating system," serving as a behavioral proxy for household heating activation. The analysis focuses on transitional periods from April (t) to March ($t+1$) across the four biennial spans, with the coefficients of interest γ_w identifying week-year fixed effects that reveal temporal patterns in heating system usage. This approach allows us to disentangle regulatory heating periods from actual behavioral responses to environmental conditions. Specifically, we aim to verify whether a strong correlation exists between temperature drops and increases in Google searches for heating-related queries. If confirmed, Google Trends data will then serve to identify heating systems activation more precisely.

Second, to empirically identify the critical temperature thresholds that trigger heating activation, we estimate:

[15] As a robustness we also use different thresholds to identify treated and controls (above 66^{th} vs below 33^{rd} or above 75^{th} vs below 25^{th} percentile)

$$\mathrm{Y}_{r,w} = \delta_0 + \sum_{k=1}^{N_k} \delta_k Temp\_bins_{r,w} + \delta_1 Wind\_speed_{r,w} + \delta_2 Precipitations_{r,w} + \delta_r + \delta_w + \psi_{r,w} \tag{2.7}$$

where r denotes the region and w the week-year observations. The dependent variable $Y_{r,w}$ captures the Google trend searches for the term "Turning on the heating system", while $Temp\_bins_{r,w}$ represents 0.5-degree temperature bins (from 28 to 0 degrees Celsius). The coefficients of interest are δ_k. We identify the critical temperature threshold for heating activation (T^*) as the first temperature bin at which Google search interest for "Turning on the heating system" becomes statistically significant ($\delta_k \neq 0$). This approach ensures that we exclude post-threshold periods where heating is already widespread, avoiding violations of the common trend assumption in subsequent causal analyses. We define the post-treatment period based on the week when temperature first falls below T^*, but operationalise it at the monthly level to match hospitalization data granularity.

This strategy allows us to capture the causal effect of heating-driven pollution exposure, avoiding the common threats to identification in the literature connected with the presence of compensatory behaviours driven by reactions to pollution alerts, Neidell (2004) for two main reasons: (i) pollution exposure is random, i.e. individuals cannot anticipate the week when the temperature drops below T^*, (ii) the control group of municipalities with under the median biomass consumption is exposed to similar pollution alerts, allowing us to net out their effects with the DD strategy. According to the latter point, one may argue that treated municipalities are likely to be exposed to higher levels of pollution alerts. However, this would bias our estimated coefficients downward, making it a lower bound.

In addition, it must be noted that the week when the outside temperature reaches T^* will be different between municipalities according to their location, year-specific weather conditions and other factors making our design compatible with a staggered DiD (De Chaisemartin & D'Haultfœuille (2020), Callaway & Sant'Anna (2021), and Wooldridge (2021)). In particular, in our analysis, we adopt the regression-adjusted (RA) version of Callaway & Sant'Anna (2021) estimator, which provides several key advantages for our research context. This approach estimates group-time average treatment effects on the treated (ATT) under three critical identifying assumptions: (1) treatment irreversibility (once a municipality presents biomass heating consumption above the median, it cannot revert to non-treated status), (2) the absence of anticipatory effects (outcomes are unaffected

by future treatment adoption), and (3) parallel trends between later-treated groups and never-treated units. The RA estimator is particularly suitable for our setting as it accommodates the observed variation in municipal heating adoption timing while mitigating potential biases from time-varying confounders through covariate adjustment.
We estimate group-time average treatment effects (ATT) as follows:

$$ATT(g,t) = \left[\frac{G_g}{(G_g)}(Y_t - Y_{g-1} - [Y_t - Y_{g-1}|X, G = NT])\right] \tag{2.8}$$

Let Y represent both pollution levels - $PM_{2.5}$ (CAMS) and NO_2[16] - and health outcomes - AMI, STEMI, NSTEMI, Ishemic and Hemorrhagic Stroke, and COPD[17] - for municipality g in month-year t. G_g indicates treatment timing (with $G_g = NT$ for never-treated units), and X represents weather controls including wind speed, temperature, and precipitation. We compute weather variables as two-week moving averages, incorporating both the current week's value and its first lag (i.e., the previous week's value). These controls are included to account for potential confounding factors that may influence both pollution levels and health outcomes, such as cardiovascular and pulmonary hospitalisations. Temperature and precipitation can directly affect air quality, while wind speed can influence the dispersion of pollutants. The main model considers municipality fixed effects control for unobserved heterogeneity.

2.5 Results

2.5.1 Identification of treated and controls and of temperature-driven heating systems activations

Initially, we conduct a descriptive analysis to examine the variations in pollution levels during the months in which residential heating systems are activated. We make a distinction between the pre-activation and post-activation periods. The pre-activation period is defined as the months from June to September, while the post-activation period spans from October to January. By comparing sub-figures of Figure A2.3 we notice that the level of $PM_{2.5}$ is higher during heating activation months (Figure A2.3b). The Po Valley is among the most polluted areas of Italy, with pollution levels exceeding those of other

[16] For robustnes pruposes we will use $PM_{2.5}$ (EEA), PM_{10}, SO_2, CO and O_3.
[17] Health outcomes are expressed as rates per 10,000 individuals, calculated by dividing the raw counts by the municipal population.

regions, even during the summer months (Figure A2.3a). This phenomenon is primarily attributable to its specific morphological characteristics, which contribute to the trapping of air pollutants, as well as to its high level of industrialisation, further exacerbating pollution. However, during the winter months, a significant increase in $PM_{2.5}$ levels is also observed in municipalities located in the Apennines, a region characterised by colder temperatures.

Figure A2.4 plots estimates of γ_w coefficients from equation 2.6 for both temperatures and Google searches for turning on the heating system; where the black dashed vertical line marks the first temperature drop and the corresponding rise in Google searches, while the red dashed vertical line represents the first week in which it is theoretically allowed to switch on the heating system (i.e. 15th of October in areas D/E). We notice that for all biennia, when the first significant drop in temperature occurs, the Google searches rapidly increase, and this happens two weeks before the legal activation time for the heating system. This behavioural response signals that Google Trends data serve as an accurate proxy for real-world heating activation timing. Critically, search trends detect when people actually turn on their heating systems, far more precisely than official seasonal dates, which consistently lag behind real behavior due to their rigid, administrative nature.

In Figure A2.5 we plot estimates of δ_k coefficients estimated from equation 2.7. Our analysis reveals that Google search activity for heating-related terms exhibits statistically significant increases, with respect to the reference week set at 16[18], when ambient temperatures fall below 18°C and remains significant until the outside temperature reaches 12°Cidentifying a temperature band where the level of uncertainty about the possibility of activating heating systems is maximum. This thermal response band serves as the primary driver of residential heating system activation. The critical temperature threshold for heating activation (T^*) is the first temperature bin at which Google search interest for "Turning on the heating system" becomes statistically significant and corresponds to 18°C.

Figure A2.6 illustrates the distribution of the treatment across Italian municipalities. Notably, when compared with the distribution of $PM_{2.5}$ levels after heating system activation in Figure A2.3b, it is evident that municipalities with high $PM_{2.5}$ emissions follow the treated municipalities.

[18]It corresponds to the last week of April.

2.5.2 Baseline results

2.5.2.1 Impact of heating system activation on pollutant emissions

Figure 2.1 shows the effects of the treated municipalities, compared to the controls, on CAMS $PM_{2.5}$ levels for different lengths of exposure to treatment. The Figure presents monthly lead-lag estimates, that are aggregated $ATT(g,t)$ estimates from Equation 2.8 to show the dynamics of T versus C n months before and after reaching T^*, for $PM_{2.5}$ (obtained from CAMS) in four biennia (2015-2016, 2016-2017, 2017-2018, 2018-2019). The x-axis indicates months relative to heating activation (time 0), with 4 lead months (pre-activation) and 5 lag months (post-activation) capturing the temporal dynamics of exposure effects. The null lead coefficients confirm the absence of differential trends between treated and control municipalities before heating system activation. In contrast, the statistically significant positive lag coefficients reveal a sustained and monotonically increasing divergence in $PM_{2.5}$ concentrations, with treated municipalities exhibiting systematically higher levels of pollution relative to controls after heating activation.

The estimated ATTs in Table 2.1 demonstrate significant effects of heating system activation on particulate matter concentrations across all biennia. For average $PM_{2.5}$ levels (Panel A), the ATT estimates show particularly strong impacts in 2015-16 (3.070 $\mu g/m^3$), 2017-18 (3.423 $\mu g/m^3$), and 2018-19 (3.416 $\mu g/m^3$), representing increases of 18.7%, 26.6%, and 25.5% relative to respective period means.

Figure 2.1: $PM_{2.5}$ CAMS main estimates for 2015-16, 2016-17, 2017-18, 2018-19.

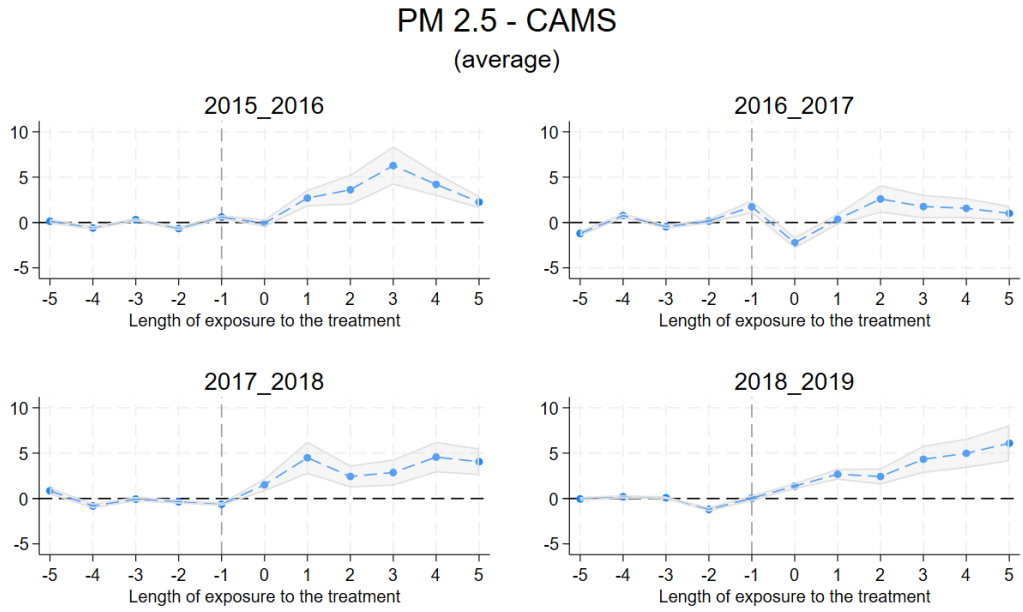

Table 2.1: Impact of Heating system activation on $PM_{2.5}$ CAMS (2015-2019)

	2015-2016	2016-2017	2017-2018	2018-2019
	(1)	(2)	(3)	(4)
A. Average Effects				
ATT	3.070***	0.831*	3.423***	3.416***
	(0.528)	(0.445)	(0.696)	(0.538)
Parallel-trends test				
χ^2	1023	508.3	395.8	430.6
p-value	0	0	0	0
df	18	18	18	19
Mean of Y	16.45	15.64	12.86	13.39
SD of Y	7.181	6.522	6.313	7.598
Observations	5,684	5,679	5,690	5,672
B. Above 75th Percentile				
ATT	0.610***	0.102	0.711***	0.759***
	(0.120)	(0.0979)	(0.147)	(0.131)
Parallel-trends test				
χ^2	207.2	169.9	232.2	237.7
p-value	0	0	0	0
df	18	18	18	19
Mean of Y	1.578	1.396	0.848	0.898
SD of Y	1.731	1.567	1.409	1.592
Observations	5,684	5,679	5,690	5,672

Notes: Table presents difference-in-differences estimates of the average treatment effect on the treated (ATT) of heating system activation on $PM_{2.5}$ CAMS levels. Panel A shows effects on average $PM_{2.5}$ CAMS levels, while Panel B focuses on the upper quartile of the outcome distribution. Standard errors at municipal level are in parentheses; *** p<0.01, ** p<0.05, * p<0.1.

The 2016-17 coefficient (0.831 μg/m^3) suggests a weaker but still detectable effect (5.3% increase), potentially reflecting milder winter conditions as visible in Figure A2.4c and A2.4d, where the 2016/2017 period exhibits a unique pattern: a sharp, singular drop in temperature occurs precisely when Google Trends searches spike. Notably, during the following weeks, temperatures remain consistently elevated and Google searches are lower compared to other years. The absolute ATT effects (3.07-3.42μg/m^3) are substantial, exceeding half of the WHO annual mean guideline (5 μg/m^3) in all cases. For extreme pollution events (Panel B: $>75^{th}$ percentile), the ATT coefficients remain statistically significant in three of four years (2015-16: 0.610; 2017-18: 0.711; 2018-19: 0.759), representing substantial relative increases of 38.7%, 83.8%, and 84.5% respectively. The significant effects in the mentioned biennia for both average and extreme $PM_{2.5}$ suggest robust heating system impacts. Moreover, all χ^2 testing the common trend hypothesis strongly reject the null of parallel pre-trends, not supporting the DiD design's validity; however, we will properly test this assumption in Section 2.5.3 employing the diagnostic

analysis proposed by Rambachan & Roth (2023).

Figure 2.2 displays monthly lead-lag estimates from Equation 2.8 for EEA NO_2 across the four biennia (2015-2019). The estimates, also in this case, confirm parallel pre-trends (null leads) and reveal treatment effects that grow monotonically post-activation (significant positive lags), consistent with the heating activation hypothesis.

The analysis reveals that heating system activation leads to statistically significant increases in NO_2 concentrations across all observed winter periods (2015-2019), as shown in Table 2.2. The estimated average treatment effects (ATT) range from 2.63 to 4.90 $\mu g/m^3$, representing 10.9% to 19.5% increases relative to seasonal means. These findings demonstrate that combustion-based heating substantially contributes to NO_2 pollution. The effects are particularly pronounced during extreme pollution episodes ($>75^{th}$ percentile), where NO_2 levels rise by 0.54-0.77 $\mu g/m^3$ (88.2-113.6% above period means).

Figure 2.2: NO_2 EEA main estimates for 2015-16, 2016-17, 2017-18, 2018-19.

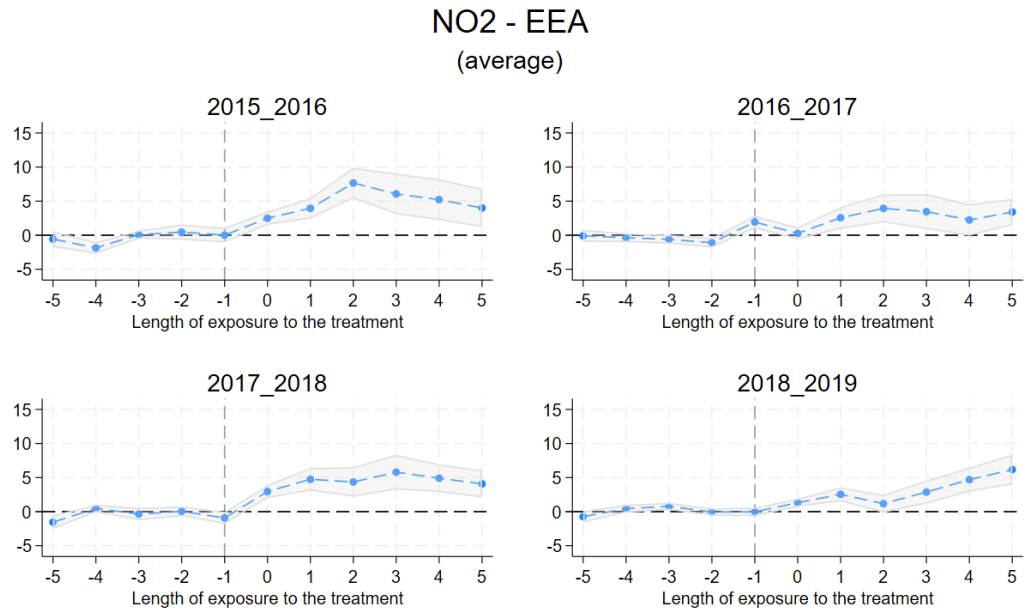

Table 2.2: Impact of Heating system activation on NO_2 EEA (2015-2019)

	2015-2016	2016-2017	2017-2018	2018-2019
	(1)	(2)	(3)	(4)
A. Average Effects				
ATT	4.896***	2.628***	4.457***	3.091***
	(1)	(0.804)	(0.873)	(0.619)
Parallel-trends test				
χ^2	726.5	95.88	79.34	103.3
p-value	0	0	1.12e-09	0
df	18	21	18	19
Mean of Y	25.13	24.09	23.05	21.49
SD of Y	15.57	15.18	14.62	13.83
Observations	4,456	4,903	5,207	5,276
B. Above 75th Percentile				
ATT	0.769***	0.543***	0.600***	0.556***
	(0.124)	(0.116)	(0.113)	(0.0806)
Parallel-trends test				
χ^2	290	52.78	33.60	33.41
p-value	0	2.83e-05	0.0141	0.0216
df	18	18	18	19
Mean of Y	0.677	0.616	0.562	0.436
SD of Y	1.476	1.394	1.263	1.118
Observations	4,473	4,978	5,237	5,327

Notes: Table presents difference-in-differences estimates of the average treatment effect on the treated (ATT) of heating system activation on NO_2 EEA levels. Panel A shows effects on average NO_2 EEA levels, while Panel B focuses on the upper quartile of the outcome distribution. Standard errors at municipal level are in parentheses; *** p<0.01, ** p<0.05, * p<0.1.

2.5.2.2 Impact of heating system activation on health outcomes

Figures 2.3a and 2.3b illustrate monthly lead-lag estimates (pre and post activation of the heating systems, respectively) of the dynamic $ATT(g,t)$ aggregation from Equation 2.8 for AMI hospitalisations and in-hospital mortality rates throughout the four winter periods (2015-2019). All the leads are clearly not statistically different from zero, showing the absence of differential trends between treated and controls before the activation of the heating systems. For hospitalisations, a clear upward trend emerges in the post-activation period for those treated with respect to controls, for all biennia, where admission rates rise sharply. This suggests a nearly simultaneous and pronounced health impact associated with the activation of heating systems. In contrast, the mortality graphs show no consistent pattern in lags, with fluctuations centred around zero, indicating weaker (2015-2016) or null effects of heating activation on in-hospital AMI deaths.

The regression results in Table 2.3 corroborate the graphical evidence. Heating system activation significantly increases AMI hospitalisation rates in three of four winters. For

2015-2016, the ATT of 1.215 per 10,000 inhabitants corresponds to a 7.6% increase relative to the mean admission rate (16.06). The most pronounced effects occur in 2017-2018 and 2018-2019, where ATTs of 2.844 and 2.675 represent 17.8% and 16.9% increases over their respective means (15.96 and 15.86). These findings align with epidemiological studies linking short-term exposure to $PM_{2.5}$ and NO_2 with acute cardiovascular events (Brook et al. (2010*b*)). For in-hospital mortality, only the 2015-2016 period exhibits a significant ATT (0.385, an 35.1% increase wrt to its 1.097 mean value), while other years show null effects, suggesting that healthcare interventions may mitigate mortality risks despite rising admissions.

Figure 2.3: ATT on AMI hospitalisations and in hospital mortality across (2015-2019)

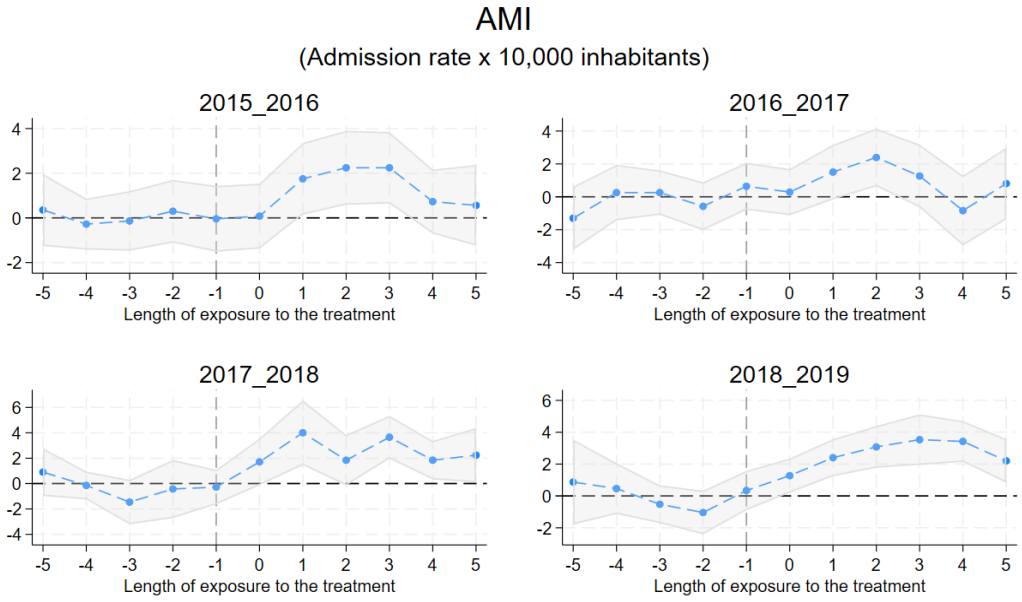

(a) ATT on AMI hospitalisations across (2015-19)

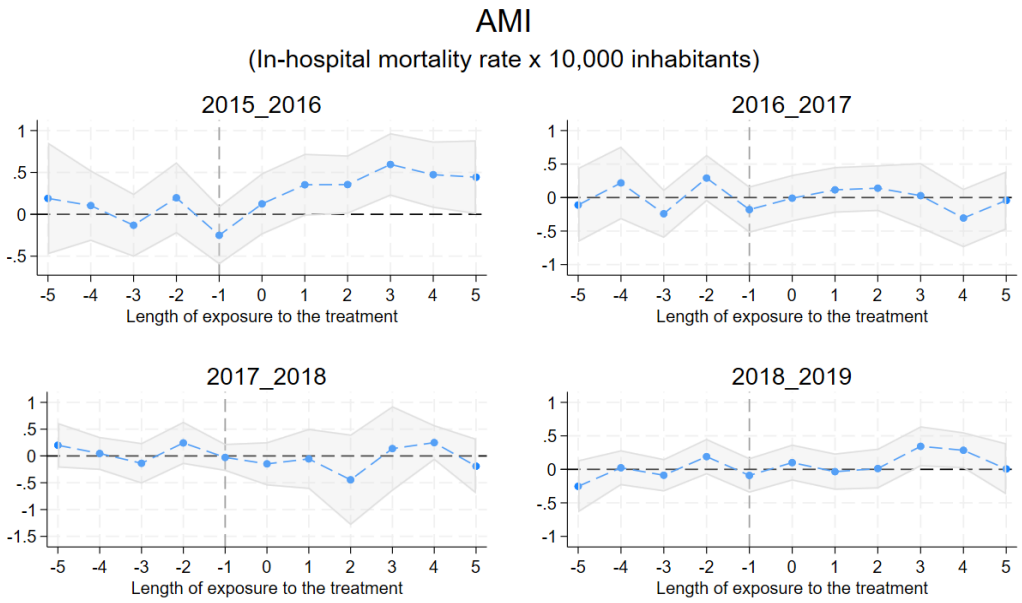

(b) ATT on AMI in-hospital mortality across (2015-19)

Table 2.3: Average Treatment Effects on the Treated on AMI Outcomes (2015-2019)

	2015-2016	2016-2017	2017-2018	2018-2019
	(1)	(2)	(3)	(4)
A. Admission Rate (per 10,000 inhabitants)				
ATT	1.215*	0.865	2.844***	2.675***
	(0.648)	(0.755)	(0.768)	(0.489)
Parallel-trends test				
χ^2	31.17	23.56	48.54	26.16
p-value	0.028	0.170	0.001	0.126
df	18	18	18	19
Mean outcome	16.06	16.14	15.96	15.86
SD outcome	21.20	21.34	20.84	20.86
Observations	5,684	5,679	5,690	5,672
B. In-Hospital Mortality Rate (per 10,000 inhabitants)				
ATT	0.385***	-0.022	-0.048	0.113
	(0.147)	(0.149)	(0.249)	(0.110)
Parallel-trends test				
χ^2	17.98	35.28	15.68	21.91
p-value	0.457	0.009	0.615	0.289
df	18	18	18	19
Mean outcome	1.097	1.101	1.098	0.985
SD outcome	2.035	2.052	2.035	1.871
Observations	5,684	5,679	5,690	5,672

Notes: Table presents difference-in-differences estimates of average treatment effects on the treated (ATT) on AMI outcomes. Panel A shows effects on hospital admission rates, while Panel B examines in-hospital mortality rates. Standard errors at municipal level are in parentheses; *** p<0.01, ** p<0.05, * p<0.1.

The analysis of STEMI outcomes (Figure 2.4) illustrates that all leads are not statistically significant, confirming parallel pre-treatment trends. The results for lags, instead, show distinct temporal patterns for admissions and mortality. For hospital admissions (Figure 2.4a), significant increases are observed during the 2017-2019 period for treated, after the activation of the eating system. Conversely, in-hospital mortality (Figure 2.4b) shows a significant elevation only in 2015-2016 that persists throughout all the 5 monthly lags, with no statistically significant effects in subsequent years.

Figure 2.4: ATT on STEMI hospitalisations and in hospital mortality across (2015-2019)

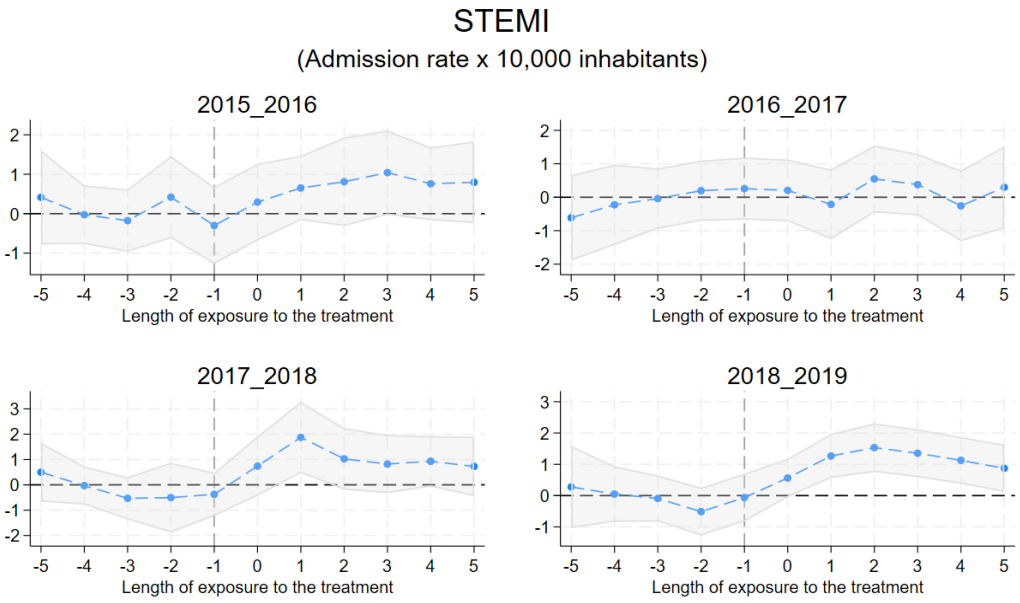

(a) ATT on STEMI hospitalisations across (2015-19)

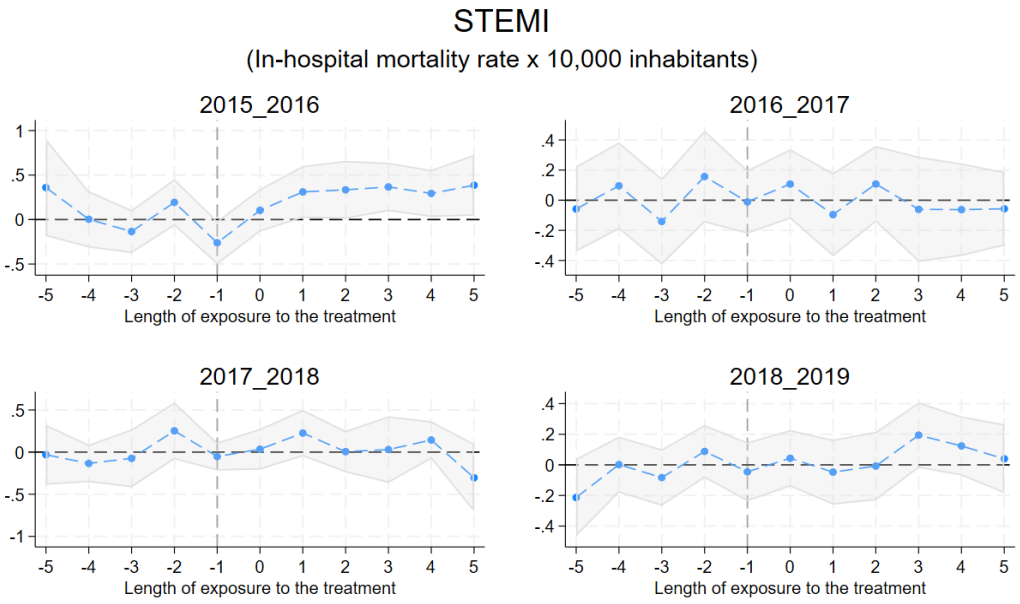

(b) ATT on STEMI in hospital mortality across (2015-19)

The estimates in Table 2.4 reveal statistically significant increases in STEMI admission rates attributable to heating system activation during the 2017-2018 (ATT = 1.051) and 2018-2019 (ATT = 1.180) winter periods. These effects correspond to substantial relative increases of 16.6% and 19.1% above their respective mean admission rates of 6.352 and 6.184 per 10,000 inhabitants. For in-hospital mortality, a significant effect emerges only in 2015-2016 (ATT = 0.287), representing a 51.0% increase from the baseline mortality rate of 0.563 per 10,000 inhabitants. These findings demonstrate that heating system activation contributes meaningfully to STEMI morbidity, with particularly robust effects on admission rates in recent years, while mortality effects appear to be more sporadic.

Table 2.4: Average Treatment Effects on the Treated on STEMI Outcomes (2015-2019)

	2015-2016	2016-2017	2017-2018	2018-2019
	(1)	(2)	(3)	(4)
A. Admission Rate (per 10,000 inhabitants)				
ATT	0.591	0.100	1.051***	1.180***
	(0.441)	(0.402)	(0.359)	(0.290)
Parallel-trends test				
χ^2	8.778	24.66	31.89	26.23
p-value	0.965	0.135	0.0226	0.124
df	18	18	18	19
Mean of Y	6.749	6.575	6.352	6.184
SD of Y	10.14	9.993	9.399	9.260
Observations	5,684	5,679	5,690	5,672
B. In-Hospital Mortality Rate (per 10,000 inhabitants)				
ATT	0.287**	-0.0130	0.0448	0.0492
	(0.116)	(0.106)	(0.106)	(0.0810)
Parallel-trends test				
χ^2	19.62	11.08	14.90	12.20
p-value	0.355	0.891	0.669	0.877
df	18	18	18	19
Mean of Y	0.563	0.565	0.550	0.513
SD of Y	1.277	1.281	1.248	1.194
Observations	5,684	5,679	5,690	5,672

Notes: Table presents difference-in-differences estimates of average treatment effects on the treated (ATT) on STEMI outcomes. Panel A shows effects on hospital admission rates, while Panel B examines in-hospital mortality rates. Standard errors at municipal level are in parentheses; *** p<0.01, ** p<0.05, * p<0.1.

For NSTEMI outcomes, lags in Figure 2.5 indicates significant increases in admission rates during 2017-2018 and 2018-2019 after heating activation, while in-hospital mortality rates show a significant rise only in 2018-2019. Null leads support parallel pre-trends.

Figure 2.5: ATT on NSTEMI hospitalisations and in hospital mortality across (2015-2019)

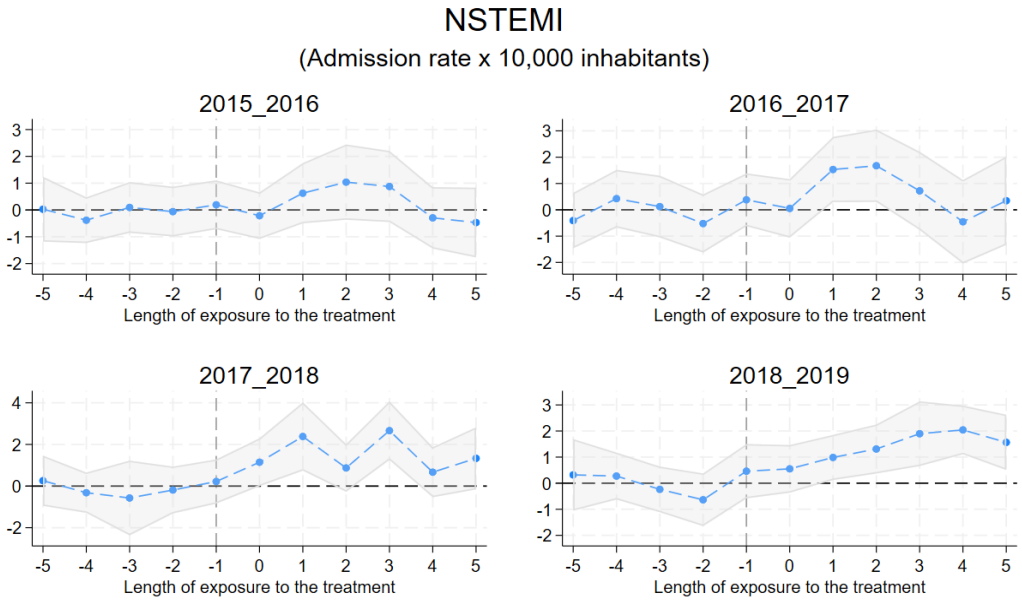

(a) ATT on NSTEMI hospitalisations across (2015-19)

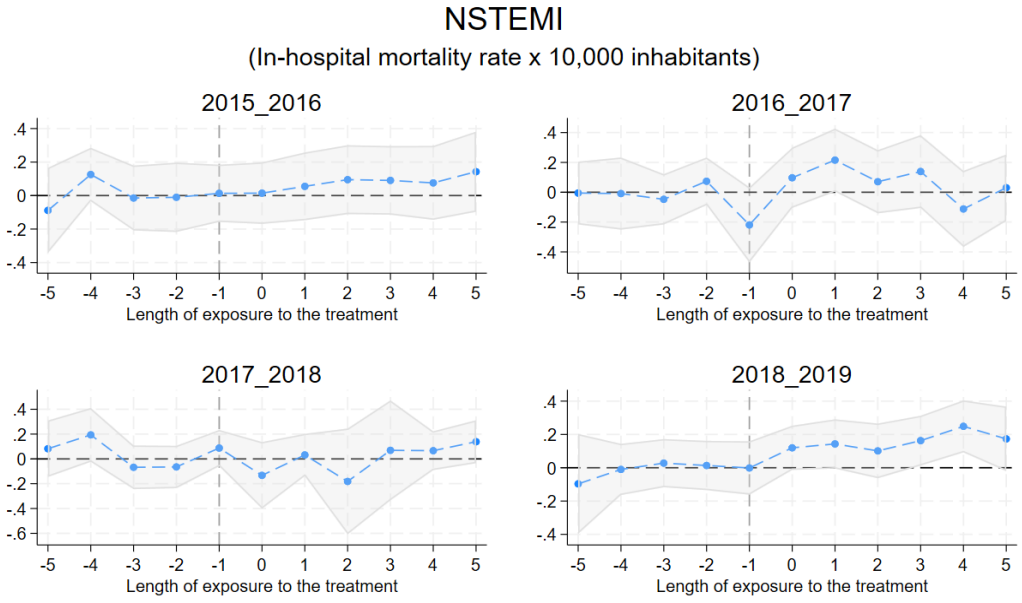

(b) ATT on NSTEMI in-hospital mortality across (2015-19)

This is confirmed by the results in Table2.5 where the estimates demonstrate significant increases in NSTEMI admission rates during 2017-2018 (ATT=1.746) and 2018-2019 (ATT=1.355), corresponding to 19.6% and 15.2% elevations relative to their respective means (8.898 and 8.913 per 10,000 inhabitants). For in-hospital mortality, only the 2018-2019 period shows statistical significance (ATT=0.161), representing a 49.5% increase

Table 2.5: Average Treatment Effects on the Treated on NSTEMI Outcomes (2015-2019)

	2015-2016	2016-2017	2017-2018	2018-2019
	(1)	(2)	(3)	(4)
A. Admission Rate (per 10,000 inhabitants)				
ATT	0.326	0.665	1.746***	1.355***
	(0.457)	(0.582)	(0.560)	(0.385)
Parallel-trends test				
χ^2	23.03	19.71	26.46	24.24
p-value	0.190	0.350	0.0898	0.187
df	18	18	18	19
Mean of Y	8.537	8.860	8.898	8.913
SD of Y	12.21	12.43	12.05	12.19
Observations	5,684	5,679	5,690	5,672
B. In-Hospital Mortality Rate (per 10,000 inhabitants)				
ATT	0.0835	0.0613	0.0105	0.161***
	(0.0909)	(0.0739)	(0.0889)	(0.0577)
Parallel-trends test				
χ^2	16.48	22.97	20.26	20.66
p-value	0.559	0.192	0.318	0.356
df	18	18	18	19
Mean of Y	0.334	0.370	0.373	0.325
SD of Y	0.918	1.048	1.003	0.897
Observations	5,684	5,679	5,690	5,672

Notes: Table presents difference-in-differences estimates of average treatment effects on the treated (ATT) on NSTEMI outcomes. Panel A shows effects on hospital admission rates, while Panel B examines in-hospital mortality rates. Standard errors at municipal level are in parentheses; *** p<0.01, ** p<0.05, * p<0.1.

from the mean mortality rate (0.325 per 10,000).

The analysis reveals divergent patterns between stroke subtypes. If we have a look at Figure 2.6 and Figure 2.7, all leads are statistically not significant, confirming parallel pre-treatment trends. At first glance, all the lags also exhibit no significant effect in the 5 months after heating activation.

For ischemic stroke, we identify no statistically significant effects of heating system activation on either admission or mortality rates across all study periods, as reported in Table 2.6. In contrast, hemorrhagic stroke outcomes show selective significant effects, see Table 2.7: admission rates increased by 26.2% (ATT=1.310) in 2016-2017 relative to the mean rate of 5.004 per 10,000 inhabitants, while mortality rates rose significantly in 2015-2016 (ATT=0.446, +37.0% vs mean 1.207/10,000) and 2017-2018 (ATT=0.528, +41.7% vs mean 1.265/10,000). These results suggest that heating-related pollution may disproportionately affect hemorrhagic stroke outcomes compared to ischemic events, particularly for acute mortality.

Figure 2.6: ATT on Ischemic Stroke hospitalisations (LHS) and in hospital mortality (RHS) across (2015-2019)

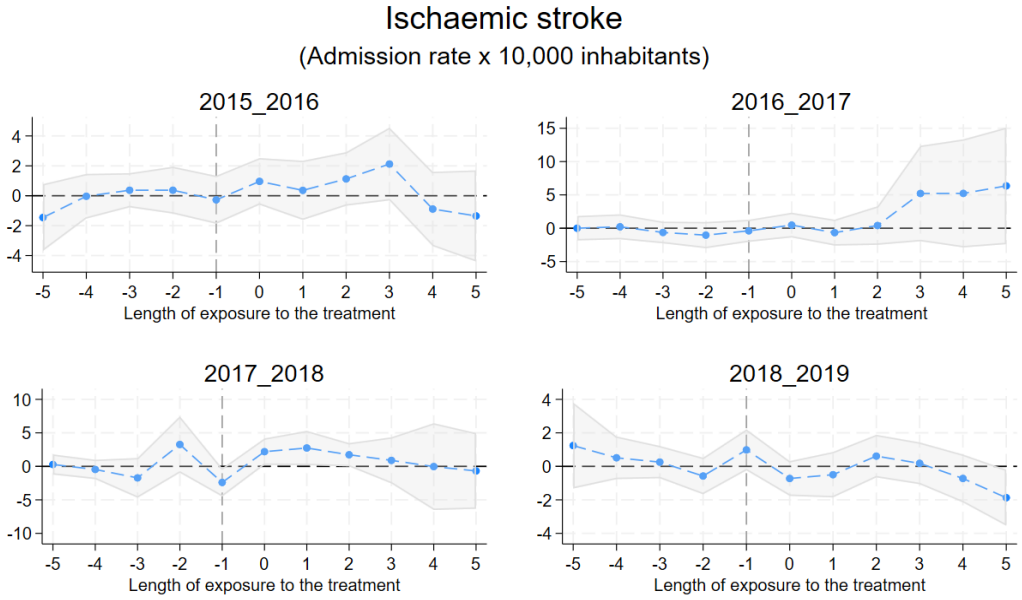

(a) ATT on Ischemic Stroke hospitalisations across (2015-19)

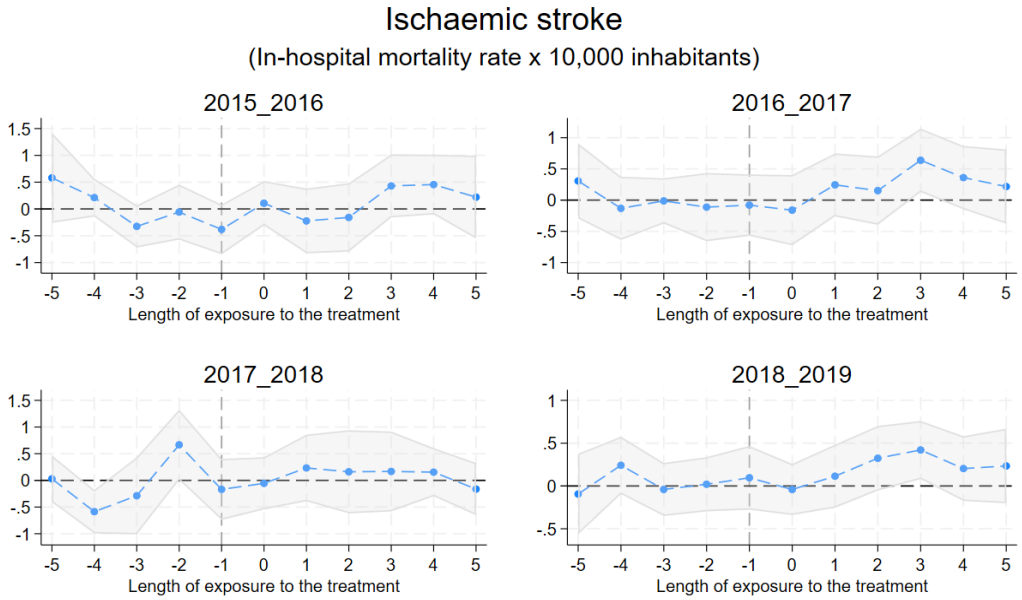

(b) ATT on Ischemic Stroke in hospital mortality across (2015-19)

Figure 2.7: ATT on Hemorrhagic Stroke hospitalisations (LHS) and in hospital mortality (RHS) across (2015-2019)

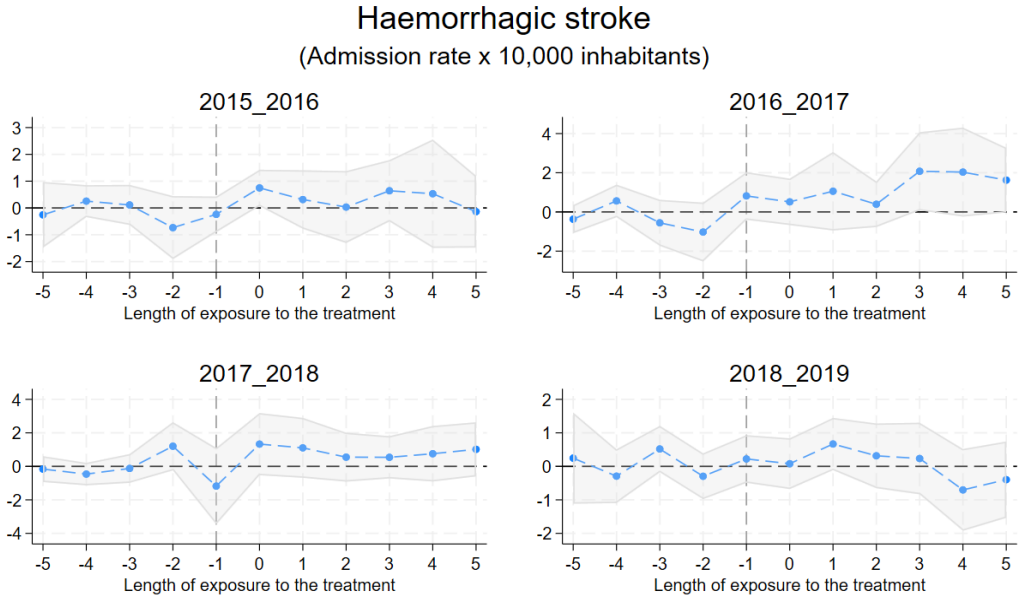

(a) ATT on Hemorrhagic Stroke hospitalisations across (2015-19)

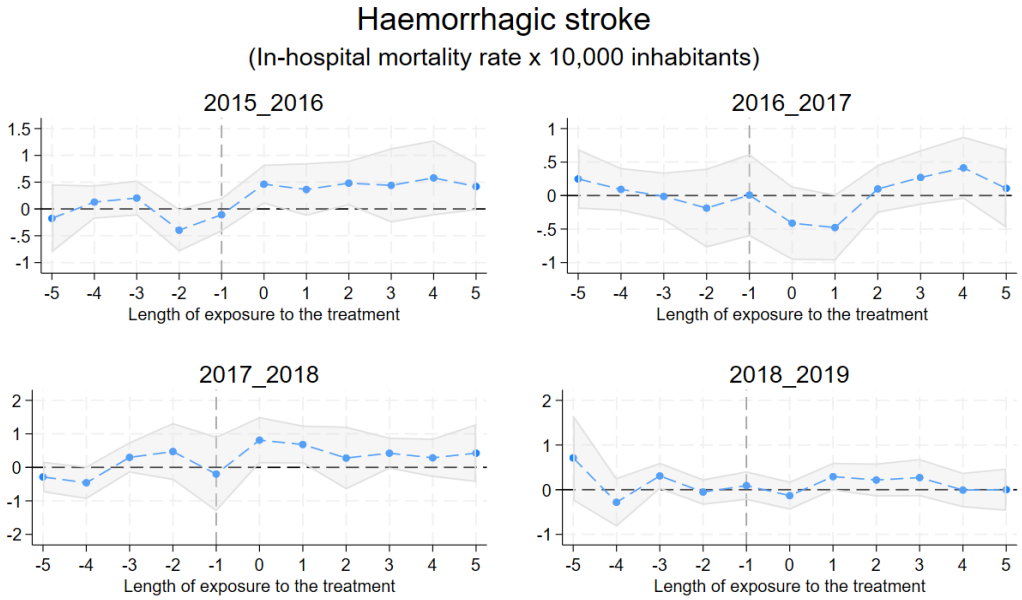

(b) ATT on Hemorrhagic Stroke in hospital mortality across (2015-19)

Table 2.6: Average Treatment Effects on the Treated on Ischemic Stroke Outcomes (2015-2019)

	2015-2016	2016-2017	2017-2018	2018-2019
	(1)	(2)	(3)	(4)
A. Admission Rate (per 10,000 inhabitants)				
ATT	0.532	2.850	0.961	-0.661
	(0.857)	(2.101)	(1.475)	(0.521)
Parallel-trends test				
χ^2	11.05	434.4	19.58	20.81
p-value	0.892	0	0.357	0.348
df	18	18	18	19
Mean of Y	15.72	15.35	14.96	14.20
SD of Y	21.02	20.72	19.65	18.62
Observations	5,684	5,679	5,690	5,672
B. In-Hospital Mortality Rate (per 10,000 inhabitants)				
ATT	0.164	0.234	0.0515	0.182
	(0.262)	(0.201)	(0.233)	(0.144)
Parallel-trends test				
χ^2	21.80	15.09	37.04	28.11
p-value	0.241	0.656	0.00518	0.0813
df	18	18	18	19
Mean of Y	1.553	1.501	1.504	1.324
SD of Y	2.782	2.723	2.711	2.386
Observations	5,684	5,679	5,690	5,672

Notes: Table presents difference-in-differences estimates of average treatment effects on the treated (ATT) on Ischemic Stroke outcomes. Panel A shows effects on hospital admission rates, while Panel B examines in-hospital mortality rates. Standard errors at municipal level are in parentheses; *** p<0.01, ** p<0.05, * p<0.1.

Table 2.7: Average Treatment Effects on the Treated on Hemorrhagic Stroke Outcomes (2015-2019)

	2015-2016	2016-2017	2017-2018	2018-2019
	(1)	(2)	(3)	(4)
A. Admission Rate (per 10,000 inhabitants)				
ATT	0.511	1.310*	0.991	0.0552
	(0.555)	(0.783)	(0.646)	(0.427)
Parallel-trends test				
χ^2	20.92	22.37	23.54	17.24
p-value	0.283	0.216	0.171	0.574
df	18	18	18	19
Mean of Y	4.921	5.004	5.158	5.031
SD of Y	7.683	7.859	7.948	7.884
Observations	5,684	5,679	5,690	5,672
B. In-Hospital Mortality Rate (per 10,000 inhabitants)				
ATT	0.446***	-0.0100	0.528*	0.124
	(0.173)	(0.164)	(0.280)	(0.128)
Parallel-trends test				
χ^2	16.92	16.50	22.07	22.98
p-value	0.528	0.558	0.229	0.238
df	18	18	18	19
Mean of Y	1.207	1.232	1.265	1.233
SD of Y	2.318	2.352	2.418	2.454
Observations	5,684	5,679	5,690	5,672

Notes: Table presents difference-in-differences estimates of average treatment effects on the treated (ATT) on Hemorrhagic Stroke outcomes. Panel A shows effects on hospital admission rates, while Panel B examines in-hospital mortality rates. Standard errors at municipal level are in parentheses; *** p<0.01, ** p<0.05, * p<0.1.

Lastly, Figure 2.8 for COPD reveals no evidence of pre-existing differential trends across its leads and a consistent upward trend in hospitalizations lags for treated municipalities with respect to controls, while showing no discernible pattern for in-hospital mortality. Table 2.8 demonstrates statistically significant increases in admission rates throughout the study period: 2015-2016 (ATT=2.136, +23.8% versus mean 8.972 per 10,000 inhabitants), 2016-2017 (ATT=1.279, +14.5% versus 8.802), 2017-2018 (ATT=2.284, +27.4% versus 8.323), and 2018-2019 (ATT=1.828, +22.5% versus 8.137). In contrast, in-hospital mortality shows no significant effects in any year. These results indicate that while heating system activation substantially exacerbates COPD morbidity (with relative increases of 14.5-27.4% above baseline admission rates), it does not appear to significantly impact short-term mortality outcomes. The consistent hospitalization effects across years, despite varying pollution mixes and meteorological conditions, underscore the particular vulnerability of COPD patients to heating-related air pollution.

Figure 2.8: ATT on COPD hospitalisations and in hospital mortality across (2015-2019)

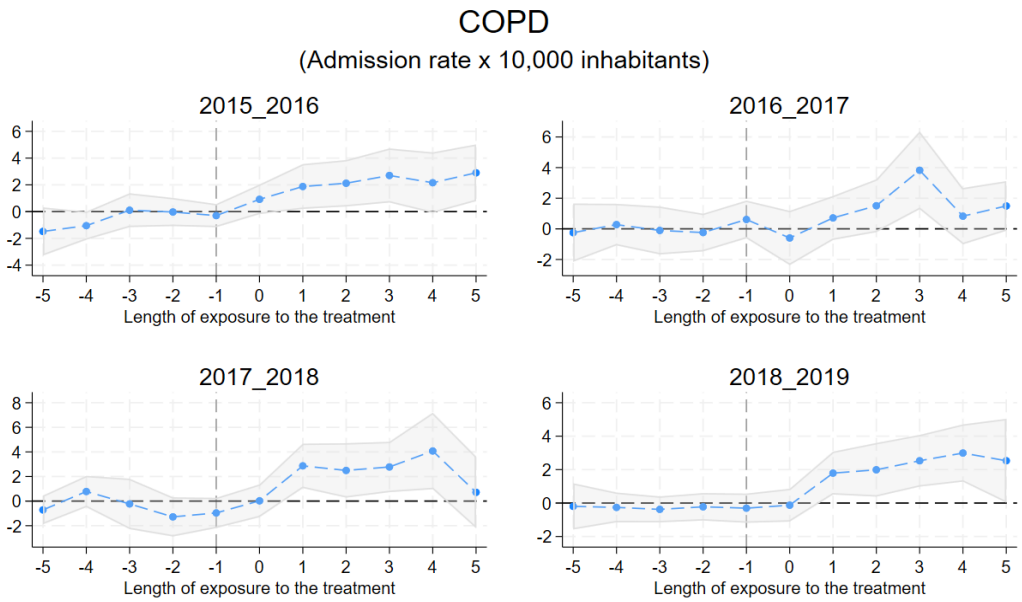

(a) ATT on COPD hospitalisations across (2015-19)

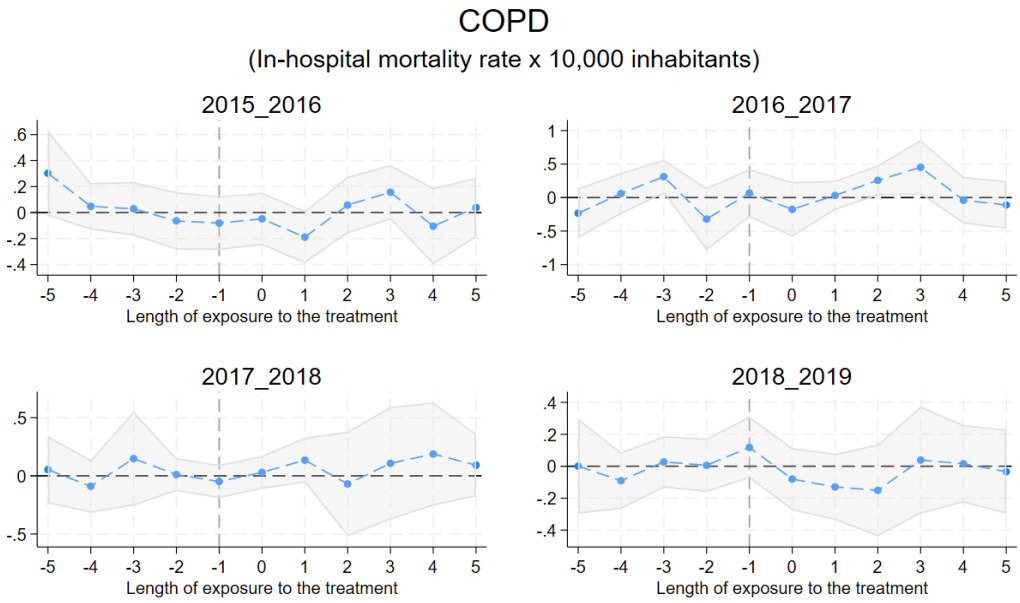

(b) ATT on COPD in-hospital mortality across (2015-19)

Table 2.8: Average Treatment Effects on the Treated on COPD Outcomes (2015-2019)

	2015-2016	2016-2017	2017-2018	2018-2019
	(1)	(2)	(3)	(4)
A. Admission Rate (per 10,000 inhabitants)				
ATT	2.136**	1.279*	2.284**	1.828***
	(0.916)	(0.668)	(1.016)	(0.664)
Parallel-trends test				
χ^2	53.12	80.72	34.28	18.02
p-value	2.51e-05	6.41e-10	0.0116	0.521
df	18	18	18	19
Mean of Y	8.972	8.802	8.323	8.137
SD of Y	13.07	13.34	12.12	11.47
Observations	5,684	5,679	5,690	5,672
B. In-Hospital Mortality Rate (per 10,000 inhabitants)				
ATT	-0.00365	0.0559	0.0459	-0.0565
	(0.0822)	(0.113)	(0.137)	(0.0923)
Parallel-trends test				
χ^2	25.46	29.89	20.64	16.89
p-value	0.113	0.0385	0.298	0.597
df	18	18	18	19
Mean of Y	0.427	0.454	0.439	0.387
SD of Y	1.094	1.293	1.220	1.075
Observations	5,684	5,679	5,690	5,672

Notes: Table presents difference-in-differences estimates of average treatment effects on the treated (ATT) on COPD outcomes. Panel A shows effects on hospital admission rates, while Panel B examines in-hospital mortality rates. Standard errors at municipal level are in parentheses; *** p<0.01, ** p<0.05, * p<0.1.

2.5.3 Robustness

To ensure the reliability of our findings, we conduct several robustness checks. First, we assess the impact of heating systems activation on other pollutants, namely $PM_{2.5}$ (EEA), PM_{10}, SO_2, CO and O_3. Second, we vary the definition of treated and control municipalities by considering alternative thresholds: (i) above the 66^{th} vs. below the 33^{rd} percentile and (ii) above the 75^{th} vs. below the 25^{th} percentile in municipal biomass consumption. This tests whether our results are sensitive to the classification of exposure intensity. Third, we apply the robust inference and sensitivity analysis framework developed by Rambachan & Roth (2023) to assess the validity of the parallel trends assumption and quantify potential bias from violations. Fourth, we conduct a falsification test on health outcomes unrelated to pollution. Furthermore, we extend our main analysis by (i) weighting estimates by municipal population to account for heterogeneous exposure across densely vs. sparsely populated areas, (ii) controlling for spillover effects from neighboring municipalities (within 30 km) to ensure pollution impacts are not confounded by cross-boundary diffusion, and (iii) implementing the augmented inverse probability weighting (AIPW) version of the Callaway & Sant'Anna (2021) estimator for improved efficiency and double robustness. Finally, we test for selective migration by examining whether individuals systematically move away from (or avoid moving into) high-pollution municipalities, which could bias our health effect estimates. These checks collectively strengthen the credibility of our causal inferences.

2.5.3.1 Impact of heating system activation on other pollutant emissions

Figure A2.7 displays the dynamic aggregation of ATTs estimated from Equation 2.8 for EEA $PM_{2.5}$ across four biennia (2015-2019). The results confirm our identification strategy: null pre-treatment trends and monotonically rising $PM_{2.5}$ divergence post-activation align with prior evidence. However, the effect magnitudes exceed CAMS estimates. The discrepancy is attributable to non-random station placement, as EEA monitors are strategically located in high-pollution urban areas. The point estimates in Table A2.5 demonstrate ATTs consistent with those reported in the previous Table 2.1, though larger in magnitude confirming the results in Figure A2.7.

Figure A2.8 displays dynamic aggregation of ATTs estimated from Equation 2.8 for EEA PM_{10} across the four biennia (2015-2019). Null lead coefficients confirm parallel pre-treatment trends, while significant positive lags indicate monotonically increasing PM_{10}

divergence post-activation, with treated municipalities exhibiting systematically higher pollution than controls, as before. The ATTs point estimates in Table A2.6, also in this case, confirm an increase in the level of PM_{10}.

Figures A2.9, A2.10, and A2.11 extend our analysis to additional pollutants. While parallel pre-trends hold for SO_2, CO, and O_3, the post-activation effects differ markedly: most lag coefficients are statistically insignificant or weak (notably SO_2 in 2018-19 and CO in 2015-16 and 2017-18). The exception is O_3, which shows a statistically significant negative response following heating system activation.

The analysis further examines the impacts of heating system activation on the additional pollutants (SO_2 Table A2.7, CO Table A2.8, and O_3 Table A2.9), which exhibit distinct patterns compared to the primary combustion-related pollutants ($PM_{2.5}$, PM_{10}, and NO_2). Although SO_2 shows modest but significant increases (0.45-0.63 μg/m^3; 15.9-22.76% increase relative to the respective average value) in most years, consistent with fossil fuel combustion, effects on CO are more sporadic, with significant spikes only in certain periods, likely reflecting incomplete combustion episodes. Most importantly, we observe these variations in mean pollutant concentrations rather than extreme (peak) exposure levels where we register an increas of 71% for SO_2 in 2018-19 and another for CO by 77.5% in 2017-2018. Notably, O_3 concentrations decline sharply (-6.4 to -11.1 μg/m^3; 11.65-18.82% decrease relative to its respective average value)[19]. These findings suggest that while PM and NO_2 remain the dominant health threats from heating systems, ancillary pollutants like SO_2 and CO may contribute to acute exposures, particularly in areas reliant on sulfur-rich fuels or inefficient combustion (Zhang & Smith (2007), WHO (2014)).

2.5.3.2 Alternative treatment thresholds

Table A2.10 demonstrates robust evidence that residential heating activation significantly increases air pollution concentrations ($PM_{2.5}$, PM_{10}, NO_2) and regulatory exceedance days across multiple treatment thresholds (66^{th} vs. 33^{rd} and 75^{th} vs. 25^{th} percentiles). Effects are consistently positive and statistically significant, with larger magnitudes under stricter thresholds, supporting a dose-response relationship. These findings confirm that

[19]During winter, the process of ozone (O_3) formation slows significantly due to reduced sunlight and colder temperatures. This leads to lower rates of photochemical reactions that produce ozone. Additionally, ozone removal through NO titration becomes more prominent, as freshly emitted NO reacts with ozone to produce NO_2. This results in net ozone loss in polluted plumes, which can persist for long distances downwind. Consequently, ozone concentrations during winter are often lower compared to other seasons. Sillman (1999)

heating systems disproportionately harm highly exposed areas.

The results are robust to alternative threshold definitions for residential heating activation, with consistent findings also observed for the estimated health effects, as shown in TableA2.11. For AMI, STEMI, and COPD hospitalisations, the treatment effects not only maintain statistical significance across all threshold specifications but also exhibit a dose-response pattern, with point estimates generally increasing in magnitude under stricter exposure cutoffs. This monotonic relationship is particularly evident for AMI hospitalisations (rising from 1.22 at median to 2.76 at 75-25) and COPD admissions (increasing from 2.14 to 4.03). Similarly for in-hospital mortality effects, results are confirmed. The few exceptions (notably ischemic and hemorrhagic strokes' null effects at median but significant estimates at higher thresholds) suggest a critical exposure-intensity threshold for cerebrovascular impacts. The consistent treatment effects across threshold specifications demonstrate robustness to exposure classification methods, with particularly pronounced health impacts observed in the most highly exposed areas.

2.5.3.3 Diagnostics for parallel trends violations

We evaluate potential violations of the parallel trends assumption using the "honest" approach developed by Rambachan & Roth (2023). This method quantifies how much the post-treatment trend can deviate from the pre-treatment pattern before our results become invalid. Specifically, we consider the break point parameter M (ranging from 0.25 to 2), where M=2 represents a 200% deviation from the pre-treatment trend that would nullify our findings.

The results in Table A2.12 demonstrate remarkable resilience: $PM_{2.5}$ and PM_{10} effects remain statistically significant up to M=1.25 at Lag 4 (4 months after heating activation), while NO_2 effects persist up to M=1. Notably, considering the number of days with pollution levels above the 75^{th} percentile, the estimates are consistent with similar deviations without falling below. These effects would only be invalidated by implausibly large violations (M>1.75), providing strong evidence that residential heating activation causally increases pollution levels. The results of Table A2.13 demonstrate varying resilience to parallel trends violations across health outcomes when measured by the M parameter (range: 0.25-2). COPD effects at Lag 5 persist up to M=1.5, indicating robust causal evidence, as this exceeds typical pre-treatment fluctuations (M<1). Acute cardiovascular outcomes remain significant up to M=1.0-1.25, still above plausible violation thresholds.

The required M values to nullify effects (M>1.5 for COPD, M>1.0-1.25 for AMI/STEMI) exceed observed pre-period deviations, supporting causal interpretation.

2.5.3.4 Placebo: effects of heating activation on unrelated-pollution health outcomes

At this stage, we assess whether heating system activation affects unrelated pollution health measures. We estimate the impact of heating activation, and its associated pollutant releases, on a set of a priori unaffected outcomes, including fractures, infections, traumatism, poisoning, elective admissions, and nervous system and mental health disorders[20]. Figure A2.12 and the DiD estimates in Table A2.14 reveal no consistent or statistically significant effects of heating system activation across the 2015-2019 period. Most average treatment effects (ATT) are negligible in magnitude and statistically insignificant, with only isolated exceptions (e.g., a marginally significant effect on traumatism hospitalizations in 2015-16 and 2018-19, and a weakly significant effect on mental health mortality in 2018-19). The absence of systematic patterns strongly suggests that heating system activation does not spuriously influence these unrelated health outcomes. This lends credibility to our identification strategy and reinforces the causal interpretation of our main findings on pollution-related health effects.

2.5.3.5 Alternative weighted estimates

The extended analyses show robust heating system effects on emissions across three critical dimensions, see Table A2.16. Population-weighted estimates show systematically larger effects than baseline results, consistent with disproportionate urban exposure, while spatial adjustments yield smaller estimates (e.g., $PM_{2.5}$ CAMS decreasing from 3.96 to 2.41 μg/m^3) due to cross-boundary pollution diffusion. The doubly robust AIPW estimates confirm our core findings, with particularly strengthened $PM_{2.5}$ effects during the 2017-18 winter period. The persistently negative ozone results serve as an effective placebo test, matching its known inverse relationship with heating emissions. These patterns remain consistent when examining threshold-exceedance days (Table A2.4), confirming our baseline estimates represent conservative lower bounds, with true causal effects likely lying between the spillover-adjusted and population-weighted values.

The health outcomes analyses in Table A2.17 show consistent treatment effects across

[20]See TableA2.15 for ICD9-CM classification of placebo outcomes.

methods, though with greater outcome-specific variation than pollution results. Population-weighting reveals stronger effects for respiratory and cardiovascular emergencies, highlighting disproportionate impacts in dense, heating-system areas. Spatial adjustments yield larger hospitalisation estimates (e.g., AMI: 3.08 vs 1.74 for 2017-18), likely reflecting cross-boundary patient mobility. AIPW estimates confirm causal effects for key outcomes (AMI, STEMI, NSTEMI, COPD), while showing nuanced mortality patterns (e.g. insignificant hemorrhagic stroke mortality). COPD effects persist across all specifications (1.42-2.53 hospitalisations), underscoring respiratory vulnerability. These results, also in this case, confirm that our baseline estimates are conservative, with true impacts likely between population-weighted and spillover-adjusted values.

2.5.3.6 Mobility

Finally, in Table A2.18, the estimated coefficients for $PM_{2.5}$, NO_2, SO_2, CO, and O_3 exposure are statistically insignificant in most specifications, with two exceptions: (i) NO_2 exposure is associated with a significant increase in emigration (coefficients ranging from 5.87-7.54). (ii) SO_2 exposure shows a weakly negative effect on emigration in specification (11) (-6.38) and the net inflow remains statistically indistinguishable from zero. This suggests that elevated SO_2 levels do not induce protective migration behaviour - individuals do not systematically relocate in response to SO_2 pollution. Critically, $PM_{2.5}$, the primary pollutant of interest in our main analysis, has no significant effect on mobility across all specifications. Similarly, income and weather controls (precipitation, wind speed) show no consistent patterns, except for precipitation's robust negative association with emigration (-5.61), likely reflecting broader seasonal migration trends. The absence of systematic evidence that pollution drives selective migration supports the exogeneity of exposure variation in our setting. While NO_2 may weakly influence emigration, its correlation is economically small (representing $<2.2\%$ of mean emigration flows) and does not meaningfully alter net population dynamics. Given the limited magnitude of this effect and the lack of systematic migration responses to most pollutants, we conclude that pollution-driven mobility is unlikely to bias our estimates substantially. We thus conclude that mobility-related confounding is unlikely to drive our main results.

2.5.4 Heterogeneity

This section examines the heterogeneity effects across key dimensions. First, we assess whether the effects of heating activation on $PM_{2.5}$, PM_{10}, and NO_2 vary between climatic zones. Second, we investigate differential effects on main health outcomes by socioeconomic and demographic characteristics, including: (1) gender, (2) age groups, (3) educational attainment, (4) comorbidity status[21] and (5) climatic zone. This stratified analysis allows us to identify vulnerable sub-populations that may bear disproportionate health burdens from seasonal heating emissions.

2.5.4.1 Climatic areas

The analysis of pollutant levels by climatic area reveals systematic differences in air quality effects during heating periods. As shown in the figures A2.13b and A2.13a, D/E zones (colder regions) exhibit consistently higher concentrations of $PM_{2.5}$ (both CAMS and EEA measurements), PM_{10}, and NO_2 compared to B/C zones across all winter periods from 2015-2019. This pattern is particularly evident for NO_2, which shows the largest absolute differences between zones. The persistent pollution gradient across years suggests that climate-related heating demands, not surprisingly, are a key driver of emissions, with colder regions experiencing substantially worse air quality during winter months. The analysis of extreme pollution events (above the 75^{th} percentile) reveals a pronounced climatic gradient in the effects of heating system activation, with significantly larger ATT estimates in colder D/E zones (figure A2.13d) compared to B/C zones (figure A2.13c) across all monitored pollutants ($PM_{2.5}$, PM_{10}, and NO_2). The D/E areas demonstrate consistently stronger impacts throughout the 2015-2019 period, particularly for $PM_{2.5}$ emissions, where the heating system's effect on extreme pollution events is nearly double that observed in milder B/C zones. These findings extend our previous observations about average pollution levels, demonstrating that the disproportionate burden on colder regions becomes even more acute during peak pollution episodes. The persistent pattern across years and pollutants suggests that climate-related heating demands not only increase baseline pollution but also dramatically amplify the frequency and intensity of extreme air quality events in northern regions.

[21] We define a co-morbidity variable that indicates if the patients present other diseases. The binary variable is equal to one if the patients present one or many of congestive heart failure, peripheral vascular disease, cerebrovascular disease, dementia, chronic pulmonary disease, connective tissue disease-rheumatic disease, peptic ulcer disease, mild liver disease, diabetes with(out) complications, paraplegia and hemiplegia, renal disease, cancer, moderate or severe liver disease, metastatic carcinoma, AIDS/HIV.

2.5.4.2 Socioeconomic and demographic factors

The subgroup analysis reveals significant heterogeneity in the health effects of heating system activation. For AMI admissions (Figure A2.14), the impacts are strongest among the elderly (65+), low-educated individuals (nearly double the effect vs. high-educated), residents of D/E climatic zones, and those without pre-existing comorbidities. STEMI admissions (Figure A2.15) show pronounced effects in 2017-18 and 2018-19 for comorbidity-free patients and D/E area residents. For what concerns in-hospital mortality we have an effect for low-educated people (secondary education) for 2015-2016 and 2016-2017. NSTEMI admissions (Figure A2.16) increase for the elderly (65+), adults (45-64), low-educated groups, comorbidity-free patients, and D/E zone residents (2017-19). In contrast, ischemic stroke shows no effects (Figure A2.17), aligning with the main estimates. For hemorrhagic stroke (figure A2.18), admissions rise weakly among the elderly and low-educated (2015-18), while in-hospital mortality spikes for the elderly and D/E area residents in 2015-16 (the most polluted winter). COPD admissions (Figure A2.19) are elevated for the elderly (2015-16, 2017-18), comorbidity-free patients (2017-18), and D/E zone residents (2016-19), with an unexpected effect in B/C zones (2017-18). Socioeconomic disparities, hence persist, with adults, the elderly, low-educated groups, free comorbidity people and those living in D/E area.

2.6 Conclusions

This paper examines the causal effects of residential heating activation on air pollution and health outcomes using a novel identification strategy employing a staggered difference-in-differences estimator (Callaway & Sant'Anna (2021)). Treatment is defined by municipal biomass consumption and heating appliance prevalence, with the post-period triggered by the first weekly temperature drop below a certain threshold.

This study makes four key contributions. First, we provide new evidence on the effect of heating-generated $PM_{2.5}$ and NO_2 on cardiovascular and respiratory diseases, distinguishing between hospitalizations and in-hospital deaths. Second, we extend previous analyses, considering also cardiovascular hospitalisations and mortality, beyond respiratory conditions. Third, we define vulnerable individuals using the CCI and present evidence of the adverse effects of pollution on those without comorbidities, regardless of age, a perspective often overlooked in previous studies. Fourth, we employ a novel identification strategy by

classifying municipalities based on their proportion of biomass-fueled heating systems and utilizing a temperature-driven approach to identify heating activation, thereby accounting for potential deviations from legal activation dates.

Our main analysis reveals that residential heating activation significantly increases air pollution concentrations for many pollutants considered in the analysis. In particular, $PM_{2.5}$ and NO_2 increase in treated municipalities with respect to controls in the post activation period in a range between 19-27% and 11-20%, respectively. This translates into substantial impacts on health with AMI, STEMI, NSTEMI, and COPD admission rates increasing by 8-18%, 17-19%, 15-20%, 15-27%, respectively. Looking at in-hospital mortality, we find more pronounced effects for cardiovascular conditions in specific years (e.g. +35% for AMI, STEMI, and NSTEMI in-hospital mortality rates increasing by 35%,51%, and 50%, respectively. Notably, we also find sporadic effects on hemorrhagic stroke mortality, which spikes during high-pollution winters (2015-16 and 2017-18 biennia), while we find no significant effects for ischemic stroke.

Our results remain robust to a series of checks. First, the analyses confirm the increase in $PM_{2.5}$ (EEA) and PM_{10} due to the activation of the heating systems, aligning with the results based on CAMS. For $S0_2$ and CO, effects appear only at mean levels (not high percentiles), while O_3 remains unaffected. Second, even considering different thresholds to define treatment the effects of heating activation on pollution concentrations and health outcomes remain statistically significant, showing larger effects when comparing treated municipalities with higher shares (i.e., above the 66-th and 75-th percentiles of the distribution) of biomass consumption with respect to those with lower values (i.e., below the 33-rd and 25-th percentiles of the distribution) showing a clear dose-response pattern. Third, the sensitivity analyses confirm that our findings are robust to a wide range of plausible deviations from the parallel trends assumption, with estimated effects remaining statistically significant unless subjected to implausibly large post-treatment trend violations. Fourth, Population-weighted and AIPW estimators are consistent with our main estimates. Fourth, placebo analysis shows null effects of heating system activation on unrelated health outcomes, and mobility analyses rule out substantial selection bias.

Our analysis reveals substantial heterogeneity in both pollution and health impacts across climatic zones and demographic groups. Colder regions (D/E zones) experience significantly larger increases in $PM_{2.5}$, PM_{10}, and NO_2 concentrations during heating periods-nearly double those in milder zones - with particularly pronounced effects during extreme

pollution events. We find evidence that health impacts are not only faced by vulnerable individuals, but also by healthy ones. For instance, AMI, STEMI, NSTEMI, and COPD admissions rise most sharply among both adults (45-64) and the elderly (65+), and also for free comorbidities individuals. Whereas mortality effects are particularly pronounced among elderly and individuals with low education. These findings highlight both the geographic and socioeconomic dimensions of inequality in pollution-related health burdens, suggesting that targeted interventions for high-risk populations and regions could yield enormous health benefits.

Our findings underscore the urgent need for policy interventions targeting residential heating emissions, particularly from biomass sources. The substantial increases in $PM_{2.5}$ and NO_2 concentrations and their significant health impacts highlight both environmental and health inequalities. Policymakers should consider to foster the implementation of the recent EU green deal to incentivize the replacement of obsolete heating systems with cleaner alternatives (e.g., heat pumps or green district heating). Our evidence points to considerable potential health gains from enhanced efficiency of residential heating, particularly in municipalities with high biomass reliance.

Closing Reflections

These two papers provide robust causal evidence on the adverse health effects of air pollution in Southern Europe, focusing on urban settings and Italian residential heating emissions.

Paper I, in chapter 1, demonstrates that elevated levels of fine particulate matter ($PM_{2.5}$) and other pollutants (PM_{10}, NO_2) significantly increase under-65 mortality from circulatory and respiratory diseases and infant mortality, with particularly severe effects in densely populated urban areas. The study employs an instrumental variable strategy that leverages rainfall as a source of exogenous variation, strengthening the causal link between pollution and premature mortality. In particular, the findings reveal unexpected socioeconomic disparities, with wealthier regions, despite a lower risk of poverty, experiencing stronger pollution-mortality effects, due to higher exposure and possibly more accurate health reporting.

Paper II, in chapter 2, complements these insights by examining the health consequences of residential heating activation, a major source of winter air pollution. Using a temperature-triggered staggered difference-in-differences design, the study finds that heating systems, especially those reliant on biomass, substantially increase $PM_{2.5}$, PM_{10}, and NO_2 concentrations, leading to spikes in cardiovascular and respiratory hospitalisations and in-hopital mortality. The effects are most acute for vulnerable groups, including adults, the elderly, low-education individuals, residents of colder regions, and people without comorbidities, underscoring the intersection of environmental and health inequalities.

Together, these studies highlight the urgent need for targeted policies to mitigate air pollution's health burden. Paper I emphasises the importance of reducing ambient $PM_{2.5}$ in urban areas, while Paper II calls for stricter regulation of residential heating emissions, particularly biomass combustion, and incentives for cleaner alternatives such as heat pumps. Both papers reveal critical disparities in pollution exposure and health outcomes across socioeconomic and geographic lines, suggesting that effective interventions must account for local conditions and vulnerable populations.

The consistency of results across methodologies, instrumental variables in Paper I and staggered DiD in Paper II, strengthens the causal interpretation of pollution's health effects. Future research should employ longitudinal and cost-benefit analyses to quantify the long-term health and economic impacts of pollution reduction policies, particularly in

areas with high exposure to traffic and biomass heating emissions. Policymakers should adopt integrated strategies that simultaneously target ambient and household pollution through measures like low-emission zones and clean heating technologies, prioritising high-risk populations in pollution hotspots. These efforts should align with climate goals, using interventions that offer dual benefits for public health and emission reduction, such as decarbonising residential heating systems.

Appendices

Appendix Paper I

Table A1.1: Summary statistics

Variable	Obs	Mean	Std. Dev.	Min	Max
A.Outcomes					
<65 Cardio-Respiratory $\times$ 100,000 pop	429	3.4012	1.1711	0.4521	11.8839
Infant MR $\times$ 1,000 pop	482	2.9665	1.6519	0	9.4118
B.Pollution					
$PM_{2.5}$ $\mu g/m^3$	1,156	13.3422	5.6934	0.5029	41.25
$PM10$ $\mu g/m^3$	1,155	24.5582	7.6912	3	83
NO_2 $\mu g/m^3$	1,156	27.1635	13.8964	3.7593	103.1538
SO_2 $\mu g/m^3$	1,055	4.5293	3.5125	0.0046	25
CO $\mu g/m^3$	1,154	4.3622	37.2224	0.0176	644.7
O_3 $\mu g/m^3$	1,130	52.1915	10.1870	1.1	83.9874
C.Weather conditions					
Avg wind speed m/s	1,156	6.4193	2.9046	1.6677	14.7733
Avg temperature $°C$	1,156	16.5247	2.4535	10.0019	22.6763
Precipitations mm	1,156	0.0529	0.0450	0	0.23337
D.Station characteristics and coverage					
Distance $< 12.5km$	1,156	4.0291	3.2909	0.1827	12.3337
Data Coverage	1,156	80.3119	25.6096	0.01	100
Urban	1,156	0.7872	0.4095	0	1
Suburban	1,156	0.2076	0.4058	0	1
Rural	1,156	0.0052	0.0719	0	1
E.Economic variables level					
Unemployment rate $NUTS2$	540	16.8193	7.865	4.9	34.8
GDP $NUTS3$	540	97.1630	25.3325	58	204
At risk of poverty $NUTS2$	540	0.5037	0.5005	0	1
F.Countries					
Croatia	540	0.0074	0.0858	0	1
Greece	540	0.0167	0.1281	0	1
Italy	540	0.35	0.4774	0	1
Portugal	540	0.0556	0.2293	0	1
Spain	540	0.5703	0.4955	0	1

Notes:: This table presents summary statistics for key variables, grouped into six categories: (A) health outcomes - Infant Mortality Rate (ratio of infant deaths to live births per 1,000 population) and <65 Cardio-Respiratory Mortality Rate (ratio of deaths due to circulatory and respiratory diseases to the total population per 100,000 population), (B) pollution levels, (C) weather conditions, (D) station characteristics and coverage, (E) economic variables, and (F) country representation.

Figure A1.1: Mortality rate under 65 per 100,000 due to diseases of the circulatory or respiratory systems (upper panel) and average yearly % variation (lower panel)

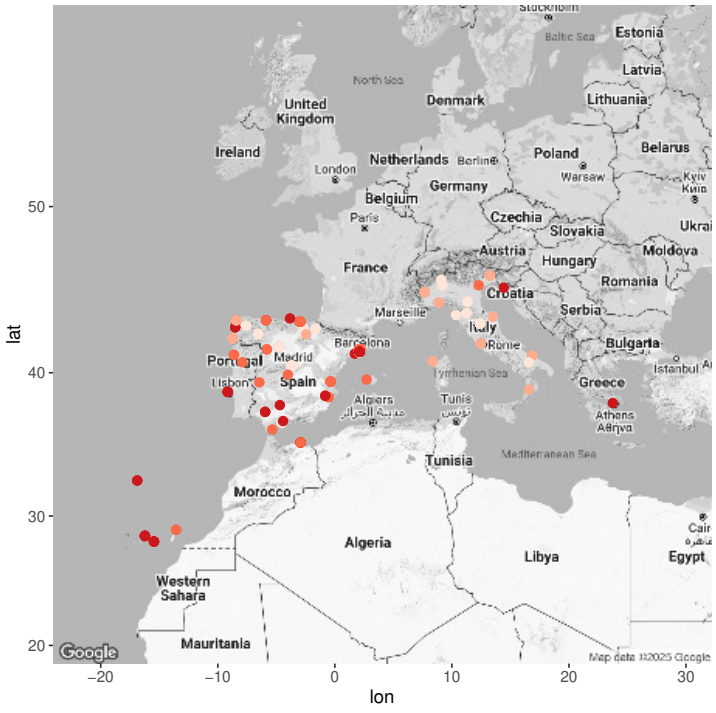

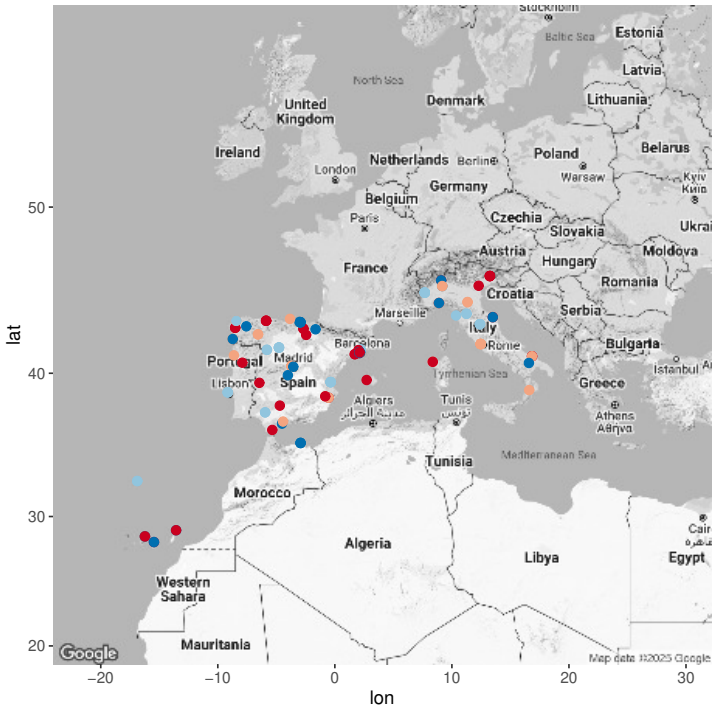

Figure A1.2: Infant mortality rate per 1,000 live births (upper panel) and average yearly % variation (lower panel)

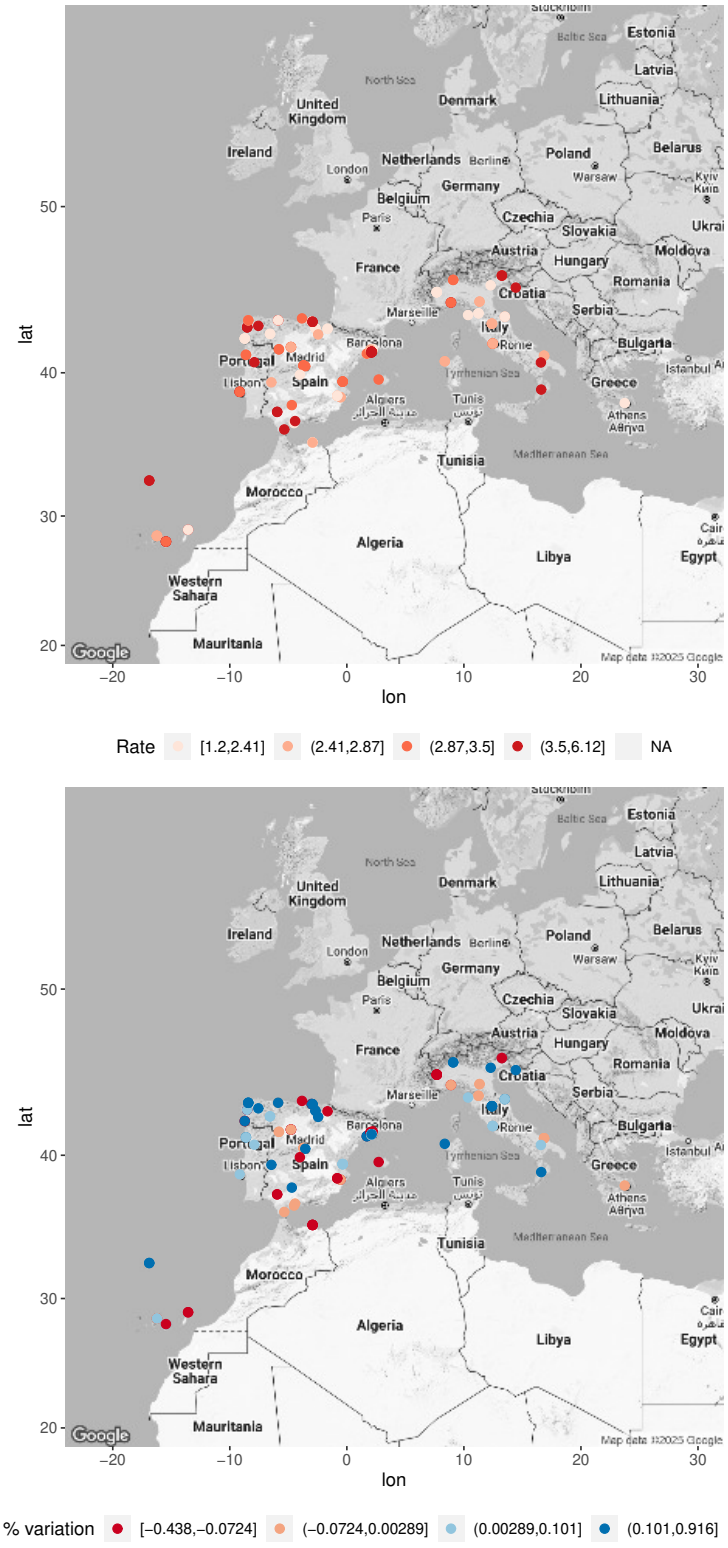

Figure A1.3: PM 2.5: average (upper panel) and average yearly % variation (lower panel)

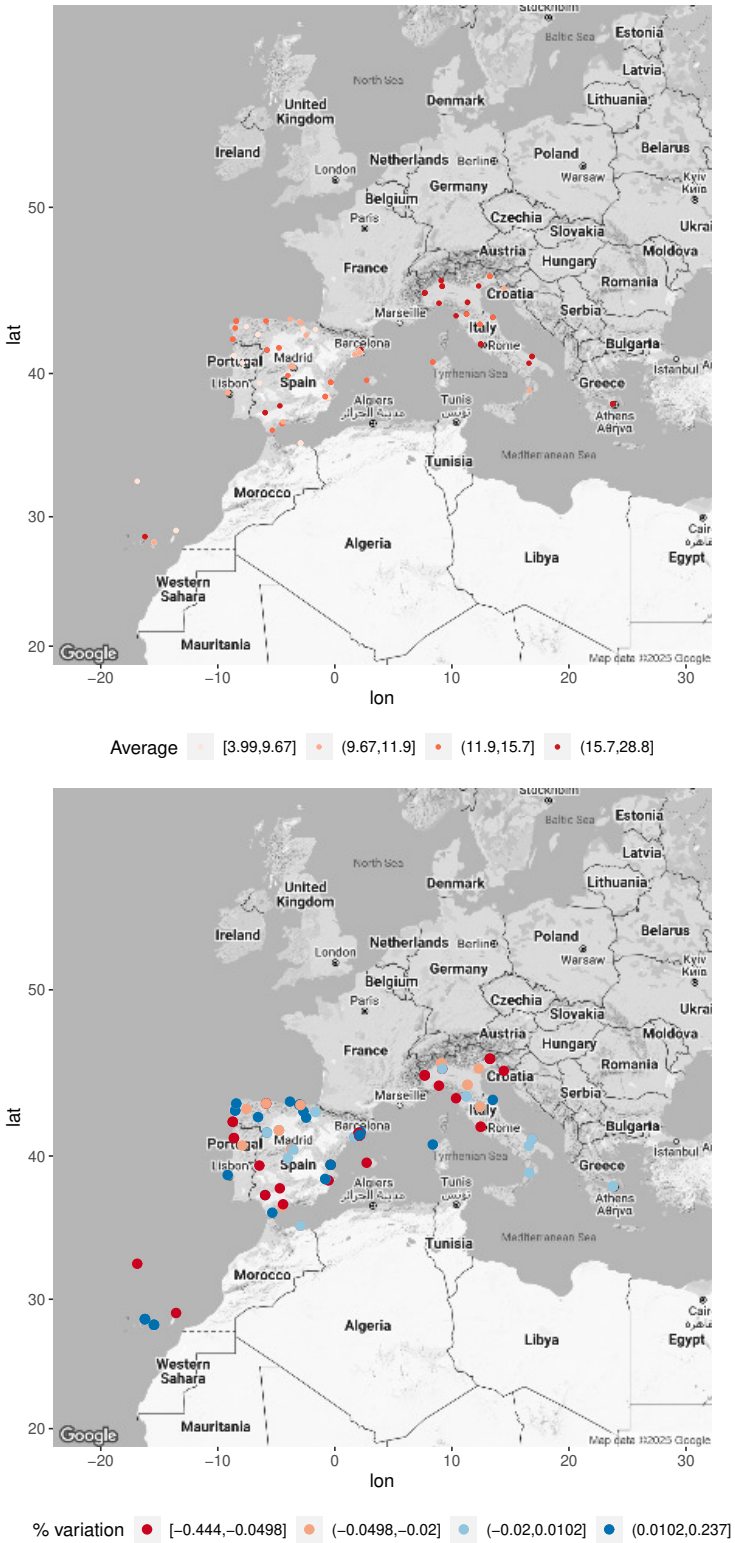

Figure A1.4: Mean precipitations: average (upper panel) and average yearly % variation (lower panel)

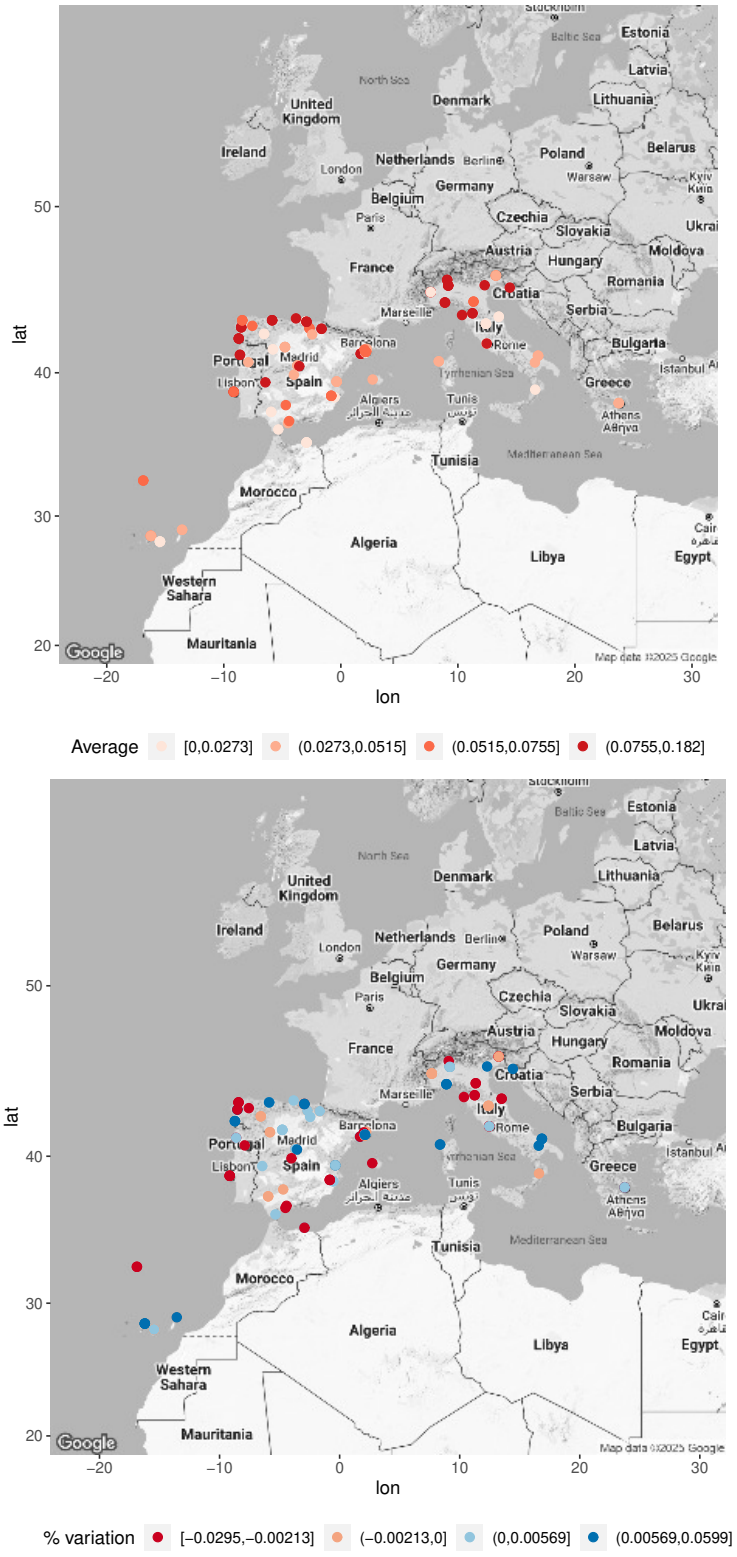

Figure A1.5: An illustration showing the location of an urban (upper part) and a suburban (lower part) air quality monitoring stations near Rome.

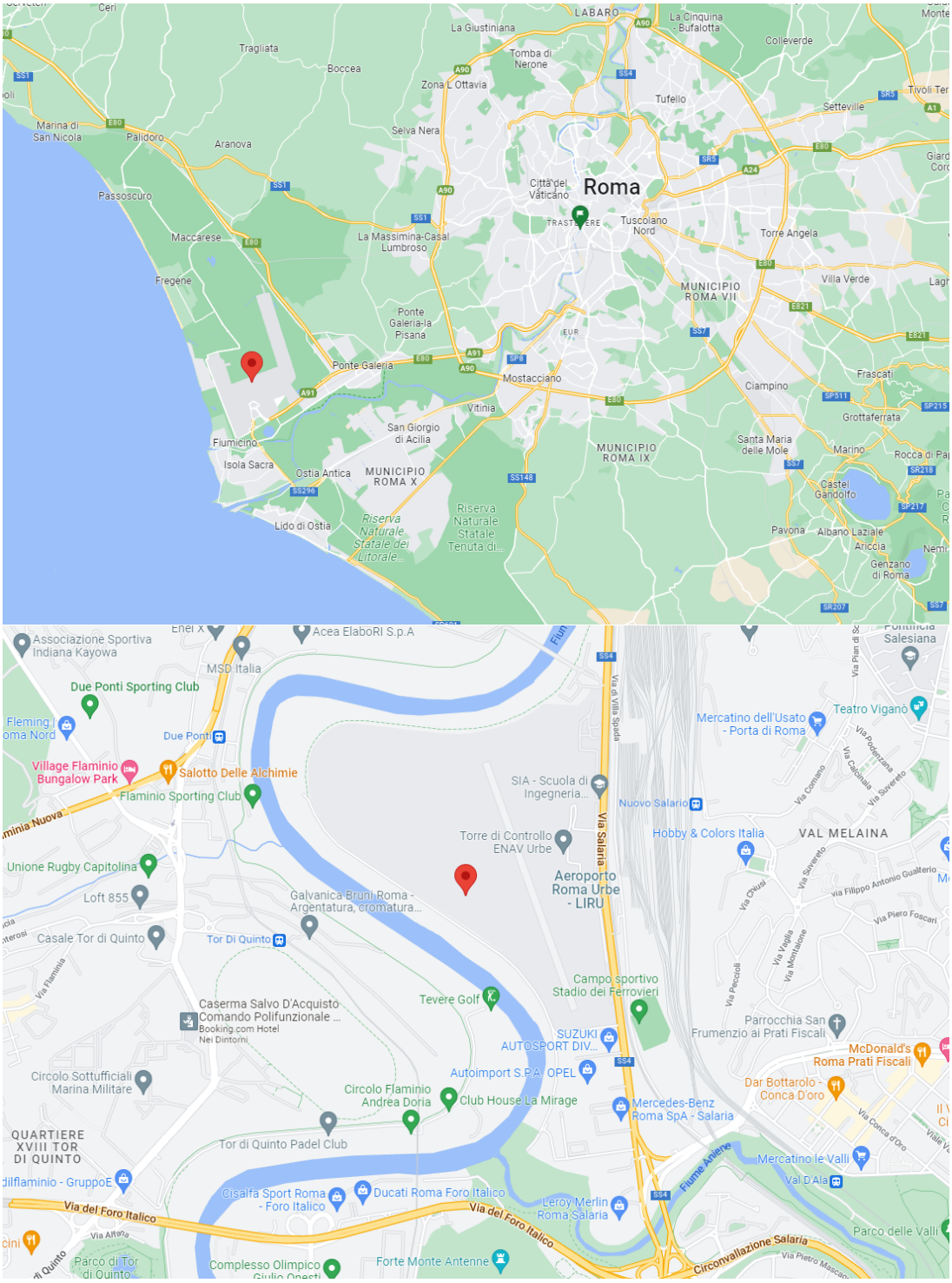

Table A1.2: < 65 Cardio-Respiratory MR × 100,000 pop - First Stage

	(1)	(2)	(3)	(4)
Precipitations	-16.9855***	-15.8956***	-17.3727***	-18.3076***
	(2.5854)	(2.7713)	(2.5703)	(2.7887)
Mean of Y	13.3422	13.3422	13.3422	13.3422
SD of Y	5.6934	5.6934	5.6934	5.6934
F-stat	29.6	62.6	31.1	53.4
p-value F-stat	8.968e-8	3.595e-14	4.58e-8	1.955e-12
Number of cities	75	75	75	75
Number of stations	180	180	180	180
Observations cities	429	429	429	429
Observations stations	915	915	915	915
Station FE	Yes	Yes	Yes	Yes
Linear trend	Yes	No	Yes	No
Quadratic trend	Yes	Yes	Yes	Yes
Station control variable	No	No	Yes	Yes
Weather control variables	No	No	Yes	Yes
City linear trend	No	Yes	No	Yes
GDP and Unemployment	No	No	Yes	Yes

Notes: Standard errors are clustered at the station level. Significant levels: *** p<0.01, ** p<0.05, * p<0.1.

Table A1.3: Infant MR × 1,000 population - First Stage

	(1)	(2)	(3)	(4)
Precipitations	-16.9855***	-15.8956***	-17.3727***	-18.3076***
	(2.5854)	(2.7115)	(2.5703)	(2.7255)
Mean of Y	13.3422	13.3422	13.3422	13.3422
SD of Y	5.6934	5.6934	5.6934	5.6934
F-stat	29.6	62.6	31.1	53.4
p-value F-stat	8.968e-8	3.595e-14	4.58e-8	1.955e-12
Number of cities	75	75	75	75
Number of stations	177	177	177	177
Observations cities	482	482	482	482
Observations stations	1,030	1,030	1,030	1,030
Station FE	Yes	Yes	Yes	Yes
Linear trend	Yes	No	Yes	No
Quadratic trend	Yes	Yes	Yes	Yes
Station control variable	No	No	Yes	Yes
Weather control variables	No	No	Yes	Yes
City linear trend	No	Yes	No	Yes
GDP and Unemployment	No	No	Yes	Yes

Notes: Standard errors are clustered at the station level. Significant levels: *** p<0.01, ** p<0.05, * p<0.1.

Table A1.4: < 65 Cardio-Respiratory MR × 100,000 and Infant MR × 1,000 - Reduced Form

	(1)	(2)	(3)	(4)
Panel A: < 65 Cardio-Respiratory MR × 100,000				
Precipitations	-5.3862***	-5.3187***	-5.0155***	-4.8699**
	(1.6389)	(1.9234)	(1.7029)	(1.9828)
Mean of Y	3.4012	3.4012	3.4012	3.4012
SD of Y	1.1711	1.1711	1.1711	1.1711
F-stat	29.6	62.6	31.1	53.4
p-value F-stat	8.968e-8	3.595e-14	4.58e-8	1.955e-12
Number of cities	75	75	75	75
Number of stations	180	180	180	180
Observations cities	429	429	429	429
Observations stations	915	915	915	915
Panel B: Infant MR × 1,000				
Precipitations	-6.4317**	-6.4181*	-5.4437*	-18.3076***
	(2.9217)	(3.3781)	(3.0244)	(3.4872)
Mean of Y	2.9665	2.9665	2.9665	2.9665
SD of Y	1.6519	1.6519	1.6519	1.6519
F-stat	29.6	62.6	31.1	53.4
p-value F-stat	8.968e-8	3.595e-14	4.58e-8	1.955e-12
Number of cities	75	75	75	75
Number of stations	177	177	177	177
Observations cities	482	482	482	482
Observations stations	1,030	1,030	1,030	1,030
Station FE	Yes	Yes	Yes	Yes
Linear trend	Yes	No	Yes	No
Quadratic trend	Yes	Yes	Yes	Yes
Station control variable	No	No	Yes	Yes
Weather control variables	No	No	Yes	Yes
City linear trend	No	Yes	No	Yes
GDP and Unemployment	No	No	Yes	Yes

Notes: Standard errors are clustered at the city level. Significant levels: *** p<0.01, ** p<0.05, * p<0.1.

Table A1.5: < 65 Cardio-Respiratory MR × 100,000 and Infant MR × 1,000 - First stage estimates by metropolitan areas type and risk of poverty rate

	Metropolitan areas		**Risk of Poverty rate**	
	Urban	Suburban	Above	Below
	(1)	(2)	(3)	(4)
Panel A: < 65 Cardio-Respiratory MR × 100,000				
Precipitations	-17.3336***	-18.0809***	-3.2843	-28.8275***
	(2.8580)	(5.7518)	(3.7547)	(3.2823)
Mean of Y	14.0865	12.7678	11.5960	15.9169
SD of Y	6.1844	4.6395	4.5773	6.3016
F-stat	30.8	2.7732	6.1475	24.3
p-value F-stat	5.788e-8	0.0981	0.0141	1.662e-6
Number of cities	67	27	46	44
Number of pollution stations	102	38	98	96
Observations cities	359	148	197	232
Observations stations	714	195	433	459
Panel B: Infant MR × 1,000				
Precipitations	-17.3336***	-18.0809***	-3.2843	-28.8275***
	(2.8580)	(5.7518)	(3.7547)	(3.2823)
Mean of Y	13.3693	12.5434	11.2802	15.1922
SD of Y	5.7819	4.4699	4.5920	5.7756
F-stat	30.8	2.7732	6.1475	24.3
p-value F-stat	5.788e-8	0.0981	0.0141	1.662e-6
Number of cities	67	27	47	44
Number of pollution stations	138	38	99	93
Observations cities	404	169	239	243
Observations stations	798	226	512	490

Notes: The specification used is that of tables 1.1 and 1.2, column (3). Standard errors are clustered at the station level. Significant levels: *** p<0.01, ** p<0.05, * p<0.1.

Table A1.6: 2IV and 3IV - TS2SLS and First stage

	2IV		**3IV**	
	Cardio-Respiratory MR $\times 100,000$	Infant MR $\times 1,000$	Cardio-Respiratory MR $\times 100,000$	Infant MR $\times 1,000$
Panel A: TS2SLS				
$PM_{2.5}$	0.279***	0.1269	0.2969***	0.1806
	(0.0949)	(0.1585)	(0.0937)	(0.1562)
Mean of Y	3.4012	2.9665	3.4012	2.9665
SD of Y	1.1711	1.6519	1.1711	1.6519
Panel B: First stage				
Precipitations	-17.3727***	-17.3727***	-17.3727***	-17.3727***
	(2.5703)	(2.5703)	(2.5703)	(2.5703)
Wind speed	-0.4946***	-0.4946***	-0.4946***	-0.4946***
	(0.1369)	(0.1369)	(0.1369)	(0.1369)
Temperature	-	-	-0.0512	-0.0512
	-	-	(0.0933)	(0.0933)
Mean of Y	13.3422	13.3422	13.3422	13.3422
SD of Y	5.6934	5.6934	5.6934	5.6934
Sargan-stat	0.0176	5.6617	1.4517	8.5917
p-value Sargan	0.8945	0.01734	0.4839	0.0136
Number of cities	75	75	75	75
Number of stations	180	177	180	177
Observations cities	429	482	429	482
Observations stations	915	1,030	915	1,030

Notes: The specification used is that of tables 1.1 and 1.2, column (3). Standard errors are clustered at the city level for TS2SLS estimates and at the station level in the first stage. Significant levels: *** p<0.01, ** p<0.05, * p<0.1.

Table A1.7: Robustness - Precipitations correlations

	Precipitations	Precipitations
	(1)	(2)
GDP_t	0.0004	-
	(0.0005)	-
$Precipitations_{t-1}$	-	-0.1100-
	-	(0.0802)
$Precipitations_{t-2}$	-	0.0696
	-	(0.0726)
Observations	540	405
Number of cities	76	76
Mean of Y	0.0591	0.0571
SD of Y	0.0484	0.0478
Station FE	Yes	Yes
Linear trend	Yes	Yes
Quadratic trend	Yes	Yes
Station control variable	Yes	Yes
Weather control variables	Yes	Yes
City linear trend	No	No
GDP and Unemployment	Yes	Yes

Notes: The linear regressions in columns (1) and (2) follow preferred specification 3. The higher observation count relative to the main specification stems from excluding mortality outcomes, allowing broader analysis of precipitation, its lags, and GDP. Standard errors are clustered at the city level. Significant levels: *** p<0.01, ** p<0.05, * p<0.1.

Table A1.8: Robustness - Mobility correlations

	Immigration	Emigration	Net inflow
	(1)	(2)	(3)
$PM_{2.5,t-1}$	-4.9507	4.7734	-9.7240
	(18.3380)	(9.2798)	(16.4163)
GDP_{t-1}	0.0082	0.0159	-0.0077
	(0.0313)	(0.0164)	(0.0304)
$Windspeed_{t-1}$	80.5946	-55.7356	136.3302
	(69.7029)	(45.1875)	(95.4888)
$Precipitations_{t-1}$	63.1966**	-2.4693	65.6658*
	(31.3974)	(12.9034)	(34.4755)
Constant	23,971.22	-18,932.33**	42,903.55**
	(16832.75)	(9068.65)	(20,216.51)
City FE	Yes	Yes	Yes
Year FE	Yes	Yes	Yes
City time trends	Yes	Yes	Yes
Observations	520	520	520
Number of cities	104	104	104
Mean of Y	3,275.833	3,047.904	227.929
SD of Y	6,031.234	5,100.002	1,378.15

Notes: The linear regressions in columns (1)–(3) cover Italy only due to limited data availability for other countries. The term t–1 denotes one-year lag. Standard errors are clustered at the city level. Significant levels: *** p<0.01, ** p<0.05, * p<0.1.

Appendix Paper II

Table A2.1: Degree-Days Range for Different Climatic Zones

Zone	Degree-Days Range
A	Municipalities with degree-days < 600
B	Municipalities with $600 <$ degree-days < 900
C	Municipalities with $901 <$ degree-days < 1400
D	Municipalities with $1401 <$ degree-days < 2100
E	Municipalities with $2101 <$ degree-days < 3000
F	Municipalities with degree-days > 3000

Figure A2.1: Italian Climatic Zones

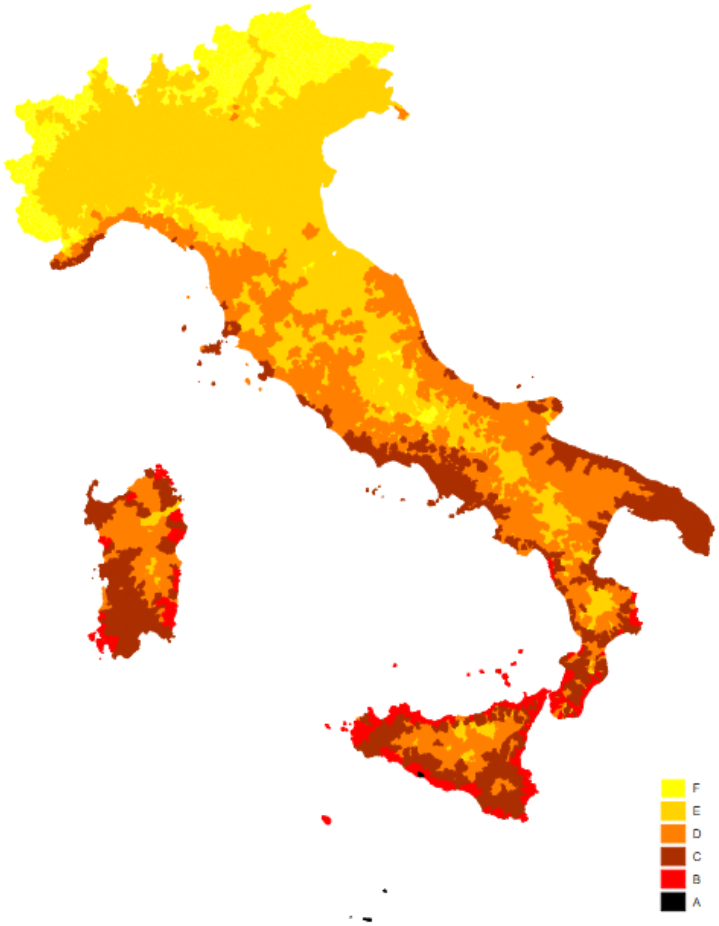

Notes: The figure illustrates Italian municipalities categorised by their classified climatic zone. Municipalities highlighted in yellow correspond to the coldest climatic zone with the highest degree days, climatic zone F. As the colour intensity increases, the zones transition in ascending order of temperature and descending degree days: zone E, D, C, B, and finally the warmest zone, characterised by a few municipalities and depicted in black, identified as climatic zone A. *Source:* own elaboration.

Table A2.2: Main Municipalities for Different Climatic Zones

Climatic Zone	**Municipalities**
A	Lampedusa, Porto Empedocle, and Linosa
B	Agrigento, Catania, Crotone, Messina, Palermo, Reggio Calabria, Siracusa, and Trapani
C	Bari, Benevento, Brindisi, Cagliari, Caserta, Catanzaro, Cosenza, Imperia, Latina, Lecce, Napoli, Oristano, Ragusa, Salerno, Sassari, and Taranto
D	Ascoli Piceno, Avellino, Caltanissetta, Chieti, Firenze, Foggia, Forlì, Genova, Grosseto, Isernia, La Spezia, Livorno, Lucca, Macerata, Massa Carrara, Matera, Nuoro, Pesaro, Pescara, Pisa, Pistoia, Prato, Roma, Savona, Siena, Teramo, Terni, Vibo Valentia, Viterbo
E	Alessandria, Aosta, Arezzo, Asti, Bergamo, Biella, Bologna, Bolzano, Brescia, Campobasso, Como, Cremona, Enna, Ferrara, Frosinone, Gorizia, L'Aquila, Lecco, Lodi, Milano, Modena, Novara, Padova, Parma, Pavia, Perugia, Piacenza, Pordenone, Potenza, Ravenna, Reggio Emilia, Rieti, Rimini, Rovigo, Sondrio, Torino, Treviso, Trieste, Udine, Varese, Venezia, Verbania, Vercelli, Verona, Vicenza
F	Belluno, Cuneo, and Trento

Figure A2.2: Italian Heating Restrictions

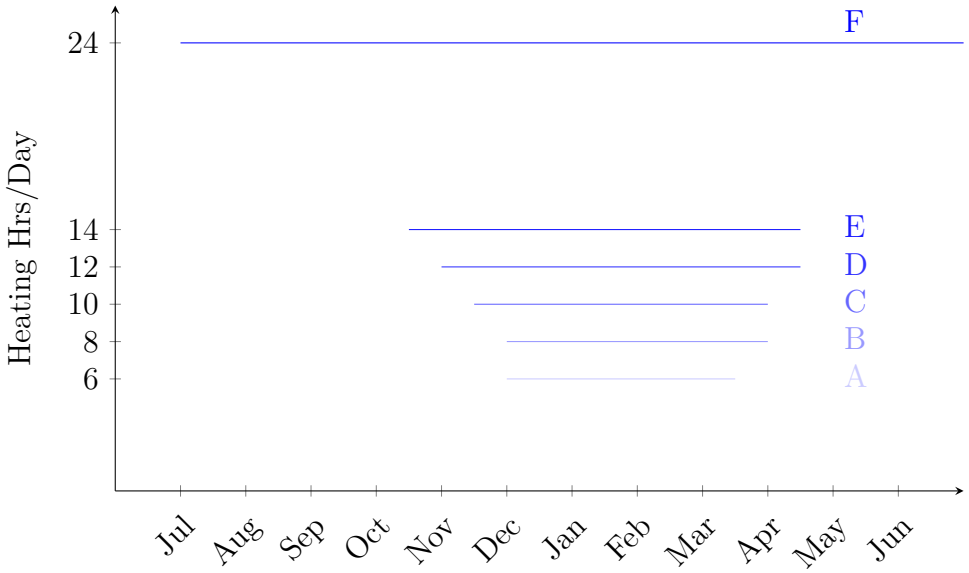

Notes: The x-axis represents the months of the year, and the y-axis denotes hours in a day. Horizontal lines indicate heating restriction zones in Italy, with highlighted lines indicating the permitted heating months and how many hrs/day: Zone A (Dec 1 - Mar 15, 6hrs/day), Zone B (Dec 1 - Mar 31, 8hrs/day), Zone C (Nov 15 - Mar 31, 10hrs/day), Zone D (Nov 1 - Apr 15, max 12hrs/day), Zone E (Oct 15 - Apr 15, up to 14hrs/day). Zone F has no restrictions.

Figure A2.3: Spatial distribution of $PM_{2.5}$ before (upper panel) and after (lowe panel) heating system activation in Italy.

(a) Average CAMS $PM_{2.5}$ levels from 2015 to 2019 during the pre-heating activation months (June, July, August, and September), focusing on the weeks spanning from the 22^{nd} to the 40^{th} week.

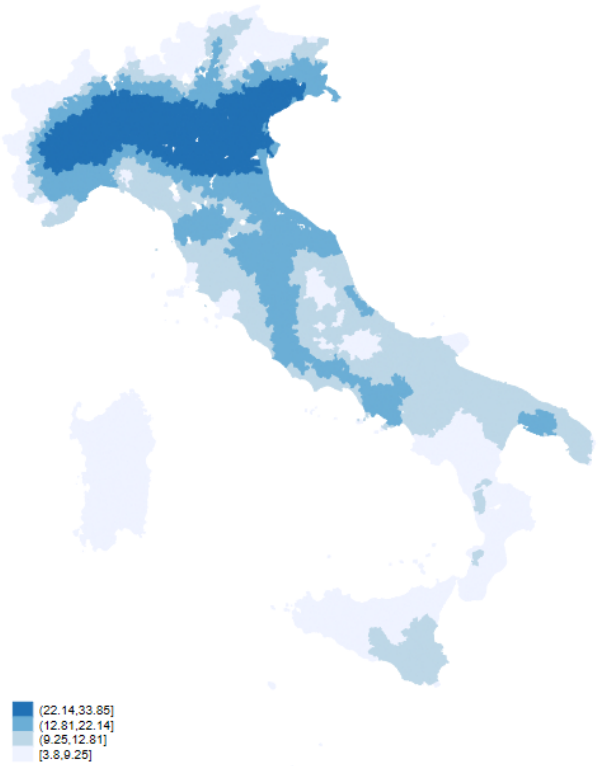

(b) Average CAMS $PM_{2.5}$ levels from 2015 to 2019 during the post-heating activation months (October, November, December, and January), specifically examining the weeks from the 41^{st} to the 52^{nd} week and the 1^{st} to the 5^{th} week.

Figure A2.4: Turning on heating: actual week vs regulation

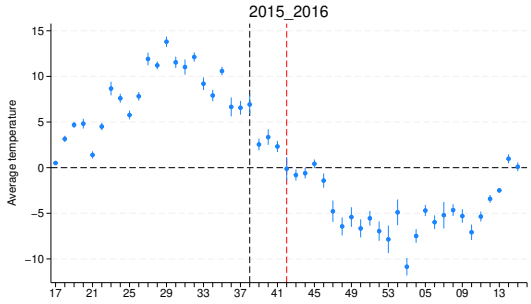

(a) Temperature 15-16

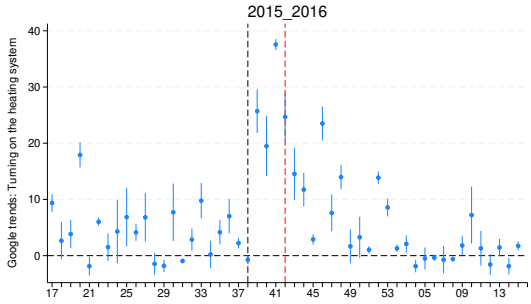

(b) Google 15-16

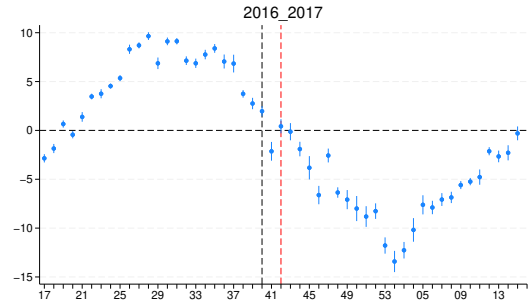

(c) Temperature 16-17

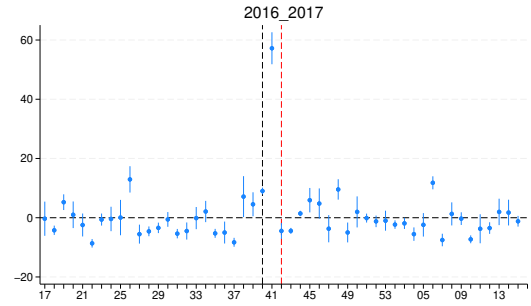

(d) Google 16-17

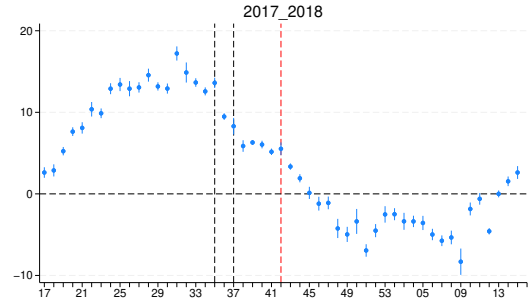

(e) Temperature 2017-18

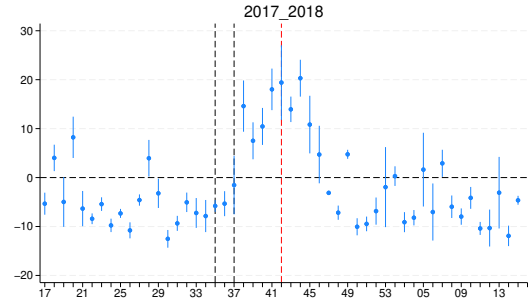

(f) Google 17-18

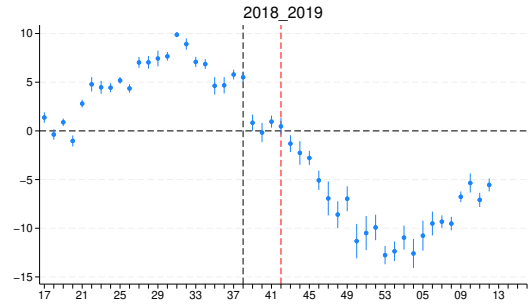

(g) Temperature 18-19

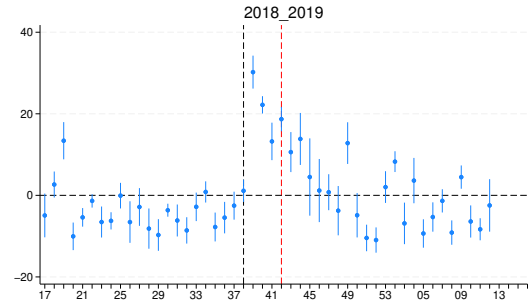

(h) Google 18-19

Notes: This Figure illustrates the trend of deviations from average temperature (left column) and the absolute number of Google searches for "Turning on the heating system" (right column) over four biennial periods: 2015-2016, 2016-2017, 2017-2018 and 2018-2019. The x-axis in all sub-figures represents weekly intervals, covering April-December of the first year and January-March of the second year. The black dashed vertical line marks the first temperature drop and the corresponding rise in Google searches. For 2017-18 (A2.4e) we highlight two remarkable drops in temperatures and the corresponding activity on Google (A2.4f). The red dashed vertical line represents the first week in which it is theoretically allowed to switch on the heating system (i.e. 15th of October in areas D/E).

Figure A2.5: Temperatures and Google searches

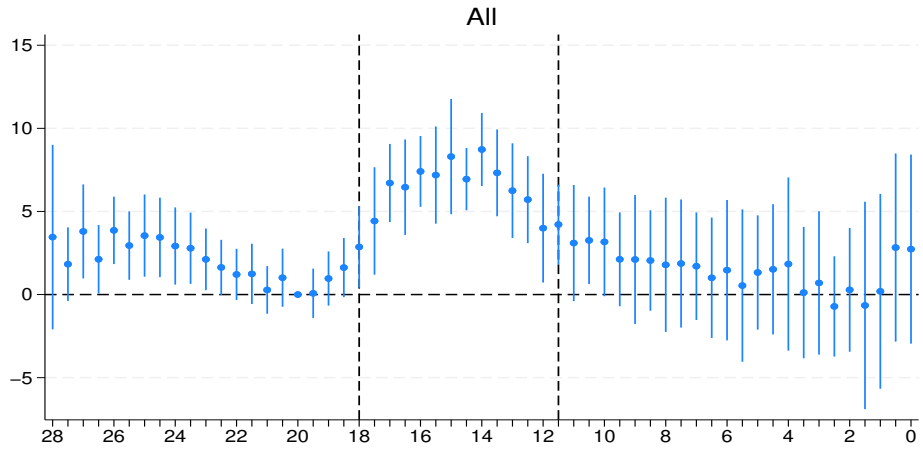

Notes: This Figure illustrates the relationship between the absolute number of Google searches for "Turning on the heating system" (y-axis) and the decrease in temperature (x-axis). The dashed vertical lines highlight the increase in Google searches as temperatures range between 18-12°C. The data cover all the considered biennial periods: 2015-2016, 2016-2017, 2017-2018, and 2018-2019.

Figure A2.6: Treatment distribution map across Italian municipalities

Figure A2.7: $PM_{2.5}$ EEA main estimates for 2015-16, 2016-17, 2017-18, 2018-19.

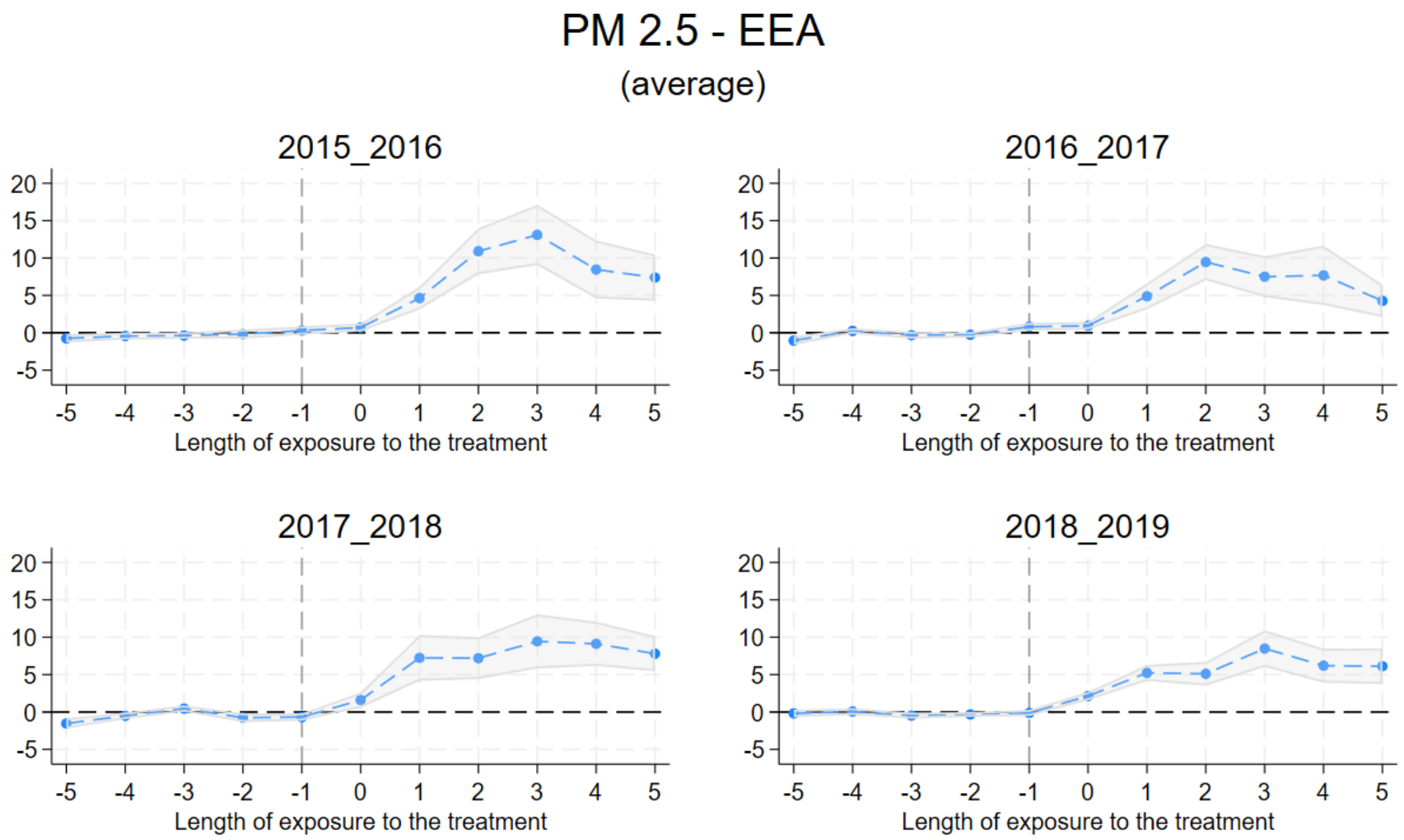

Figure A2.8: PM_{10} EEA main estimates for 2015-16, 2016-17, 2017-18, 2018-19.

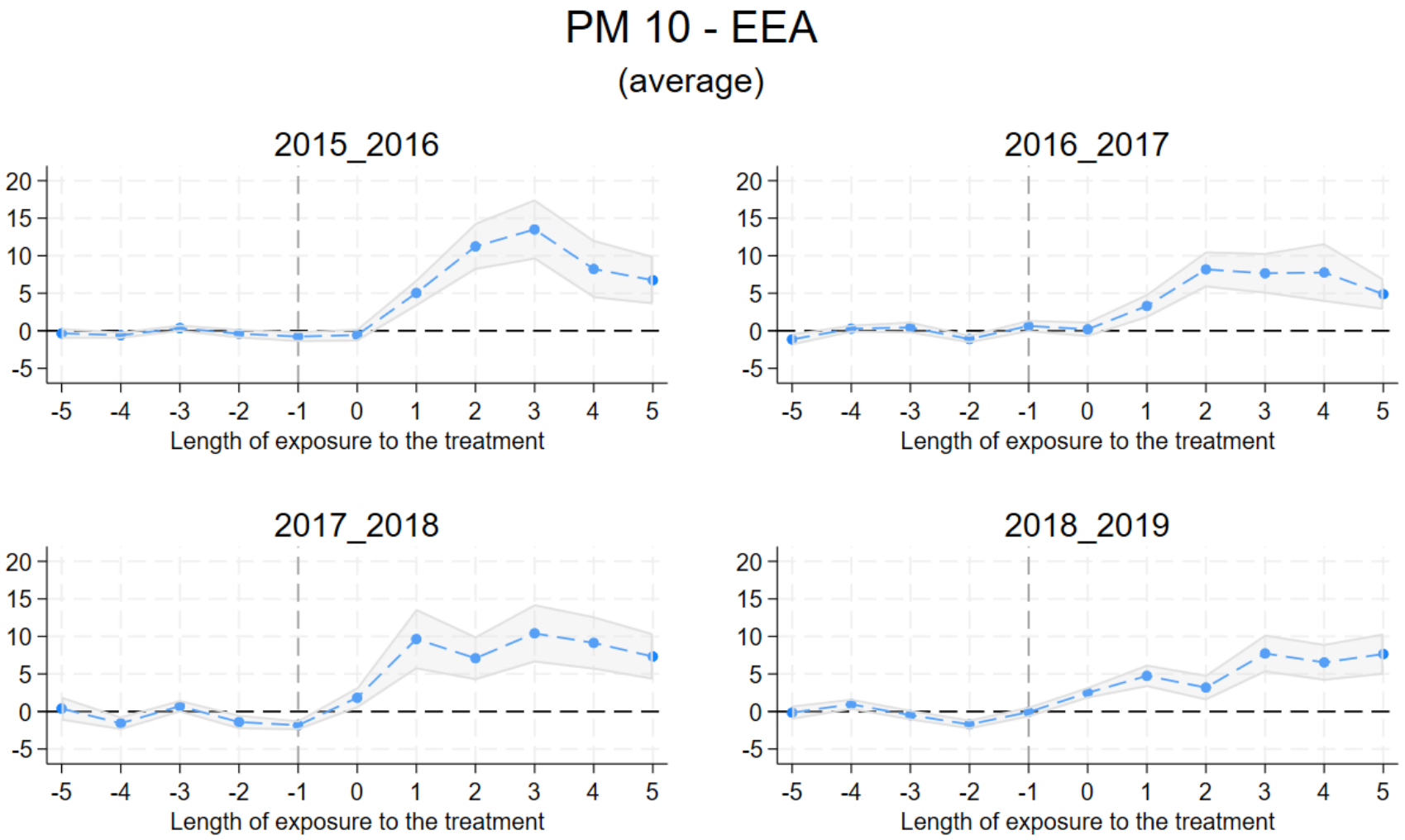

Figure A2.9: SO_2 EEA main estimates for 2015-16, 2016-17, 2017-18, 2018-19.

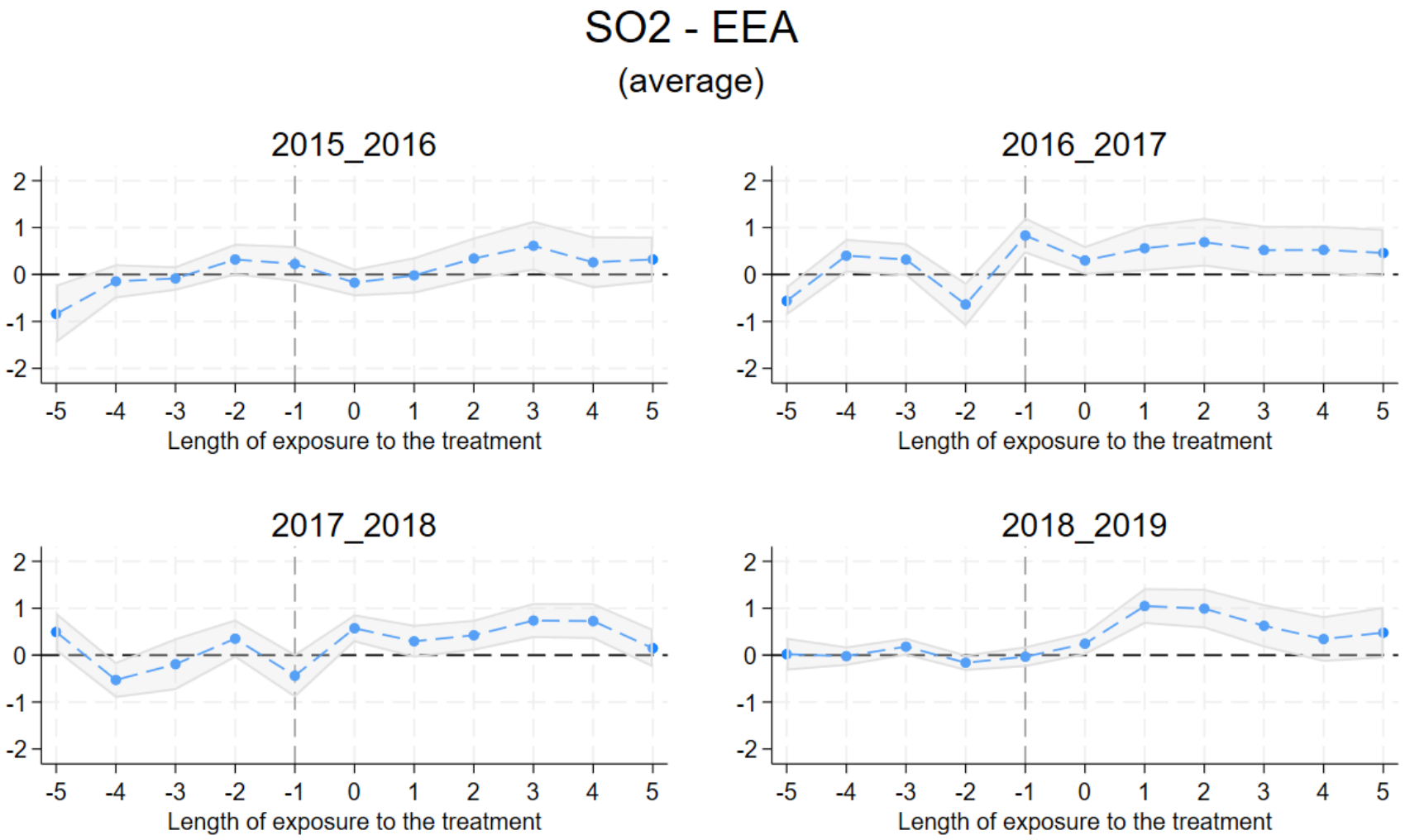

Figure A2.10: *CO* EEA main estimates for 2015-16, 2016-17, 2017-18, 2018-19.

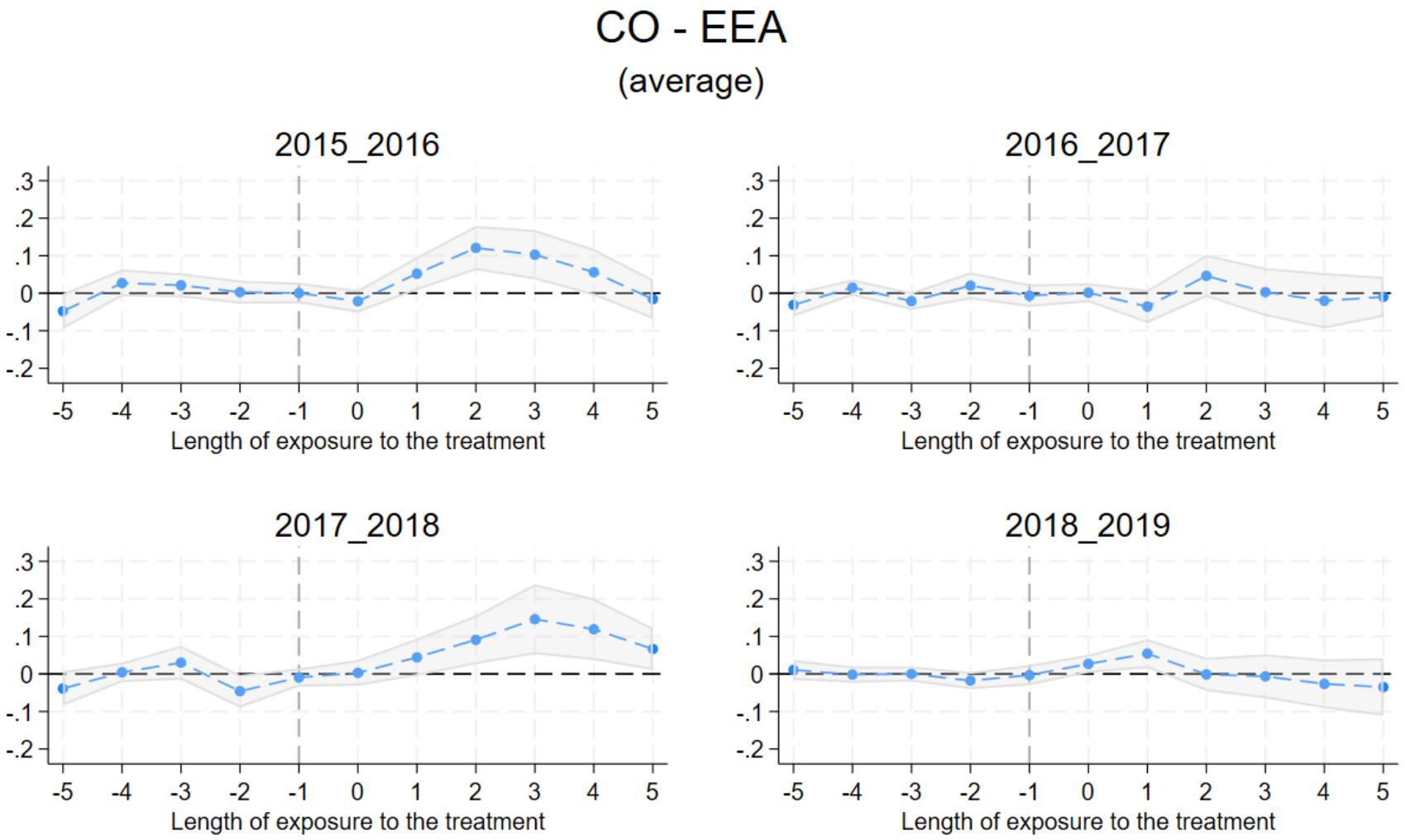

Figure A2.11: O_3 EEA main estimates for 2015-16, 2016-17, 2017-18, 2018-19.

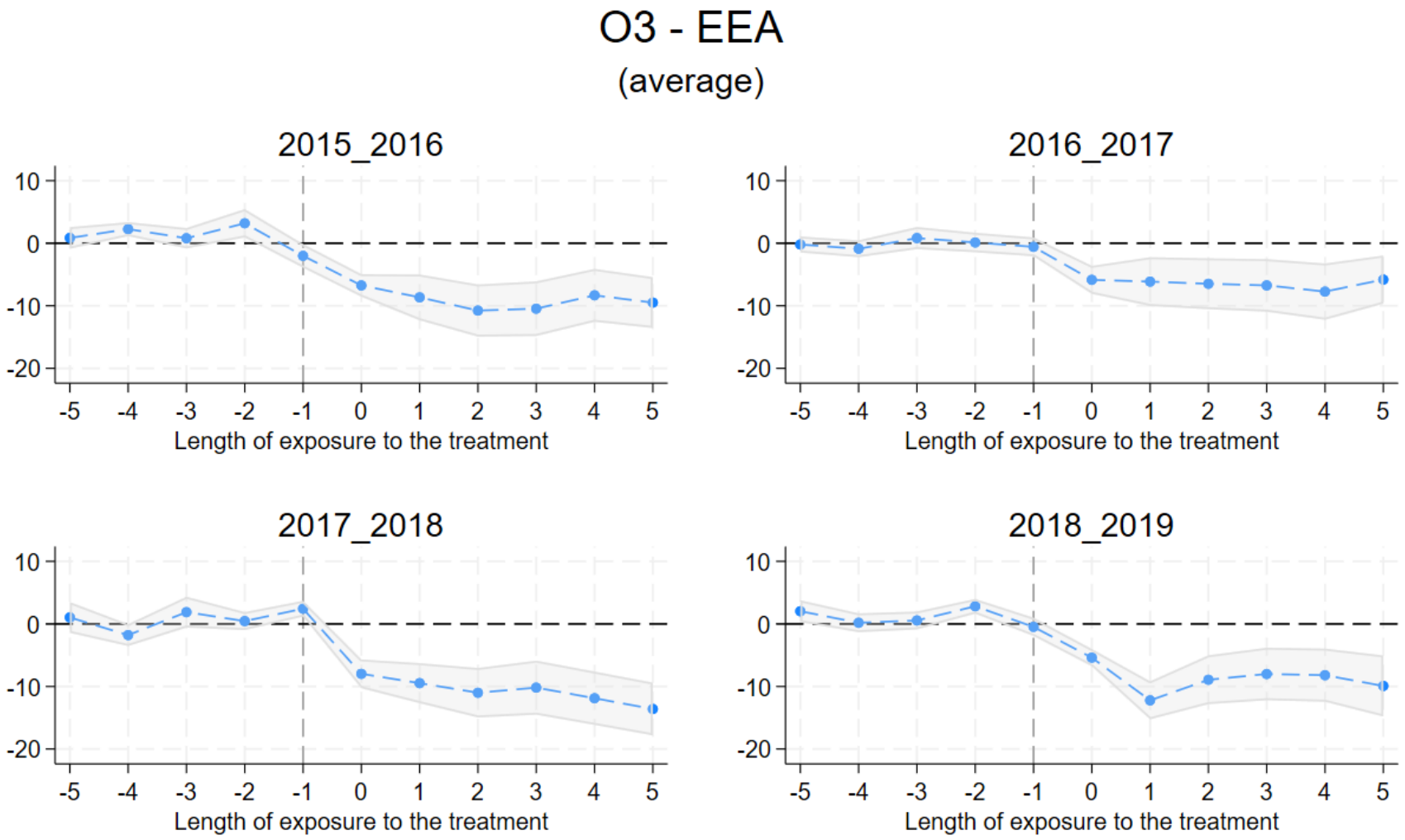

Figure A2.12: Average Treatment Effects on Placebo Outcomes: Hospitalization Rates (LHS) and In-Hospital Mortality Rates (RHS) per 10,000 Inhabitants, across 2015-2019

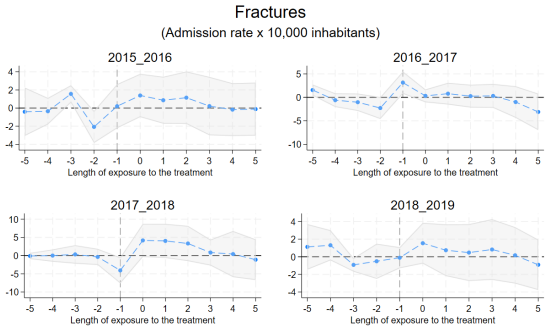

(a) Hospitalisations

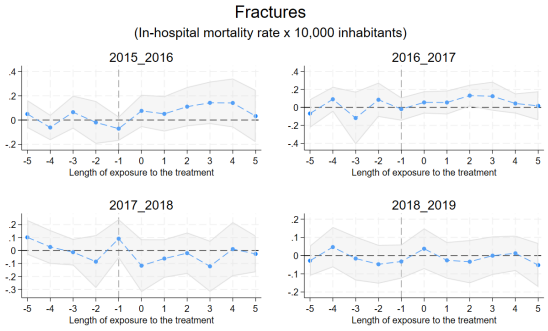

(b) In-hospital mortality

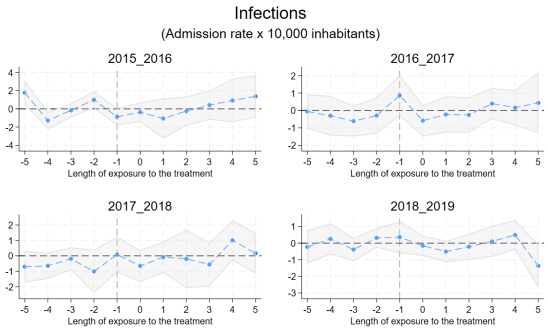

(c) Hospitalisations

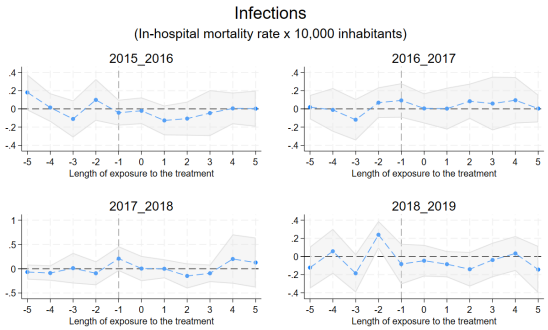

(d) In-hospital mortality

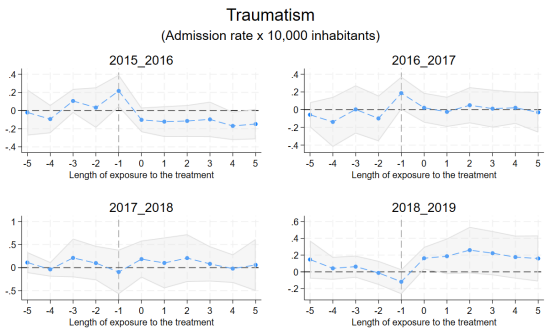

(e) Hospitalisations

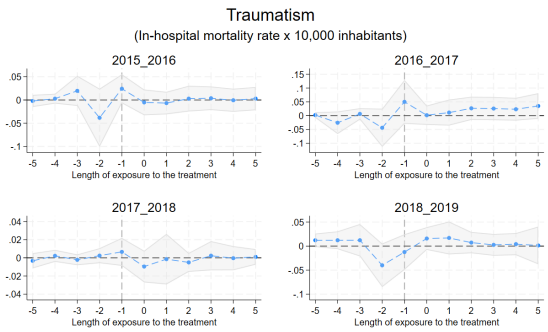

(f) In-hospital mortality

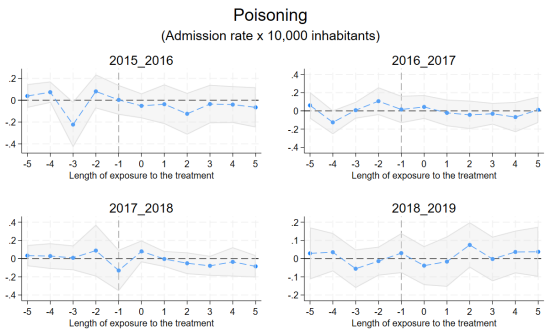

(g) Hospitalisations

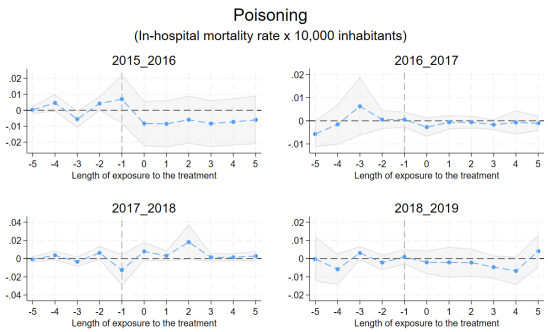

(h) In-hospital mortality

Notes: This Figure presents the Average Treatment Effect on the Treated (ATT) of residential heating activation on (a) hospitalisation rates (left panels) and (b) in-hospital mortality rates (right panels) (both per 10,000 inhabitants) for placebo outcomes: (a,b) fractures (top row), (c,d) infections (second row), (e,f) trauma (third row), and (g, h) poisoning (bottom row). Estimates reflect biennial comparisons across the 2015-2019 period. The Figure continues on the following page.

Figure A2.12: Average Treatment Effects on Placebo Outcomes: Hospitalization Rates (LHS) and In-Hospital Mortality Rates (RHS) per 10,000 Inhabitants, across 2015-2019 (Continued)

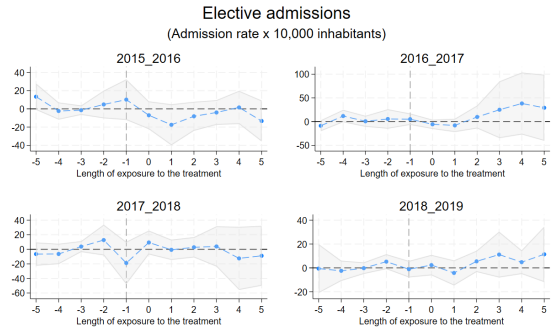

(i) Hospitalisations

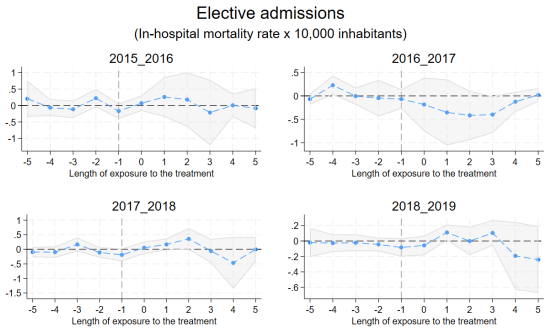

(j) In-hospital mortality

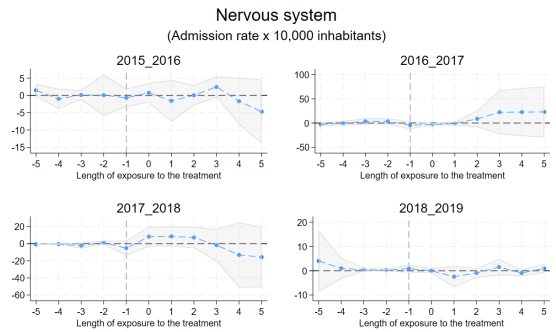

(k) Hospitalisations

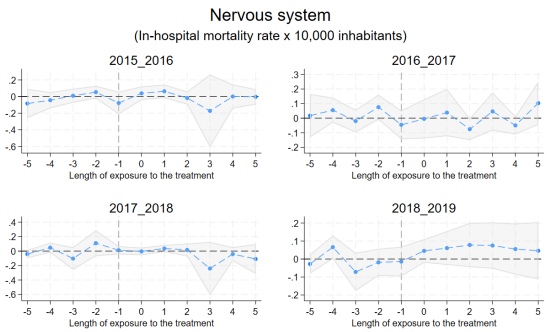

(l) In-hospital mortality

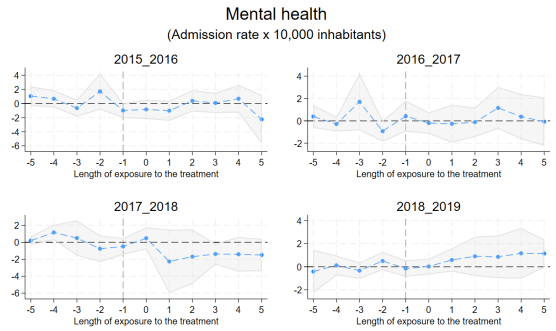

(m) Hospitalisations

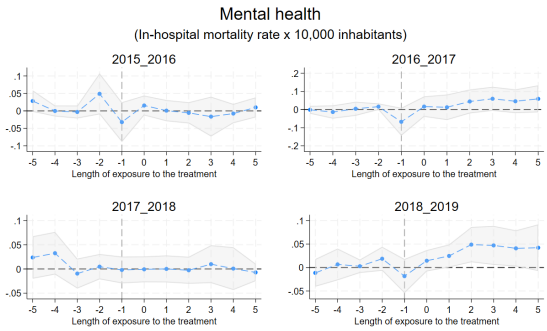

(n) In-hospital mortality

Notes (continued): This Figure presents the Average Treatment Effect on the Treated (ATT) of residential heating activation on (a) hospitalisation rates (left panels) and (b) in-hospital mortality rates (right panels) (both × 10,000 inhabitants) for additional placebo outcomes: (i,j) elective admissions (top row), (k,l) nervous system disorders (second row), and (m,n) mental health conditions (bottom row). Estimates reflect biennial comparisons across the 2015-2019 period.

Figure A2.13: Average Treatment Effects (ATT) of residential heating activation on $PM_{2.5}$ (CAMS and EEA), PM_{10} and NO_2 by climatic areas: B/C and D/E.

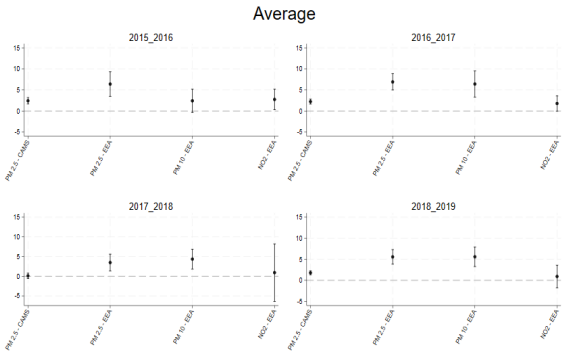

(a) ATT of residential heating activation on mean pollutants' concentrations in climatic zone B/C

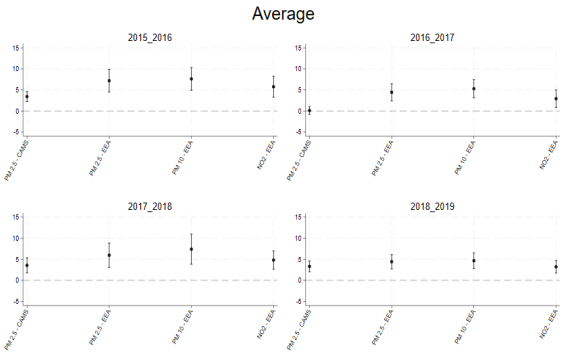

(b) ATT of residential heating activation on mean pollutants' concentrations in climatic zone D/E

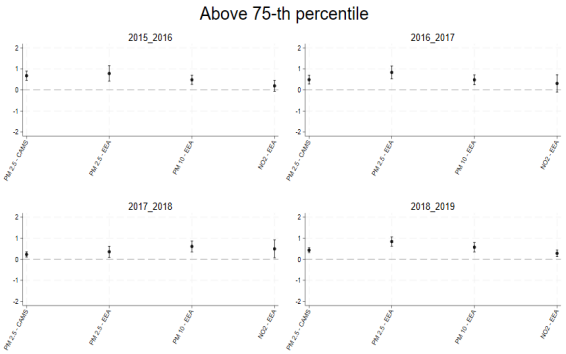

(c) ATT of residential heating activation on 75^{th} percentile pollutants' concentrations in climatic zone B/C

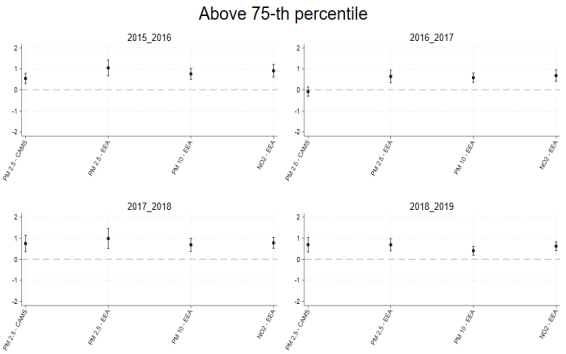

(d) ATT of residential heating activation on 75^{th} percentile pollutants' concentrations in climatic zone D/E

Notes: The Figure presents the Average Treatment Effects (ATT) of residential heating system activation on air pollution concentrations across different climatic zones. Panels (a) and (b) show impacts on mean pollution levels, with (a) focusing on climatic zone B/C and (b) on zone D/E, examining $PM_{2.5}$ (from both CAMS and EEA data), PM_{10}, and NO_2. The lower panels analyze effects at the 75^{th} percentile, with (c) for zone B/C and (d) for zone D/E, revealing how heating activation influences upper-tail pollution events.

Figure A2.14: Heterogeneous Average Treatment Effects (ATT) of residential heating activation on AMI

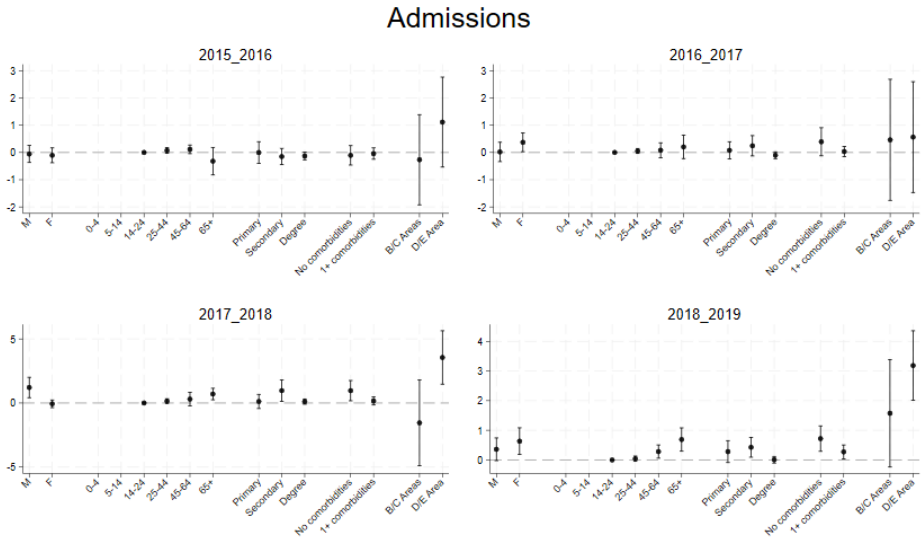

(a) Heterogeneous Average Treatment Effects (ATT) of residential heating activation on AMI - Hospitalisations

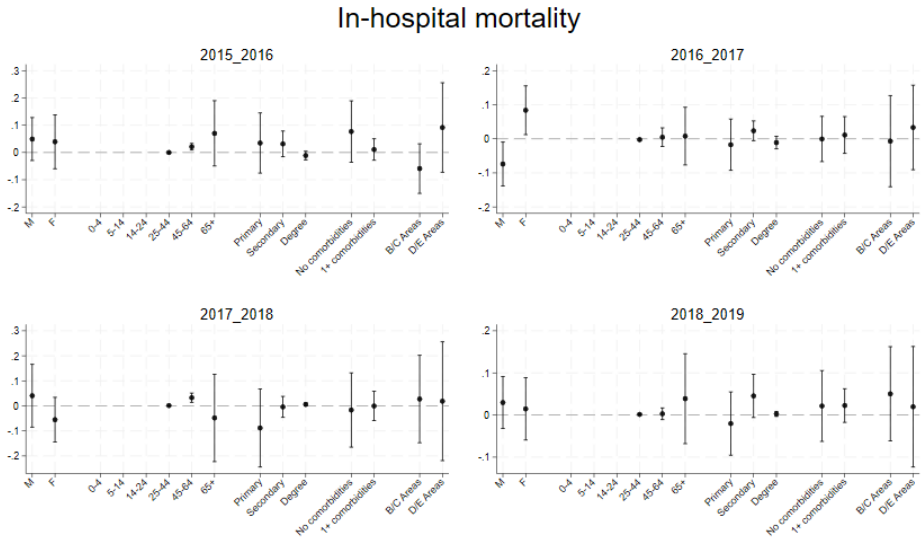

(b) Heterogeneous Average Treatment Effects (ATT) of residential heating activation on AMI - In hospital mortality

Notes: The Figure displays the Average Treatment Effect on the Treated (ATT) of residential heating activation on (a) AMI hospitalisations (upper panel) and (b) in-hospital mortality (lower panel). Results are stratified by gender, age group, educational attainment, comorbidity status (with/without), and climatic zone (B/C vs. D/E)

Figure A2.15: Heterogeneous Average Treatment Effects (ATT) of residential heating activation on STEMI

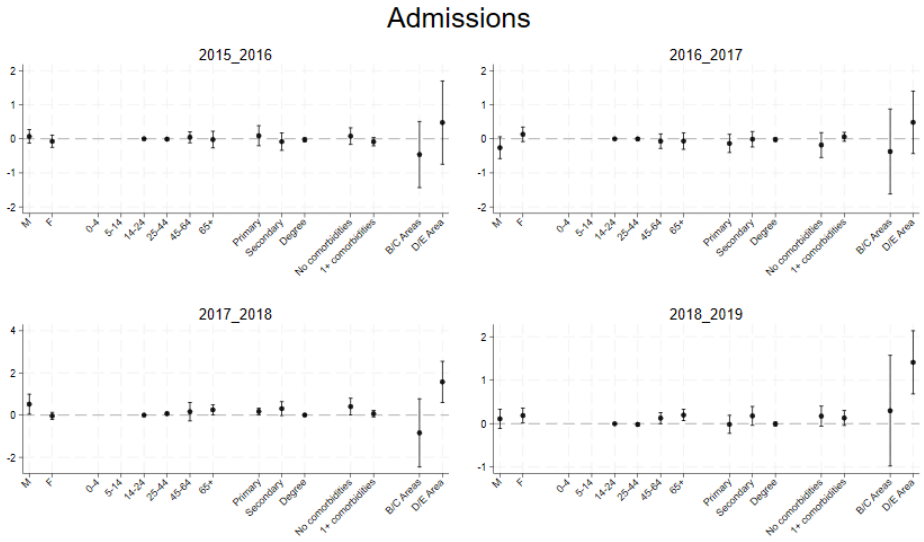

(a) Heterogeneous Average Treatment Effects (ATT) of residential heating activation on STEMI - Hospitalisations

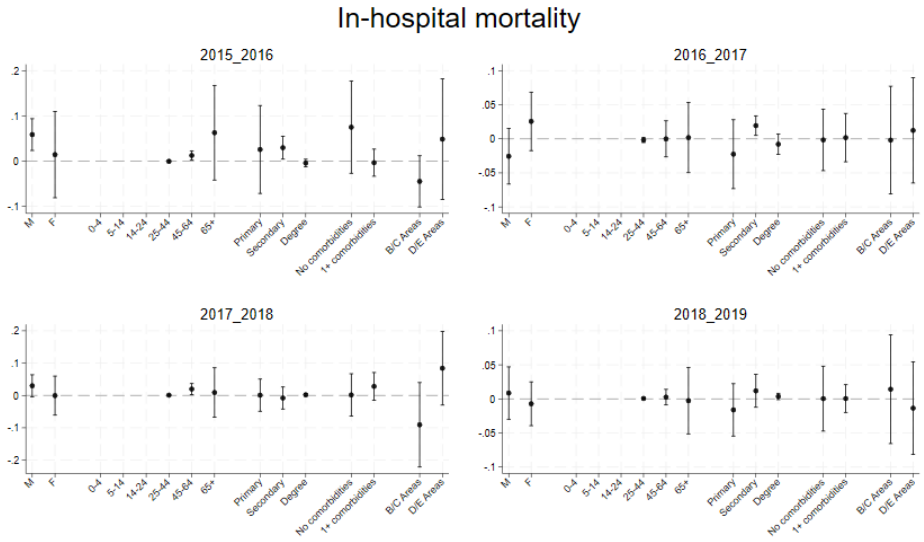

(b) Heterogeneous Average Treatment Effects (ATT) of residential heating activation on STEMI - In hospital mortality

Notes: The Figure displays the Average Treatment Effect on the Treated (ATT) of residential heating activation on (a) STEMI hospitalisations (upper panel) and (b) in-hospital mortality (lower panel). Results are stratified by gender, age group, educational attainment, comorbidity status (with/without), and climatic zone (B/C vs. D/E)

Figure A2.16: Heterogeneous Average Treatment Effects (ATT) of residential heating activation on NSTEMI

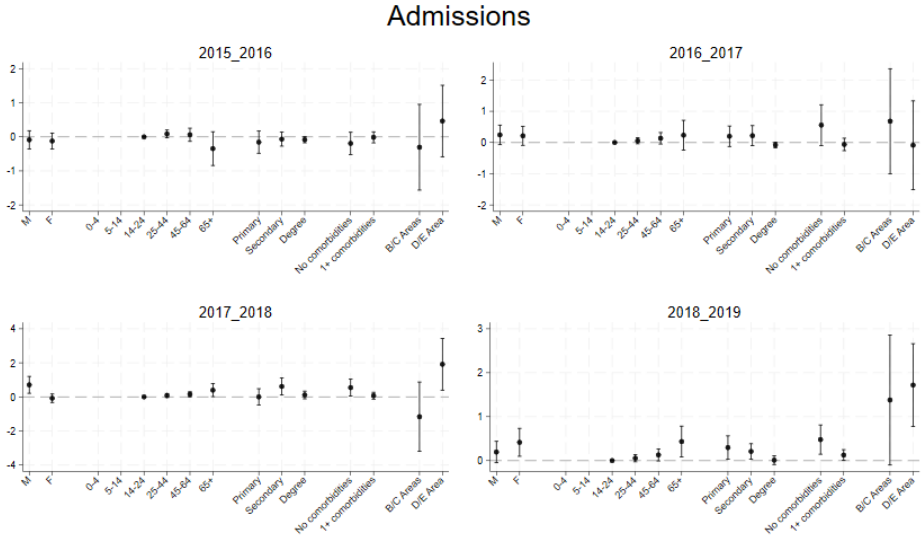

(a) Heterogeneous Average Treatment Effects (ATT) of residential heating activation on NSTEMI - Hospitalisations

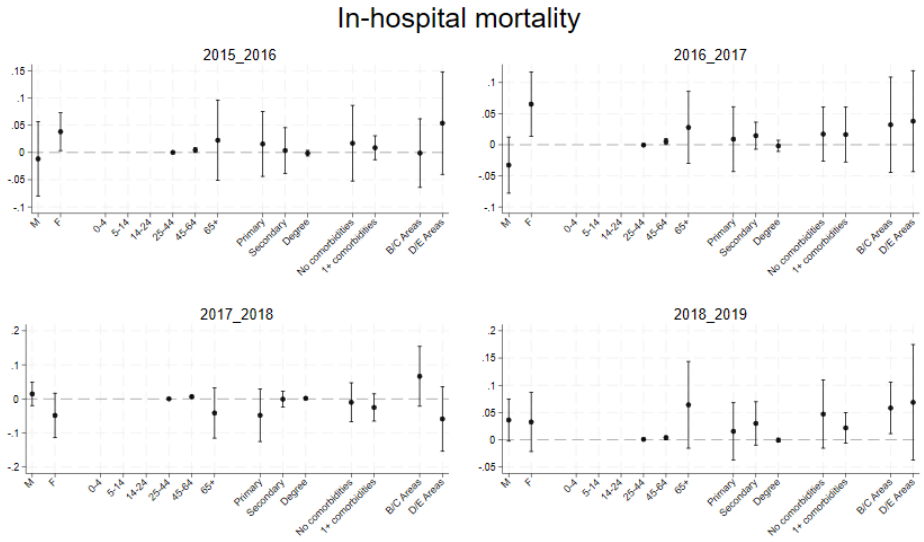

(b) Heterogeneous Average Treatment Effects (ATT) of residential heating activation on NSTEMI - In hospital mortality

Notes: The Figure displays the Average Treatment Effect on the Treated (ATT) of residential heating activation on (a) NSTEMI hospitalisations (upper panel) and (b) in-hospital mortality (lower panel). Results are stratified by gender, age group, educational attainment, comorbidity status (with/without), and climatic zone (B/C vs. D/E)

Figure A2.17: Heterogeneous Average Treatment Effects (ATT) of residential heating activation on Ischemic Stroke

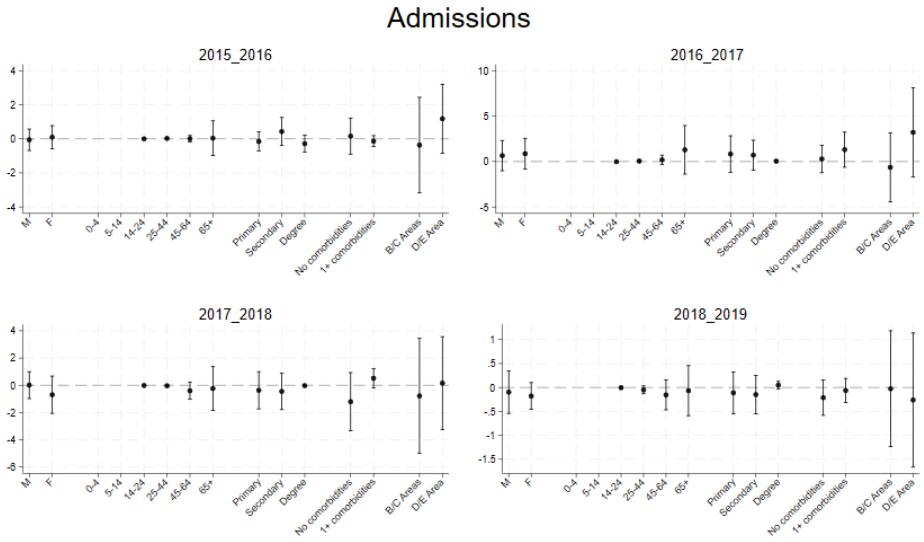

(a) Heterogeneous Average Treatment Effects (ATT) of residential heating activation on Ischemic Stroke - Hospitalisations

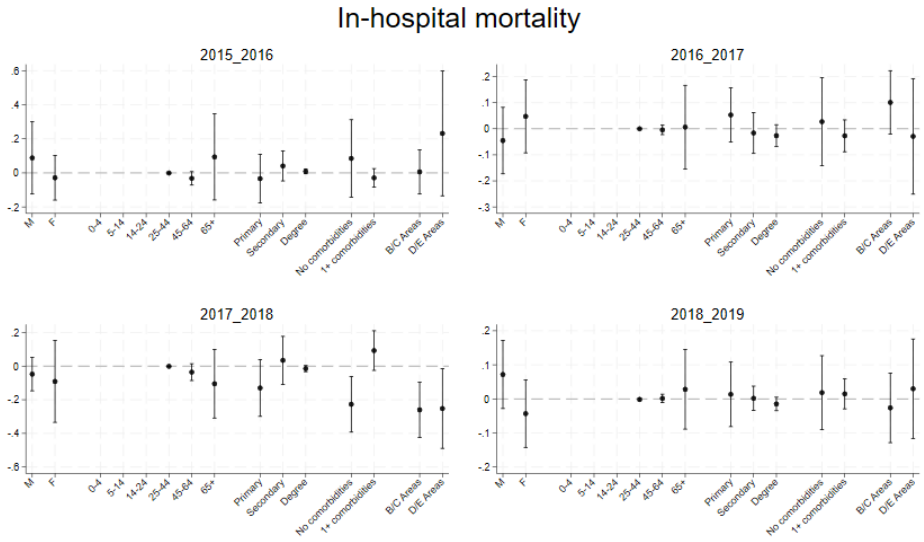

(b) Heterogeneous Average Treatment Effects (ATT) of residential heating activation on Ischemic Stroke - In hospital mortality

Notes: The Figure displays the Average Treatment Effect on the Treated (ATT) of residential heating activation on (a) Ischemic Stroke hospitalisations (upper panel) and (b) in-hospital mortality (lower panel). Results are stratified by gender, age group, educational attainment, comorbidity status (with/without), and climatic zone (B/C vs. D/E)

Figure A2.18: Heterogeneous Average Treatment Effects (ATT) of residential heating activation on Hemorrhagic Stroke

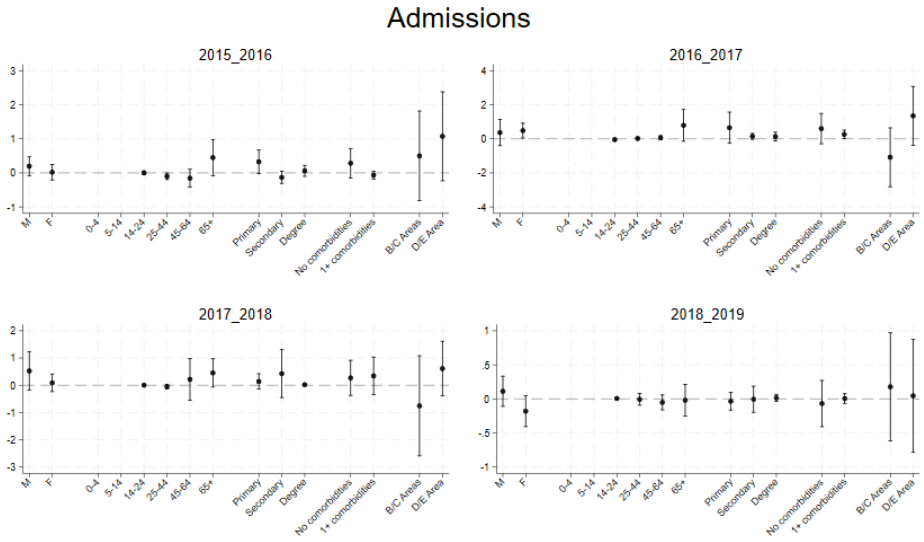

(a) Heterogeneous Average Treatment Effects (ATT) of residential heating activation on Hemorrhagic Stroke - Hospitalisations

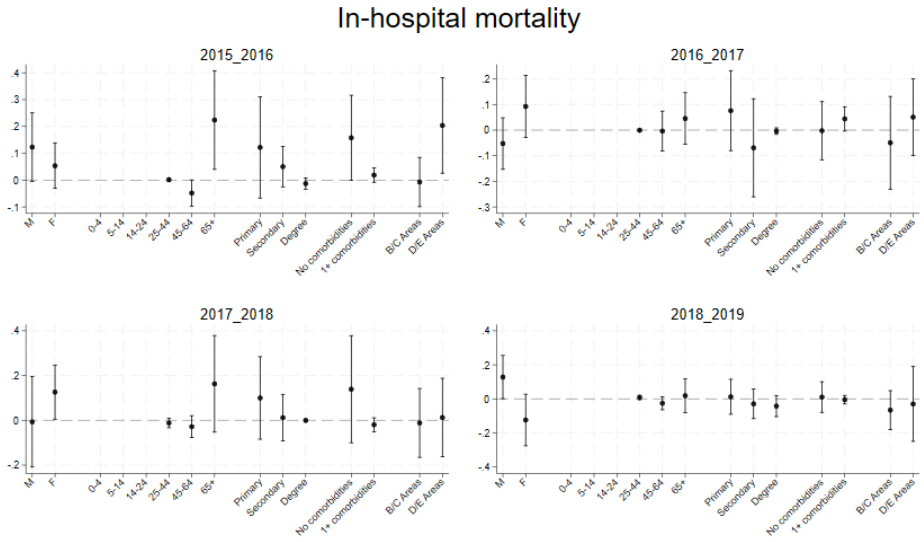

(b) Heterogeneous Average Treatment Effects (ATT) of residential heating activation on Hemorrhagic Stroke - In hospital mortality

Notes: The Figure displays the Average Treatment Effect on the Treated (ATT) of residential heating activation on (a) Hemorrhagic Stroke hospitalisations (upper panel) and (b) in-hospital mortality (lower panel). Results are stratified by gender, age group, educational attainment, comorbidity status (with/without), and climatic zone (B/C vs. D/E)

Figure A2.19: Heterogeneous Average Treatment Effects (ATT) of residential heating activation on COPD

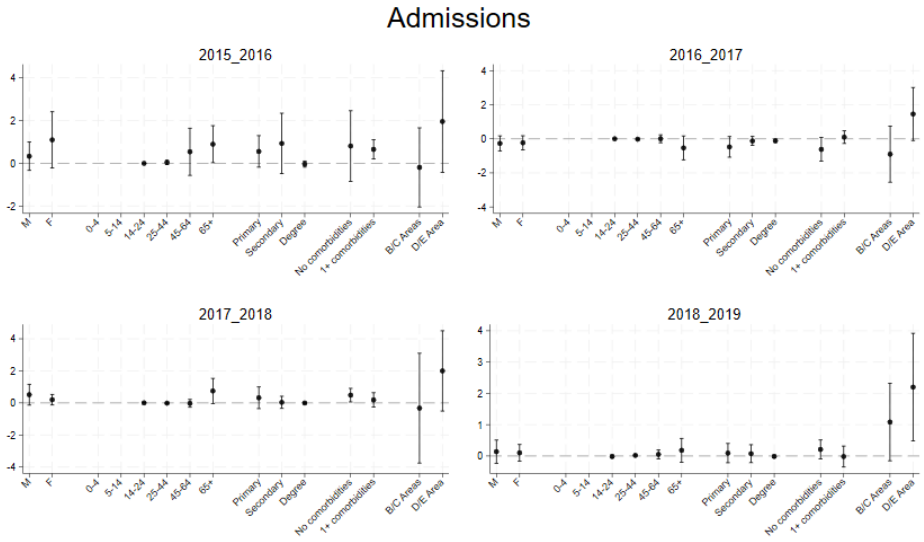

(a) Heterogeneous Average Treatment Effects (ATT) of residential heating activation on COPD - Hospitalisations

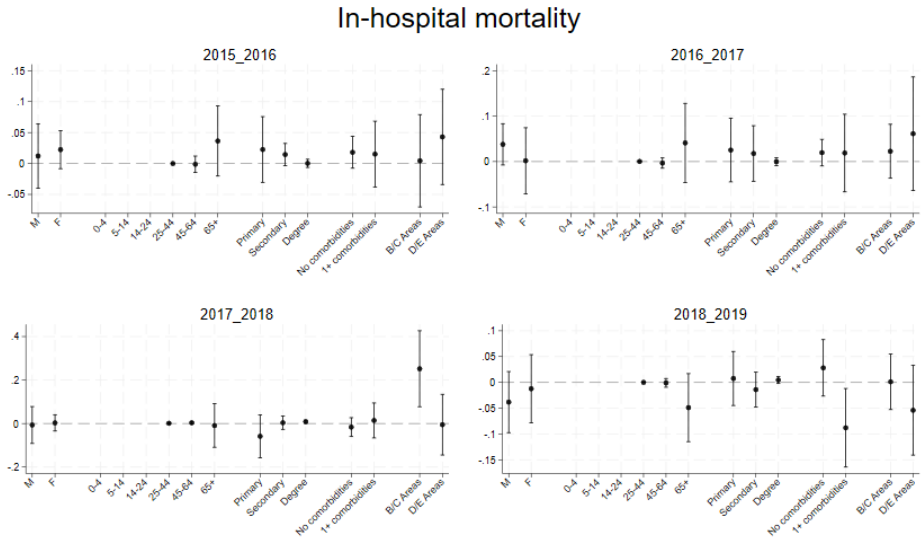

(b) Heterogeneous Average Treatment Effects (ATT) of residential heating activation on COPD - In hospital mortality

Notes: The Figure displays the Average Treatment Effect on the Treated (ATT) of residential heating activation on (a) COPD hospitalisations (upper panel) and (b) in-hospital mortality (lower panel). Results are stratified by gender, age group, educational attainment, comorbidity status (with/without), and climatic zone (B/C vs. D/E)

Table A2.3: Summary of Health Outcomes, Mortality, and Pollution Data (2015-2019)

	2015-2016			2016-2017			2017-2018			2018-2019		
	Obs	Mean	SD.	Obs	Mean	SD	Obs	Mean	SD	Obs	Mean	SD
I. Health outcomes - Hospitalisations												
AMI	5693	4.44	6.60	5694	4.41	6.48	5698	4.32	6.35	5687	4.40	7.91
STEMI	5693	1.86	3.65	5694	1.76	3.27	5698	1.65	2.84	5687	1.69	4.44
NSTEMI	5693	2.35	3.58	5694	2.44	3.77	5698	2.46	3.81	5687	2.49	3.96
Ischemic Stroke	5693	4.65	9.32	5694	4.49	9.20	5698	4.17	7.51	5687	3.83	6.09
Hemorrhagic Stroke	5693	1.33	2.84	5694	1.34	2.80	5698	1.34	2.69	5687	1.31	2.93
COPD	5693	3.07	6.15	5694	2.88	5.32	5698	2.66	4.74	5687	2.82	12.75
II. Health outcomes - Mortality												
AMI	5693	0.30	0.71	5694	0.30	0.73	5698	0.29	0.69	5687	0.28	0.92
STEMI	5693	0.15	0.49	5694	0.14	0.41	5698	0.14	0.43	5687	0.13	0.45
NSTEMI	5693	0.10	0.36	5694	0.11	0.46	5698	0.11	0.39	5687	0.11	0.63
Ischemic Stroke	5693	0.42	0.95	5694	0.40	0.94	5698	0.40	0.94	5687	0.35	0.80
Hemorrhagic Stroke	5693	0.32	0.86	5694	0.31	0.80	5698	0.32	0.85	5687	0.33	1.02
COPD	5693	0.13	0.44	5694	0.13	0.46	5698	0.13	0.46	5687	0.11	0.39
III. Pollution												
PM 2.5 (CAMS)	5693	16.40	7.06	5694	15.49	6.29	5698	12.83	6.23	5687	13.35	7.48
> 15 μg/m^3	5693	3.20	1.77	5694	2.88	1.69	5698	1.90	1.79	5687	1.88	1.97
> 25 μg/m^3	5693	1.04	1.50	5694	0.96	1.35	5698	0.60	1.17	5687	0.66	1.35
$> 75^{th}$ perc	5693	3.40	1.75	5694	3.09	1.67	5698	2.07	1.82	5687	2.05	1.99
$> 90^{th}$ perc	5693	1.56	1.70	5694	1.37	1.52	5698	0.85	1.39	5687	0.89	1.57
PM 2.5 (EEA)	4526	18.77	12.08	5061	17.74	11.35	5294	16.13	9.17	5539	15.63	8.57
> 15 μg/m^3	4578	2.69	1.97	5077	2.38	1.89	5347	2.17	1.87	5642	2.13	1.82
> 25 μg/m^3	4578	1.26	1.81	5077	1.10	1.60	5347	0.97	1.47	5642	0.84	1.43
$> 75^{th}$ perc	4578	2.49	1.99	5077	2.18	1.88	5347	1.98	1.86	5642	1.90	1.80
$> 90^{th}$ perc	4578	1.26	1.81	5077	1.10	1.60	5347	0.97	1.47	5642	0.84	1.43

Notes: The table provides summary statistics for the four biennia: 2015-16, 2016-17, 2017-18 and 2018-19. Panel (I) reports hospitalization rates, and Panel (II) presents in-hospital mortality for acute myocardial infarction (AMI), ST-elevation MI (STEMI), non-ST-elevation MI (NSTEMI), ischemic stroke, hemorrhagic stroke, and chronic obstructive pulmonary disease (COPD). Panel (III) provides summary statistics for air pollution exposure, including daily averages of $PM_{2.5}$ (CAMS and EEA), PM_{10} (EEA), O_3 (EEA), CO (EEA), NO_2 (EEA), and SO_2 (EEA). For each pollutant, the table also reports the number of days exceeding the WHO-defined hazardous thresholds. Air Quality Guidelines, updated 2021 by WHO, for various pollutants: $PM_{2.5}$ has a 1-day limit of 15μg/m^3 (99th percentile: 5 μg/m^3, 3-4 exceedance days/year); PM_{10} has a 1-day limit of 45 μg/m^3 (99th percentile: 15 μg/m^3, 3-4 exceedance days/year); Nitrogen Dioxide ($NO2$) has a 1-hour limit of 200 μg/m^3, a 1-day limit of 25 μg/m^3, and a calendar year limit of 10 μg/m^3 (3-4 exceedance days/year); Sulfur dioxide (SO_2) has 24-hour limit of 40μg/m^3 and a 10 minutes limit of 500; Carbon Monoxide (CO) has a 1-hour limit of 30 mg/m^3, a maximum daily 8-hour mean of 10 mg/m^3, and a 1-day limit of 4 mg/m^3 (3-4 exceedance days/year); Ozone ($O3$) has a maximum daily 8-hour mean of 100 μg/m^3 (99th percentile: 60 μg/m^3, 3-4 exceedance days/year);. Panel (IV) presents the average wind speed, temperature and precipitation. Panel (V) summarises the number of municipalities and hospital institutes for each biennium.

Table A2.3: Summary of Health Outcomes, Mortality, and Pollution Data (2015-2019)

	2015-2016			2016-2017			2017-2018			2018-2019		
	Obs	Mean	SD	Obs	Mean	SD	Obs	Mean	SD	Obs	Mean	SD
III. Pollution												
PM 10 (EEA)	5097	26.66	13.43	5427	26.12	12.91	5523	24.88	11.76	5533	25.13	10.91
> 45 μg/m^3	5114	0.72	1.33	5475	0.69	1.16	5544	0.63	1.05	5603	0.59	1.06
> 50 μg/m^3	5114	0.57	1.17	5475	0.54	1.00	5544	0.49	0.89	5603	0.44	0.90
$> 75^{th}$ perc	5114	1.67	1.77	5475	1.55	1.63	5544	1.46	1.60	5603	1.47	1.64
$> 90^{th}$ perc	5114	0.72	1.33	5475	0.69	1.16	5544	0.63	1.05	5603	0.59	1.06
NO2 (EEA)	5327	24.05	13.43	5542	23.01	13.09	5637	22.19	12.48	5662	20.78	11.90
> 25 μg/m^3	5333	2.47	2.19	5557	2.30	2.10	5638	2.28	2.10	5663	2.07	2.06
> 25 μg/m^3	5333	2.47	2.19	5557	2.30	2.10	5638	2.28	2.10	5663	2.07	2.06
$> 75^{th}$ perc	5333	1.75	1.98	5557	1.59	1.86	5638	1.57	1.83	5663	1.36	1.75
$> 90^{th}$ perc	5333	0.61	1.23	5557	0.56	1.13	5638	0.51	1.01	5663	0.39	0.88
SO2 (EEA)	5079	2.96	2.28	5443	2.79	2.21	5520	2.81	2.02	5543	2.75	2.20
> 40 μg/m^3	5087	0.00	0.01	5458	0.00	0.01	5527	0.00	0.02	5562	0.00	0.01
> 20 μg/m^3	5087	0.01	0.05	5458	0.01	0.09	5527	0.01	0.08	5562	0.01	0.05
$> 75^{th}$ perc	5087	0.00	0.01	5458	0.71	1.39	5527	0.72	1.34	5562	0.69	1.43
$> 90^{th}$ perc	5087	0.18	0.57	5458	0.17	0.60	5527	0.15	0.50	5562	0.19	0.77
CO (EEA)	5044	0.60	0.36	5374	0.55	0.32	5416	0.51	0.27	5471	0.48	0.26
> 4 mg/m^3	5049	0.00	0.00	5410	0.00	0.00	5431	0.00	0.01	5513	0.00	0.01
> 4 mg/m^3	5049	0.00	0.00	5410	0.00	0.00	5431	0.00	0.01	5513	0.00	0.01
$> 75^{th}$ perc	5049	2.57	2.41	5410	2.25	2.25	5431	2.05	2.17	5513	1.81	2.11
$> 90^{th}$ perc	5049	1.13	1.82	5410	0.87	1.54	5431	0.69	1.31	5513	0.61	1.23

Notes: The table provides summary statistics for the four biennia: 2015-16, 2016-17, 2017-18 and 2018-19. Panel (I) reports hospitalization rates, and Panel (II) presents in-hospital mortality for acute myocardial infarction (AMI), ST-elevation MI (STEMI), non-ST-elevation MI (NSTEMI), ischemic stroke, hemorrhagic stroke, and chronic obstructive pulmonary disease (COPD). Panel (III) provides summary statistics for air pollution exposure, including daily averages of $PM_{2.5}$ (CAMS and EEA), PM_{10} (EEA), O_3 (EEA), CO (EEA), NO_2 (EEA), and SO_2 (EEA). For each pollutant, the table also reports the number of days exceeding the WHO-defined hazardous thresholds. Air Quality Guidelines, updated 2021 by WHO, for various pollutants: $PM_{2.5}$ has a 1-day limit of 15μg/m^3 (99th percentile: 5 μg/m^3, 3-4 exceedance days/year); PM_{10} has a 1-day limit of 45 μg/m^3 (99th percentile: 15 μg/m^3, 3-4 exceedance days/year); Nitrogen Dioxide ($NO2$) has a 1-hour limit of 200 μg/m^3, a 1-day limit of 25 μg/m^3, and a calendar year limit of 10 μg/m^3 (3-4 exceedance days/year); Sulfur dioxide (SO_2) has 24-hour limit of 40μg/m^3 and a 10 minutes limit of 500; Carbon Monoxide (CO) has a 1-hour limit of 30 mg/m^3, a maximum daily 8-hour mean of 10 mg/m^3, and a 1-day limit of 4 mg/m^3 (3-4 exceedance days/year); Ozone ($O3$) has a maximum daily 8-hour mean of 100 μg/m^3 (99th percentile: 60 μg/m^3, 3-4 exceedance days/year);. Panel (IV) presents the average wind speed, temperature and precipitation. Panel (V) summarises the number of municipalities and hospital institutes for each biennium.

Table A2.3: Summary of Health Outcomes, Mortality, and Pollution Data (2015-2019)

	2015-2016			2016-2017			2017-2018			2018-2019		
	Obs	Mean	SD	Obs	Mean	SD.	Obs	Mean	SD.	Obs	Mean	SD
III. Pollution												
O3 (EEA)	5084	56.41	27.09	5433	55.16	23.46	5569	58.74	24.81	5614	58.93	23.18
> 100 μg/m^3	5087	0.48	1.01	5486	0.27	0.68	5572	0.40	0.86	5621	0.34	0.79
> 100 μg/m^3	5087	0.48	1.01	5486	0.27	0.68	5572	0.40	0.86	5621	0.34	0.79
$> 75^{th}$ perc	5087	1.83	2.10	5486	1.59	1.85	5572	1.90	2.07	5621	1.88	2.00
$> 90^{th}$ perc	5087	0.94	1.50	5486	0.67	1.18	5572	0.91	1.41	5621	0.83	1.35
IV. Weather conditions												
Avg. wind speed	5693	2.46	0.84	5694	2.62	0.85	5698	2.73	0.90	5687	2.58	0.86
Avg. temperature	5693	15.75	6.85	5694	15.34	6.78	5698	15.16	7.18	5687	15.93	6.84
Precipitations	5693	1.82	1.41	5694	1.91	1.44	5698	1.90	1.53	5687	1.87	1.66
V. Data Coverage												
Municipalities		477			482			478			479	
Hospital Institutes		911			912			874			869	

Notes: The table provides summary statistics for the four biennia: 2015-16, 2016-17, 2017-18 and 2018-19. Panel (I) reports hospitalization rates, and Panel (II) presents in-hospital mortality for acute myocardial infarction (AMI), ST-elevation MI (STEMI), non-ST-elevation MI (NSTEMI), ischemic stroke, hemorrhagic stroke, and chronic obstructive pulmonary disease (COPD). Panel (III) provides summary statistics for air pollution exposure, including daily averages of $PM_{2.5}$ (CAMS and EEA), PM_{10} (EEA), O_3 (EEA), CO (EEA), NO_2 (EEA), and SO_2 (EEA). For each pollutant, the table also reports the number of days exceeding the WHO-defined hazardous thresholds. Air Quality Guidelines, updated 2021 by WHO, for various pollutants: $PM_{2.5}$ has a 1-day limit of 15μg/m^3 (99th percentile: 5 μg/m^3, 3-4 exceedance days/year); PM_{10} has a 1-day limit of 45 μg/m^3 (99th percentile: 15 μg/m^3, 3-4 exceedance days/year); Nitrogen Dioxide ($NO2$) has a 1-hour limit of 200 μg/m^3, a 1-day limit of 25 μg/m^3, and a calendar year limit of 10 μg/m^3 (3-4 exceedance days/year); Sulfur dioxide (SO_2) has 24-hour limit of 40μg/m^3 and a 10 minutes limit of 500; Carbon Monoxide (CO) has a 1-hour limit of 30 mg/m^3, a maximum daily 8-hour mean of 10 mg/m^3, and a 1-day limit of 4 mg/m^3 (3-4 exceedance days/year); Ozone ($O3$) has a maximum daily 8-hour mean of 100 μg/m^3 (99th percentile: 60 μg/m^3, 3-4 exceedance days/year);. Panel (IV) presents the average wind speed, temperature and precipitation. Panel (V) summarises the number of municipalities and hospital institutes for each biennium.

Table A2.4: 2021 World Health Organization (WHO) air quality guidelines (AQGs)

	$PM_{2.5}$	PM_{10}	NO_2	SO2	CO	O3
Annual	5	15	10	-	-	60
Daily	15	45	25	40	4	100

Notes: Air Quality Guidelines, updated 2021 by WHO, for various pollutants: $PM_{2.5}$ has a 1-day limit of 15μg/m^3 (99th percentile: 5 μg/m^3, 3-4 exceedance days/year); PM_{10} has a 1-day limit of 45 μg/m^3 (99th percentile: 15 μg/m^3, 3-4 exceedance days/year); Nitrogen Dioxide ($NO2$) has a 1-hour limit of 200 μg/m^3, a 1-day limit of 25 μg/m^3, and a calendar year limit of 10 μg/m^3 (3-4 exceedance days/year); Sulfur dioxide (SO_2) has 24-hour limit of 40μg/m^3 and a 10 minutes limit of 500; Carbon Monoxide (CO) has a 1-hour limit of 30 mg/m^3, a maximum daily 8-hour mean of 10 mg/m^3, and a 1-day limit of 4 mg/m^3 (3-4 exceedance days/year); Ozone ($O3$) has a maximum daily 8-hour mean of 100 μg/m^3 (99th percentile: 60 μg/m^3, 3-4 exceedance days/year);.

Table A2.5: Impact of Heating system activation on $PM_{2.5}$ EEA (2015-2019)

	2015-2016	2016-2017	2017-2018	2018-2019
	(1)	(2)	(3)	(4)
A. Average Effects				
ATT	7.127***	5.675***	6.967***	5.215***
	(1.171)	(1.043)	(1.256)	(0.763)
Parallel-trends test				
$\chi^2 2$	83.51	137.6	191.7	1539
p-value	0	0	0	0
df	16	18	18	19
Mean of Y	19	18.17	16.31	15.67
SD of Y	12.29	11.93	9.622	8.922
Observations	3,792	4,434	4,819	5,169
B. Above 75th Percentile				
ATT	0.993***	0.811***	0.984***	0.865***
	(0.166)	(0.150)	(0.196)	(0.125)
Parallel-trends test				
χ^2	194.8	193.7	106.8	78.02
p-value	0	0	0	4.08e-09
df	16	18	18	19
Mean of Y	1.302	1.154	0.994	0.840
SD of Y	1.887	1.683	1.544	1.482
Observations	3,831	4,446	4,889	5,307

Notes: This table presents difference-in-differences estimates of the average treatment effect on the treated (ATT) of heating system activation on $PM_{2.5}$ EEA levels. Panel A shows effects on average $PM_{2.5}$ EEA levels, while Panel B focuses on the upper quartile of the outcome distribution. Standard errors at municipal level are in parentheses; *** p<0.01, ** p<0.05, * p<0.1.

Table A2.6: Impact of Heating system activation on PM_{10} EEA (2015-2019)

	2015-2016	2016-2017	2017-2018	2018-2019
	(1)	(2)	(3)	(4)
A. Average Effects				
ATT	6.776***	5.232***	7.331***	5.038***
	(1.153)	(0.972)	(1.480)	(0.810)
Parallel-trends test				
χ^2	302.8	516.7	179.4	771.8
p-value	0	0	0	0
df	18	22	18	19
Mean of Y	27.01	26.56	25.29	25.45
SD of Y	13.57	13.66	12.12	11.54
Observations	4,320	4,763	4,965	5,088
B. Above 75th Percentile				
ATT	0.709***	0.530***	0.651***	0.500***
	(0.111)	(0.0986)	(0.134)	(0.0891)
Parallel-trends test				
χ^2	295.2	147.2	132.1	96.48
p-value	0	0	0	0
df	18	18	18	19
Mean of Y	0.737	0.715	0.647	0.593
SD of Y	1.392	1.235	1.118	1.116
Observations	4,366	4,840	5,000	5,201

Notes: This table presents difference-in-differences estimates of the average treatment effect on the treated (ATT) of heating system activation on PM_{10} EEA levels. Panel A shows effects on average PM_{10} EEA levels, while Panel B focuses on the upper quartile of the outcome distribution. Standard errors at municipal level are in parentheses; *** p<0.01, ** p<0.05, * p<0.1.

Table A2.7: Impact of Heating system activation on SO_2 EEA (2015-2019)

	2015-2016	2016-2017	2017-2018	2018-2019
	(1)	(2)	(3)	(4)
A. Average Effects				
ATT	0.211	0.528***	0.447***	0.627***
	(0.200)	(0.197)	(0.141)	(0.188)
Parallel-trends test				
χ^2	104.5	152.1	98.66	35.30
p-value	0	0	0	0.0129
df	16	18	18	19
Mean of Y	2.994	2.864	2.815	2.753
SD of Y	2.400	2.437	2.211	2.424
Observations	4,265	4,728	4,973	5,204
B. Above 75th Percentile				
ATT	-0.0622	0.0733	0.0203	0.130**
	(0.0486)	(0.0490)	(0.0573)	(0.0599)
Parallel-trends test				
χ^2	44.28	43.11	45.52	48.25
p-value	0.000179	0.000771	0.000348	0.000236
df	16	18	18	19
Mean of Y	0.159	0.171	0.130	0.183
SD of Y	0.588	0.679	0.533	0.867
Observations	4,273	4,839	5,009	5,282

Notes: This table presents difference-in-differences estimates of the average treatment effect on the treated (ATT) of heating system activation on SO_2 EEA levels. Panel A shows effects on average SO_2 EEA levels, while Panel B focuses on the upper quartile of the outcome distribution. Standard errors at municipal level are in parentheses; *** p<0.01, ** p<0.05, * p<0.1.

Table A2.8: Impact of Heating system activation on *CO* EEA (2015-2019)

	2015-2016	2016-2017	2017-2018	2018-2019
	(1)	(2)	(3)	(4)
A. Average Effects				
ATT	0.0470**	-0.00676	0.0725**	-0.00286
	(0.0216)	(0.0219)	(0.0290)	(0.0217)
Parallel-trends test				
χ^2	1170	250.1	69.54	96.65
p-value	0	0	5.41e-08	0
df	18	18	18	19
Mean of Y	0.607	0.545	0.503	0.479
SD of Y	0.397	0.332	0.300	0.282
Observations	4,240	4,623	4,742	4,867
B. Above 75th Percentile				
ATT	0.179	0.0711	0.502***	0.0806
	(0.135)	(0.134)	(0.135)	(0.131)
Parallel-trends test				
χ^2	4799	36.20	53.93	37.62
p-value	0	0.00665	1.88e-05	0.00663
df	18	18	18	19
Mean of Y	1.138	0.861	0.648	0.561
SD of Y	1.976	1.681	1.387	1.339
Observations	4,252	4,729	4,848	4,946

Notes: This table presents difference-in-differences estimates of the average treatment effect on the treated (ATT) of heating system activation on *CO* EEA levels. Panel A shows effects on average *CO* EEA levels, while Panel B focuses on the upper quartile of the outcome distribution. Standard errors at municipal level are in parentheses; *** p<0.01, ** p<0.05, * p<0.1.

Table A2.9: Impact of Heating system activation on O_3 EEA (2015-2019)

	2015-2016	2016-2017	2017-2018	2018-2019
	(1)	(2)	(3)	(4)
A. Average Effects				
ATT	-9.277***	-6.372***	-11.06***	-8.808***
	(1.841)	(1.831)	(1.800)	(1.725)
Parallel-trends test				
χ^2	630.3	1350	98.28	171.9
p-value	0	0	0	0
df	16	24	18	18
Mean of Y	55.92	54.71	58.78	59.13
SD of Y	28.17	24.59	26.05	24.76
Observations	4,242	4,641	4,992	5,150
B. Above 75th Percentile				
ATT	0.129	-0.0456	-0.459***	-0.0653
	(0.164)	(0.136)	(0.153)	(0.128)
Parallel-trends test				
χ^2	229.1	138.4	97.85	158.1
p-value	0	0	0	0
df	16	18	18	18
Mean of Y	0.932	0.675	0.934	0.869
SD of Y	1.606	1.302	1.559	1.524
Observations	4,251	4,722	5,044	5,208

Notes: This table presents difference-in-differences estimates of the average treatment effect on the treated (ATT) of heating system activation on O_3 EEA levels. Panel A shows effects on average O_3 EEA levels, while Panel B focuses on the upper quartile of the outcome distribution. Standard errors at municipal level are in parentheses; *** p<0.01, ** p<0.05, * p<0.1.

Table A2.10: Average Treatment Effects of heating system activation under alternative treatment threshold definitions on: Pollutant Concentrations (Left Panel) vs. Regulatory Threshold Exceedances (Right Panel), across 2015-2019

	Pollutant Concentration				Days Over Threshold			
	2015-16	2016-17	2017-18	2018-19	2015-16	2016-17	2017-18	2018-19
PM 2.5 (CAMS)								
Above vs below median	3.070***	0.831*	3.423***	3.416***	0.610***	0.102	0.711***	0.759***
	(0.528)	(0.445)	(0.696)	(0.538)	(0.120)	(0.0979)	(0.147)	(0.131)
Above 66-33 percentile	3.970***	1.160	4.611***	4.611***	0.970***	0.148	0.969***	0.969***
	(0.784)	(0.728)	(0.781)	(0.781)	(0.228)	(0.154)	(0.187)	(0.187)
Above 75-25 percentile	5.971***	2.152**	5.606***	5.677***	1.604***	0.304	1.208***	1.256***
	(0.863)	(1.029)	(0.961)	(0.915)	(0.239)	(0.213)	(0.195)	(0.190)
PM 2.5 (EEA)								
Above vs below median	7.127***	5.675***	6.967***	5.215***	0.993***	0.811***	0.984***	0.865***
	(1.171)	(1.043)	(1.256)	(0.763)	(0.166)	(0.150)	(0.196)	(0.125)
Above 66-33 percentile	7.127***	5.675***	6.967***	5.215***	0.987***	0.591**	1.125***	1.125***
	(1.171)	(1.043)	(1.256)	(0.763)	(0.212)	(0.257)	(0.214)	(0.214)
Above 75-25 percentile	12.65***	8.576***	12.53***	9.582***	1.798***	1.070***	1.697***	1.412***
	(1.468)	(2.099)	(1.788)	(1.416)	(0.175)	(0.309)	(0.265)	(0.209)
PM 10 (EEA)								
Above vs below median	6.776***	5.232***	7.331***	5.038***	0.709***	0.530***	0.651***	0.500***
	(1.153)	(0.972)	(1.480)	(0.810)	(0.111)	(0.0986)	(0.134)	(0.0891)
Above 66-33 percentile	6.206***	4.865***	7.073***	7.073***	0.848***	0.559***	0.616***	0.616***
	(1.766)	(1.861)	(1.411)	(1.411)	(0.131)	(0.176)	(0.148)	(0.148)
Above 75-25 percentile	14.06***	11.23***	16.61***	10.36***	1.240***	0.940***	1.238***	0.881***
	(1.645)	(1.949)	(1.877)	(1.399)	(0.138)	(0.188)	(0.158)	(0.128)
NO2 (EEA)								
Above vs below median	4.896***	2.628***	4.457***	3.091***	0.769***	0.543***	0.600***	0.556***
	(0.998)	(0.804)	(0.873)	(0.619)	(0.124)	(0.116)	(0.113)	(0.0806)
Above 66-33 percentile	6.860***	2.391*	4.130***	4.130***	0.886***	0.617***	0.734***	0.734***
	(1.244)	(1.332)	(1.090)	(1.090)	(0.179)	(0.192)	(0.0831)	(0.0831)
Above 75-25 percentile	7.811***	4.767***	12.84***	6.126***	1.004***	0.906***	1.458***	0.899***
	(1.862)	(1.762)	(1.688)	(1.201)	(0.256)	(0.186)	(0.150)	(0.0870)

Notes: This table presents difference-in-differences estimates of the Average Treatment Effect on the Treated (ATT) of residential heating activation under alternative treatment thresholds. The left panel reports effects on air pollutant concentrations ($PM_{2.5}$, PM_{10}, and NO_2, measured in μg/m^3), while the right panel shows effects on annual exceedance days of regulatory thresholds. Treatment effects are estimated for three comparison groups: (i) above versus below median exposure, (ii) above the 66$^{\text{th}}$ versus below the 33$^{\text{rd}}$ percentile, and (iii) above the 75$^{\text{th}}$ versus below the 25$^{\text{th}}$ percentile of the treatment intensity distribution. Standard errors appear in parentheses with *** $p < 0.01$, ** $p < 0.05$, and * $p < 0.1$.

Table A2.11: Average Treatment Effects of heating system activation under Alternative Treatment Threshold Definitions on: Hospitalizations (Left Panel) vs. In-hospital mortality rates (Right Panel), across 2015-2019

	Hospitalizations				In-hospital mortality			
	2015-16	2016-17	2017-18	2018-19	2015-16	2016-17	2017-18	2018-19
AMI								
Above vs below median	1.215*	0.865	2.844***	2.675***	0.385***	-0.0224	-0.0475	0.113
	(0.648)	(0.755)	(0.768)	(0.489)	(0.147)	(0.149)	(0.249)	(0.110)
Above 66-33 percentile	1.639*	-0.266	2.520**	2.935***	0.711***	0.0283	-0.148	0.258*
	(0.964)	(1.138)	(1.252)	(0.710)	(0.200)	(0.185)	(0.192)	(0.136)
Above 75-25 percentile	2.603**	-0.652	2.984**	2.757***	1.111***	-0.0165	-0.235	0.390***
	(1.287)	(1.204)	(1.201)	(0.737)	(0.218)	(0.264)	(0.227)	(0.150)
STEMI								
Above vs below median	0.591	0.100	1.051***	1.180***	0.287**	-0.0130	0.0448	0.0492
	(0.441)	(0.402)	(0.359)	(0.290)	(0.116)	(0.106)	(0.106)	(0.0810)
Above 66-33 percentile	1.577***	-0.402	1.439**	1.590***	0.503***	0.0693	-0.150	0.0960
	(0.460)	(0.692)	(0.709)	(0.389)	(0.188)	(0.0964)	(0.148)	(0.0857)
Above 75-25 percentile	1.666**	-0.340	1.442**	1.290***	0.940***	0.0896	-0.134	0.131
	(0.676)	(0.940)	(0.676)	(0.439)	(0.183)	(0.133)	(0.140)	(0.0888)
NSTEMI								
Above vs below median	0.326	0.665	1.746***	1.355***	0.0835	0.0613	0.0105	0.161***
	(0.457)	(0.582)	(0.560)	(0.385)	(0.0909)	(0.0739)	(0.0889)	(0.0577)
Above 66-33 percentile	-0.436	0.311	1.673**	1.148**	0.0959	0.133	0.120	0.212***
	(0.659)	(1.035)	(0.710)	(0.550)	(0.0840)	(0.0968)	(0.0789)	(0.0775)
Above 75-25 percentile	0.245	0.0417	1.333*	1.047*	0.0387	0.125	0.0827	0.286***
	(0.663)	(0.775)	(0.787)	(0.556)	(0.103)	(0.125)	(0.101)	(0.0845)
Ischemic Stroke								
Above vs below median	0.532	2.850	0.961	-0.661	0.164	0.234	0.0515	0.182
	(0.857)	(2.101)	(1.475)	(0.521)	(0.262)	(0.201)	(0.233)	(0.144)
Above 66-33 percentile	-0.572	1.964	2.554*	-1.552	-0.0435	0.501	-0.295	-0.174
	(1.710)	(1.391)	(1.481)	(1.184)	(0.487)	(0.311)	(0.250)	(0.161)
Above 75-25 percentile	-0.193	3.620*	2.931*	-1.432	-0.517	0.999**	-0.465	-0.0734
	(2.829)	(1.956)	(1.716)	(1.091)	(0.776)	(0.397)	(0.366)	(0.184)
Hemorrhagic Stroke								
Above vs below median	0.511	1.310*	0.991	0.0552	0.446***	-0.0100	0.528*	0.124
	(0.555)	(0.783)	(0.646)	(0.427)	(0.173)	(0.164)	(0.280)	(0.128)
Above 66-33 percentile	-0.294	0.149	3.089	0.0972	0.336	-0.342	1.481**	0.142
	(0.679)	(0.706)	(2.031)	(0.641)	(0.248)	(0.272)	(0.619)	(0.186)
Above 75-25 percentile	-0.898	0.679	5.726**	0.782	0.479	-0.351	2.027***	0.307
	(1.108)	(0.882)	(2.252)	(0.621)	(0.332)	(0.368)	(0.750)	(0.200)
COPD								
Above vs below median	2.136**	1.279*	2.284**	1.828***	-0.00365	0.0559	0.0459	-0.0565
	(0.916)	(0.668)	(1.016)	(0.664)	(0.0822)	(0.113)	(0.137)	(0.0923)
Above 66-33 percentile	2.752***	1.523	2.889***	2.721***	0.0299	0.0389	0.0648	0.0257
	(0.999)	(1.345)	(0.904)	(0.850)	(0.131)	(0.149)	(0.130)	(0.113)
Above 75-25 percentile	2.997***	1.476	4.028***	3.122***	-0.162	-0.136	0.0319	0.0118
	(0.916)	(2.050)	(1.146)	(1.100)	(0.146)	(0.172)	(0.186)	(0.147)

Notes: This table presents difference-in-differences estimates of the Average Treatment Effect on the Treated (ATT) under alternative treatment thresholds. The left panel shows effects on the number of hospitalizations, while the right panel reports effects on in-hospital mortality rate for AMI, STEMI, NSTEMI, Ischemic Stroke, Hemorrhagic Stroke and COPD. Treatment effects are estimated for three comparison groups: (i) above versus below median, (ii) above the 66^{th} vs. below the 33^{rd} percentile, and (iii) above the 75^{th} vs. below the 25^{th} percentile based on the treatment intensity distribution. Standard errors are reported in parentheses. Significance levels: *** $p < 0.01$, ** $p < 0.05$, * $p < 0.1$.

Table A2.12: Robust Inference and Sensitivity Analysis on pollutants concentration using Honest DiD

	Average					Above 75-th Percentile				
	Lag 1	Lag 2	Lag 3	Lag 4	Lag 5	Lag 1	Lag 2	Lag 3	Lag 4	Lag 5
PM 2.5 (CAMS)										
2015-2016	0-25%	50-75%	75-100%	150-175%	100-125%	0-25%	50-75%	75-100%	150-175%	100-125%
2016-2017	50-75%	0-25%	100-125%	75-100%	75-100%	50-75%	0-25%	100-125%	75-100%	75-100%
2017-2018	50-75%	100-125%	50-75%	75-100%	100-125%	50-75%	100-125%	50-75%	75-100%	100-125%
2018-2019	25-50%	50-75%	75-100%	100-125%	125-150%	25-50%	50-75%	75-100%	100-125%	125-150%
PM 2.5 (EEA)										
2015-2016	0-25%	25-50%	100-125%	150-175%	100-125%	0-25%	25-50%	100-125%	150-175%	100-125%
2016-2017	-	50-75%	100-125%	75-100%	125-150%	-	50-75%	100-125%	75-100%	125-150%
2017-2018	25-50%	75-100%	75-100%	100-125%	100-125%	25-50%	75-100%	75-100%	100-125%	100-125%
2018-2019	25-50%	50-75%	75-100%	125-150%	100-125%	25-50%	50-75%	75-100%	125-150%	100-125%
PM 10 (EEA)										
2015-2016	-	25-50%	100-125%	150-175%	100-125%	-	25-50%	100-125%	150-175%	100-125%
2016-2017	-	25-50%	100-125%	75-100%	125-150%	-	25-50%	100-125%	75-100%	125-150%
2017-2018	25-50%	75-100%	75-100%	100-125%	75-100%	25-50%	75-100%	75-100%	100-125%	75-100%
2018-2019	25-50%	25-50%	50-75%	100-125%	75-100%	25-50%	25-50%	50-75%	100-125%	75-100%
NO_2 (EEA)										
2015-2016	-	25-50%	75-100%	75-100%	75-100%	-	25-50%	75-100%	75-100%	75-100%
2016-2017	-	25-50%	75-100%	75-100%	50-75%	-	25-50%	75-100%	75-100%	50-75%
2017-2018	25-50%	75-100%	75-100%	100-125%	75-100%	25-50%	75-100%	75-100%	100-125%	75-100%
2018-2019	-	25-50%	25-50%	75-100%	75-100%	-	25-50%	25-50%	75-100%	75-100%

Notes: This table reports the sensitivity analysis based on the Honest Difference-in-Differences framework developed by Rambachan & Roth (2023). The left panel presents results averaged across different lag specifications, while the right panel shows results for the top quartile of the treatment distribution (above the 75-th percentile). Lag columns correspond to treatment lags of 1 to 5 months before heating system activation. "-" indicates insufficient data for robust estimation in that cell.

Table A2.13: Robust Inference and Sensitivity Analysis on Hospitalisations Outcomes using Honest DiD

	Years	Lag 1	Lag 2	Lag 3	Lag 4	Lag 5
		(1)	(2)	(3)	(4)	(5)
Hospitalisations						
AMI	2015-2016	-	-	-	-	-
	2017-2018	-	50-75%	-	25-50%	25-50%
STEMI	2017-2018	-	25-50%	-	25-50%	-
NSTEMI	2017-2018	-	25-50%	-	-	25-50%
COPD	2015-2016	-	25-50%	25-50%	25-50%	25-50%
	2017-2018	-	25-50%	50-75%	50-75%	75-100%

Notes: This table shows sensitivity analyses for health-related hospitalisation outcomes using the Honest Difference-in-Differences methodology (Rambachan & Roth (2023)). Each column corresponds to a different lag (1–5 months before heating activation) between exposure and outcome. Dash "-" indicates insufficient data for robust estimation in that cell.

Table A2.14: Average Treatment Effects Estimates of heating system activation on Placebo Outcomes: Hospitalization Rates (left panel) and In-Hospital Mortality Rates (right panel) × 10,000 Inhabitants, across 2015-2019

	Hospitalizations				In-Hospital Mortality			
	2015-16	2016-17	2017-18	2018-19	2015-16	2016-17	2017-18	2018-19
	(1)	(2)	(3)	(4)	(1)	(2)	(3)	(4)
Fractures								
ATT	0.427	-0.595	1.707	0.449	0.0921	0.0625	-0.0428	-0.0111
	(1.186)	(0.995)	(2.249)	(1.325)	(0.0765)	(0.0538)	(0.0648)	(0.0386)
Infections								
ATT	0.207	-0.0814	0.00873	-0.446	-0.0369	0.0504	0.0247	-0.0751
	(0.886)	(0.476)	(0.550)	(0.386)	(0.0693)	(0.0832)	(0.148)	(0.0810)
Traumatism								
ATT	-0.128*	0.0243	0.127	0.193*	0.00320	0.0242	-0.00116	0.00542
	(0.0654)	(0.0879)	(0.238)	(0.116)	(0.0139)	(0.0224)	(0.00607)	(0.0140)
Poisoning								
ATT	-0.0387	-0.0228	-0.0307	0.0214	-0.00780	-0.00116	0.00218	0.00218
	(0.0714)	(0.0671)	(0.0321)	(0.0529)	(0.00780)	(0.00132)	(0.00209)	(0.00265)
Elective admissions								
ATT	-9.652	13.55	-2.683	5.595	-0.0290	-0.230	0.0206	-0.0549
	(9.142)	(18.68)	(10.92)	(6.251)	(0.243)	(0.143)	(0.166)	(0.0973)
Nervous system								
ATT	-1.299	11.43	-2.018	-0.138	-0.0485	0.00298	-0.0579	0.0582
	(2.523)	(13.60)	(9.408)	(0.378)	(0.0507)	(0.0487)	(0.0492)	(0.0549)
Mental health								
ATT	-0.532	0.0649	-1.364	0.931	0.000827	0.0384	-0.000147	0.0365**
	(0.380)	(0.642)	(0.950)	(0.755)	(0.0132)	(0.0311)	(0.0112)	(0.0147)

Notes: The left panel reports ATT estimates for hospitalization rates, while the right panel shows estimates for in-hospital mortality rates. All outcomes are measured × 10,000 inhabitants. Standard errors in parentheses. *** p<0.01, ** p<0.05, * p<0.1.

Table A2.15: ICD9-CM Classification of Placebo Outcomes

Variable	**ICD9-CM Classification**[22]	**Explanation**
Trauma	(dpr_3_n $\geq$ 800 and dpr_3_n $\leq$ 904) OR (dsec1_3_n $\geq$ 800 and dsec1_3_n $\leq$ 904)	Fractures, dislocations, and injuries
Nutrition	dpr_3_n = 783	Symptoms related to nutrition, metabolism, and development
Traumatism	dpr_3_n $\geq$ 950 and dpr_3_n $\leq$ 959	Traumatisms of nervous system and spinal cord, including traumatic complications
Poisoning	dpr_3_n $\geq$ 960 and dpr_3_n $\leq$ 979	Poisoning from drugs, medicines and biological substances
Elective	tiporic = 1	Planned/elective hospital admissions
Nervous System	dpr_3_n $\geq$ 320 and dpr_3_n $\leq$ 389	Diseases of nervous system and sensory organs
Mental Health	dpr_3_n $\geq$ 290 and dpr_3_n $\leq$ 319	Mental and behavioral disorders

Notes: This table presents the ICD-9-CM classification criteria used to identify placebo outcomes in the analysis. The diagnostic codes are drawn from primary diagnosis fields (dpr_3_n) and secondary diagnosis fields (dsec1_3_n) where specified.

Table A2.16: Robustness of Average Treatment Effects of heating system activation to alternative estimation strategies: population weighting, spillover adjustment, and augmented IPW estimation

	Pollutant Concentration				Days Over Threshold			
	2015-16	2016-17	2017-18	2018-19	2015-16	2016-17	2017-18	2018-19
PM 2.5 (CAMS)								
Weighted	3.956***	1.211**	3.676***	4.434***	0.861***	0.187	0.816***	0.948***
	(0.603)	(0.536)	(0.779)	(0.562)	(0.142)	(0.131)	(0.164)	(0.140)
Neighbors	2.408***	0.415	2.588***	1.813***	0.425***	0.031	0.527***	0.351**
	(0.576)	(0.456)	(0.765)	(0.620)	(0.132)	(0.102)	(0.166)	(0.159)
AIPW	3.424***	1.736**	6.171***	3.551***	0.567***	0.301*	1.239***	0.816***
	(0.524)	(0.764)	(1.791)	(0.470)	(0.114)	(0.164)	(0.323)	(0.126)
PM 2.5 (EEA)								
Weighted	8.979***	6.416***	7.522***	5.513***	1.223***	0.904***	1.017***	0.912***
	(1.302)	(1.178)	(1.248)	(0.667)	(0.158)	(0.170)	(0.206)	(0.118)
Neighbors	6.690***	4.889***	5.977***	3.186***	0.892***	0.631***	0.794***	0.468***
	(1.072)	(0.965)	(1.305)	(0.855)	(0.160)	(0.139)	(0.201)	(0.146)
AIPW	8.767***	6.265***	9.183***	5.236***	1.202***	0.879***	1.368***	0.900***
	(1.332)	(1.175)	(1.902)	(0.692)	(0.191)	(0.164)	(0.304)	(0.122)
NO_2 (EEA)								
Weighted	7.649***	3.466***	4.372***	4.547***	1.202***	0.725***	0.959***	0.866***
	(1.122)	(0.998)	(1.345)	(0.765)	(0.183)	(0.176)	(0.200)	(0.147)
Neighbors	5.026***	2.157***	3.612***	1.453***	0.744***	0.456***	0.474***	0.456***
	(0.742)	(0.706)	(0.735)	(0.551)	(0.086)	(0.088)	(0.098)	(0.065)
AIPW	3.956***	3.840***	5.324***	3.124***	0.776***	0.612***	1.143***	0.543***
	(1.087)	(0.840)	(1.471)	(0.550)	(0.119)	(0.120)	(0.303)	(0.087)
O_3 (EEA)								
Weighted	-10.26***	-6.411***	-10.04***	-11.62***	0.230	0.049	-0.406*	-0.132
	(1.995)	(2.257)	(2.340)	(2.177)	(0.175)	(0.223)	(0.219)	(0.144)
Neighbors	-7.933***	-3.846**	-8.340***	-4.017**	0.064	-0.049	-0.337***	0.001
	(1.732)	(1.646)	(1.666)	(1.586)	(0.131)	(0.110)	(0.126)	(0.112)
AIPW	-10.44***	-6.546***	-10.11***	-11.34***	0.004	-0.054	-0.246	-0.131
	(2.034)	(2.234)	(2.674)	(2.345)	(0.214)	(0.139)	(0.248)	(0.123)

Notes: This table extends the main results by applying alternative estimation strategies. Specifically, we consider: (i) weighting estimates by the municipal population, (ii) adjusting for potential spillover effects from neighboring municipalities within a 30 km radius, and (iii) using the augmented Inverse Probability Weighting (AIPW) version of the Callaway & Sant'Anna (2021) estimator. The left panel reports effects on air pollutant concentrations ($PM_{2.5}$, PM_{10}, NO_2, and O_3, measured in $\mu g/m^3$), while the right panel presents effects on the number of days exceeding regulatory pollution thresholds. Standard errors are reported in parentheses. Significance levels: *** $p < 0.01$, ** $p < 0.05$, * $p < 0.1$.

Table A2.17: Robustness of Average Treatment Effects of heating system activation on hospitalisations and in-hospital mortality to alternative estimation strategies: population weighting, spillover adjustment, and augmented IPW estimation

	Hospitalizations				In-hospital Mortality			
	2015-16	2016-17	2017-18	2018-19	2015-16	2016-17	2017-18	2018-19
AMI								
Weighted by population	0.832	0.713	1.740***	1.893***	0.292***	-0.0267	0.0507	0.112
	(0.506)	(0.570)	(0.567)	(0.358)	(0.0855)	(0.103)	(0.122)	(0.0730)
Nearest neighbours	1.475**	1.117	3.084***	2.669***	0.408***	-0.0293	-0.000410	0.0660
	(0.646)	(0.908)	(0.888)	(0.567)	(0.141)	(0.169)	(0.243)	(0.125)
AIPW	1.515*	0.0234	4.263***	2.951***	0.242*	-0.128	-0.221	0.0441
	(0.885)	(1.078)	(1.443)	(0.536)	(0.143)	(0.158)	(0.255)	(0.107)
STEMI								
Weighted by population	0.407*	0.151	0.804***	0.482**	0.163***	0.0131	0.0899	0.0211
	(0.246)	(0.258)	(0.263)	(0.233)	(0.0602)	(0.0655)	(0.0696)	(0.0547)
Nearest neighbours	0.715*	0.170	1.159***	1.170***	0.293**	-0.0419	0.0529	0.0195
	(0.406)	(0.445)	(0.367)	(0.304)	(0.114)	(0.126)	(0.101)	(0.0882)
AIPW	0.230	-0.0452	1.677***	1.159***	0.243**	-0.116	-0.0257	-0.0258
	(0.701)	(0.337)	(0.600)	(0.272)	(0.111)	(0.109)	(0.104)	(0.0748)
NSTEMI								
Weighted by population	0.299	0.530	0.959**	1.290***	0.113***	-0.00165	-0.00805	0.130***
	(0.375)	(0.441)	(0.379)	(0.257)	(0.0430)	(0.0521)	(0.0525)	(0.0447)
Nearest neighbours	0.486	0.826	1.865***	1.408***	0.117	0.0859	0.0204	0.138**
	(0.507)	(0.719)	(0.621)	(0.470)	(0.0947)	(0.0802)	(0.0864)	(0.0642)
AIPW	0.784	0.0162	2.393**	1.719***	-0.000670	0.0387	-0.0392	0.130**
	(0.579)	(0.985)	(1.033)	(0.465)	(0.0877)	(0.0788)	(0.0914)	(0.0578)
Ischemic Stroke								
Weighted by population	0.625	1.323***	1.075**	0.352	0.192**	0.241***	0.0859	0.0580
	(0.464)	(0.496)	(0.495)	(0.291)	(0.0961)	(0.0914)	(0.111)	(0.0875)
Nearest neighbours	0.554	2.358	0.983	-0.489	0.188	0.235	0.0480	0.208
	(0.900)	(2.116)	(1.386)	(0.613)	(0.268)	(0.218)	(0.270)	(0.142)
AIPW	0.232	4.404	2.457	-0.505	0.0683	0.143	-0.0564	0.0834
	(1.114)	(2.865)	(2.014)	(0.519)	(0.264)	(0.199)	(0.235)	(0.138)
Hemorrhagic Stroke								
Weighted by population	0.243	0.272	0.772**	0.478**	0.228**	-0.0258	0.398***	0.175**
	(0.252)	(0.264)	(0.300)	(0.206)	(0.0916)	(0.129)	(0.127)	(0.0839)
Nearest neighbours	0.612	1.334*	1.010*	0.243	0.521***	0.0601	0.552**	0.190
	(0.605)	(0.772)	(0.576)	(0.571)	(0.202)	(0.183)	(0.270)	(0.147)
AIPW	1.813	1.700	0.998	0.612	0.258	-0.0233	0.426	0.0177
	(1.277)	(1.221)	(0.836)	(0.583)	(0.161)	(0.163)	(0.278)	(0.112)
COPD								
Weighted by population	1.418**	1.051**	1.980***	1.425***	-0.0567	0.111**	0.0473	0.0129
	(0.567)	(0.498)	(0.490)	(0.379)	(0.0557)	(0.0539)	(0.0675)	(0.0516)
Nearest neighbours	2.527***	1.326*	2.426**	1.448*	0.0231	0.0313	0.0378	-0.0487
	(0.922)	(0.724)	(1.058)	(0.812)	(0.0906)	(0.129)	(0.136)	(0.109)
AIPW	2.026***	0.478	1.981**	1.553**	0.0154	-0.0121	-0.0278	-0.135
	(0.747)	(0.702)	(0.972)	(0.687)	(0.0750)	(0.117)	(0.140)	(0.0885)

Notes: This table extends the main results by applying alternative estimation strategies. Specifically, we consider: (i) weighting estimates by the municipal population, (ii) adjusting for potential spillover effects from neighboring municipalities within a 30 km radius, and (iii) using the augmented Inverse Probability Weighting (AIPW) version of the Callaway & Sant'Anna (2021) estimator. The left panel reports effects on hospitalisations, while the right panel presents effects on in-hospital mortality for AMI, STEMI, NSTEMI, Ischemic Stroke, Hemorrhagic Stroke and COPD. Standard errors are reported in parentheses. Significance levels: *** $p < 0.01$, ** $p < 0.05$, * $p < 0.1$.

Table A2.18: Correlations of environmental pollutants on immigration, emigration, and net inflow in municipalities.

	Immigration	Emigration	Net inflow	Immigration	Emigration	Net inflow	Immigration	Emigration	Net inflow	Immigration	Emigration	Net inflow	Immigration	Emigration	Net inflow
	(1)	(2)	(3)	(4)	(5)	(6)	(7)	(8)	(9)	(10)	(11)	(12)	(13)	(14)	(15)
PM 2.5 (CAMS), Lag 1	-1.3361	3.7390	-5.0743	-4.8826	2.0633	-6.9459	-4.8273	1.3445	-6.1719	-0.9815	0.4716	-1.4531	-1.3173	1.7942	-3.1114
	(3.023)	(2.627)	(3.862)	(3.912)	(3.498)	(4.904)	(4.308)	(3.812)	(5.372)	(4.666)	(4.006)	(5.709)	(4.944)	(4.216)	(6.031)
NO2 (EEA), Lag 1				2.7043	7.5399***	-4.8355	2.4101	6.4567**	-4.0465	2.6038	6.1740**	-3.5703	3.8393	5.8729**	-2.0337
				(2.740)	(2.479)	(3.502)	(2.967)	(2.646)	(3.816)	(3.058)	(2.644)	(3.979)	(3.201)	(2.742)	(4.138)
SO2 (EEA), Lag 1							-4.3876	-1.0269	-3.3607	-1.4938	-6.3786**	4.8847	-4.6919	-5.1081	0.4163
							(2.980)	(3.172)	(4.363)	(3.081)	(2.802)	(4.174)	(3.401)	(3.108)	(4.477)
CO (EEA), Lag 1										2.8905	-1.1187	4.0094	2.7564	-0.6581	3.4145
										(2.085)	(1.924)	(2.648)	(2.189)	(2.027)	(2.758)
O3 (EEA), Lag 1													2.4262	-2.5389	4.9651
													(2.869)	(2.763)	(3.732)
Income, Lag 1	0.0004	-0.0009	0.0014	-0.0000	-0.0027	0.0027	0.0002	-0.0025	0.0027	-0.0002	-0.0029	0.0027	0.0002	-0.0035	0.0037
	(0.003)	(0.003)	(0.005)	(0.004)	(0.003)	(0.005)	(0.004)	(0.004)	(0.006)	(0.005)	(0.004)	(0.006)	(0.005)	(0.004)	(0.007)
Wind speed, Lag 1	-2.6279	-2.3748	-0.2523	-6.0093	-3.4196	-2.5898	-4.9947	-3.5573	-1.4376	-4.6514	-2.0895	-2.5620	-0.0179	-3.9357	3.9178
	(3.313)	(3.085)	(4.380)	(4.206)	(3.985)	(5.544)	(4.747)	(4.381)	(6.170)	(5.004)	(4.541)	(6.477)	(5.536)	(4.705)	(6.738)
Precipitations, Lag 1	-0.0106	-5.6074***	5.5980***	-1.1892	-5.1177***	3.9284	-0.6272	-5.5044***	4.8770*	0.6410	-2.4491	3.0900	0.4266	-0.6889	1.1154
	(1.561)	(1.399)	(2.079)	(1.842)	(1.788)	(2.455)	(2.112)	(2.115)	(2.863)	(2.248)	(2.017)	(2.855)	(2.403)	(2.134)	(3.008)
Constant	297.9368***	311.5024***	-13.5482	326.3402***	342.5775***	-16.2350	323.1113***	342.9060***	-19.7920	319.2874***	343.7409***	-24.4518	304.6163***	356.3817***	-51.7655
	(51.861)	(45.076)	(71.826)	(61.727)	(54.817)	(85.120)	(65.181)	(58.029)	(90.711)	(73.672)	(64.207)	(102.037)	(79.219)	(67.751)	(108.953)
Muncipal FE	Y	Y	Y	Y	Y	Y	Y	Y	Y	Y	Y	Y	Y	Y	Y
Year FE	Y	Y	Y	Y	Y	Y	Y	Y	Y	Y	Y	Y	Y	Y	Y
Municipal time trends	Y	Y	Y	Y	Y	Y	Y	Y	Y	Y	Y	Y	Y	Y	Y
Observations	38,126	38,126	38,126	31,182	31,182	31,182	28,762	28,762	28,762	25,853	25,853	25,853	23,629	23,629	23,629
R-squared															
Mean of Y	300.8	294.8	5.997	300.8	294.8	5.997	300.8	294.8	5.997	300.8	294.8	5.997	300.8	294.8	5.997
SD of Y	148.8	140.7	131.7	148.8	140.7	131.7	148.8	140.7	131.7	148.8	140.7	131.7	148.8	140.7	131.7

Notes: This table presents regression estimates examining the correlations of air pollution on migration patterns at the municipal level. The dependent variables are immigration, emigration, and net inflow (immigration minus emigration), with all independent variables lagged by one year. Key pollutants include $PM_{2.5}$, NO_2, SO_2, CO, and O_3 concentrations, as well as income, wind speed, and precipitation. The models control for municipal fixed effects, year fixed effects, and municipal time trends. Coefficients for each pollutant are shown with standard errors in parentheses with statistical significance levels: *** $p < 0.01$, ** $p < 0.05$, * $p < 0.1$.

Bibliography

Achakulwisut P, Brauer M, H. P. A. S. (2019), 'Global,national, and urban burdens of paediatric asthma incidence attributable to ambient no2 pollution: estimates from global datasets.', *The Lancet Planetary Health* **3**(1), e166–78.

Anenberg, S. C. e. a. (2022), 'Long-term trends in urban no2 concentrations and associated paediatric asthma incidence: estimates from global datasets', *The Lancet Planetary Health* **6**(1), 49–58.

Angrist, J. D. & Krueger, A. B. (1992), 'The effect of age at school entry on educational attainment: An application of instrumental variables with moments from two samples', *Journal of the American Statistical Association* **87**, 328–336.

Arceo, E., Hanna, R. & Oliva, P. (2016), 'Does the effect of pollution on infant mortality differ between developing and developed countries? evidence from mexico city', *The Economic Journal* **126**(591), 257–280.

Ardon-Dryer, K., Huang, Y.-W. & Cziczo, D. J. (2015), 'Laboratory studies of collection efficiency of sub-micrometer aerosol particles by cloud droplets on a single-droplet basis', *Atmospheric Chemistry and Physics* **15**(16), 9159–9171.

Bauernschuster, S., Hener, T. & Rainer, H. (2017*a*), 'When labor disputes bring cities to a standstill: The impact of public transit strikes on traffic, accidents, air pollution, and health', *American Economic Journal: Economic Policy* **9**(1), 1–37.

Bauernschuster, S., Hener, T. & Rainer, H. (2017*b*), 'When labor disputes bring cities to a standstill: The impact of public transit strikes on traffic, accidents, air pollution, and health', *American Economic Journal: Economic Policy* **9**, 1–37.

Borjas, G. J. (1999), 'The economic analysis of immigration'.

Brook, R. D., Rajagopalan, S., Pope, C. A., Brook, J. R., Bhatnagar, A., Diez-Roux, A. V., Holguin, F., Hong, Y., Luepker, R. V., Mittleman, M. A., Peters, A., Siscovick, D., Smith, S. C., Whitsel, L. & Kaufman, J. D. (2010*a*), 'Particulate matter air pollution and cardiovascular disease', *Circulation* **121**(21), 2331–2378.
URL: *https://www.ahajournals.org/doi/abs/10.1161/CIR.0b013e3181dbece1*

Brook, R. D., Rajagopalan, S., Pope, C. A., Brook, J. R., Bhatnagar, A., Diez-Roux, A. V., Holguin, F., Hong, Y., Luepker, R. V., Mittleman, M. A., Peters, A., Siscovick, D., Smith, S. C., Whitsel, L. & Kaufman, J. D. (2010*b*), 'Particulate matter air pollution and cardiovascular disease: An update to the scientific statement from the american heart association'.

Cakaj, A., Lisiak-Zielińska, M., Khaniabadi, Y. O. & Sicard, P. (2023), 'Premature deaths related to urban air pollution in poland', *Atmospheric Environment* **301**.

Callaway, B. & Sant'Anna, P. H. (2021), 'Difference-in-Differences with multiple time periods', *Journal of Econometrics* **225**(2), 200–230.

Cesur, R., Tekin, E. & Ulker, A. (2017), 'Air pollution and infant mortality: Evidence from the expansion of natural gas infrastructure', *The Economic Journal* **127**, 330–362.

Chay, K., DOBKIN, C. & GREENSTONE, M. (2003), 'The clean air act of 1970 and adult mortality', *Journal of Risk and Uncertainty* **27**(3), 279–300.

Chay, K. Y. & Greenstone, M. (2003), 'The impact of air pollution on infant mortality: Evidence from geographic variation in pollution shocks induced by a recession', *The Quarterly Journal of Economics* **118**(3), 1121–1167.

Cheung, C. W., He, G. & Pan, Y. (2020), 'Mitigating the air pollution effect? the remarkable decline in the pollution-mortality relationship in hong kong', *Journal of Environmental Economics and Management* **101**, 102316.

Curci, G., Depalo, D. & Palma, A. (2023), 'The dirtier you breathe, the less safe you are. the effect of air pollution on work accidents', *SSRN Electronic Journal* .
URL: *https://papers.ssrn.com/abstract=4370149*

Currie, J. & Neidell, M. (2005), 'Air pollution and infant health: What can we learn from california's recent experience?', *The Quarterly Journal of Economics* **120**(3), 1003–1030.

De Chaisemartin, C. & D'Haultfœuille, X. (2020), 'Two-way fixed effects estimators with heterogeneous treatment effects', *American Economic Review* **110**(9), 2964–96.
URL: *https://www.aeaweb.org/articles?id=10.1257/aer.20181169*

DeCicca, P. & Malak, N. (2020), 'When good fences aren't enough: The impact of neighboring air pollution on infant health', *Journal of Environmental Economics and Management* **102**, 102324.

Deryugina, T., Heutel, G., Miller, N. H., Molitor, D. & Reif, J. (2019), 'The mortality and medical costs of air pollution: Evidence from changes in wind direction', *American Economic Review* **109**(12), 4178–4219.

Di Porto, E., Kopinska, J. & Palma, A. (2021), 'Labor market effects of dirty air. evidence from administrative data', *Economia Politica* **38**, 887–921.

Dominici, F., Greenstone, M. & Sunstein, C. R. (2014), 'Particulate matter matters', *Science* **344**(6181), 257–259.

EEA (2024), 'European union emission inventory report 1990-2022 — under the unece convention on'.
URL: *https://european-union.europa.eu/index*$_e$*n*.

EEA, E. (2021), 'Air quality in europe in 2021', *Tech. rep.* .

European Commission, E. C. (2022), 'Eu action plan: Towards zero pollution for air, water and soil', *Tech. rep.* .

European Environment Agency (2022), 'Health impacts of air pollution in europe, 2022 — european environment agency'.
URL: *https://www.eea.europa.eu/publications/air-quality-in-europe-2022/health-impacts-of-air-pollution*

European Environment Agency (2023), 'Europe's air quality status 2023 — european environment agency'.
URL: *https://www.eea.europa.eu/publications/europes-air-quality-status-2023*

European Parliament and Council (2008), 'Directive 2008/50/ec of the european parliament and of the council of 21 may 2008 on ambient air quality and cleaner air for europe', Official Journal of the European Union, L 152/1.
URL: *https://eur-lex.europa.eu/eli/dir/2008/50/oj/eng*

European Parliament and Council (2010), 'Directive 2010/75/eu of the european parliament and of the council of 24 november 2010 on industrial emissions (integrated

pollution prevention and control)', Official Journal of the European Union, L 334/17.
URL: *https://eur-lex.europa.eu/eli/dir/2010/75/oj/eng*

European Parliament and Council (2016), 'Directive (eu) 2016/2284 of the european parliament and of the council of 14 december 2016 on the reduction of national emissions of certain atmospheric pollutants, amending directive 2003/35/ec and repealing directive 2001/81/ec', Official Journal of the European Union, L 344/1.
URL: *https://eur-lex.europa.eu/eli/dir/2016/2284/oj/eng*

Fan, M., He, G. & Zhou, M. (2020), 'The winter choke: Coal-fired heating, air pollution, and mortality in china', *Journal of Health Economics* **71**, 102316.

Fan, M., Jiang, H. & Zhou, M. (2023), 'Beyond particulate matter: New evidence on the causal effects of air pollution on mortality', *Journal of Health Economics* **91**, 102799.

Feng, S., Gao, D., Liao, F., Zhou, F. & Wang, X. (2016), 'The health effects of ambient pm2.5 and potential mechanisms', *Ecotoxicology and Environmental Safety* **128**, 67–74.
URL: *https://www.sciencedirect.com/science/article/pii/S014765131630029X*

Filomena, M. ., Picchio, M. & Filomena, M. (2023), 'Unsafe temperatures, unsafe jobs: The impact of weather conditions on work-related injuries'.

Gazzetta Ufficiale della Repubblica Italiana - DPR 412/1993 (1993), 'Dpr 412/1993'. Regolamento recante norme per la progettazione, l'installazione, l'esercizio e la manutenzione degli impianti termici degli edifici ai fini del contenimento dei consumi di energia, in attuazione dell'art. 4, comma 4, della legge 9 gennaio 1991, n. 10.
URL: *https://www.gazzettaufficiale.it/eli/id/1993/10/14/093G0451/sg*

Gazzetta Ufficiale della Repubblica Italiana - DPR 74/2013 (2013), 'Dpr 74/2013'. Regolamento recante definizione dei criteri generali in materia di esercizio, conduzione, controllo, manutenzione e ispezione degli impianti termici per la climatizzazione invernale ed estiva degli edifici e per la preparazione dell'acqua calda per usi igienici sanitari, a norma dell'articolo 4, comma 1, lettere a) e c), del decreto legislativo 19 agosto 2005, n. 192.
URL: *https://www.gazzettaufficiale.it/eli/id/2013/06/27/13G00114/sg*

Giaccherini, M., Kopinska, J. & Palma, A. (2021), 'When particulate matter strikes cities: Social disparities and health costs of air pollution', *Journal of Health Economics* **78**, 102478.

Godzinski, A. & Suarez Castillo, M. (2021), 'Disentangling the effects of air pollutants with many instruments', *Journal of Environmental Economics and Management* **109**, 102489.

Graff Zivin, J. & Neidell, M. (2013), 'Environment, health, and human capital', *Journal of Economic Literature* **51**(3), 689–730.

Guo, L.-C., Zhang, Y., Lin, H., Zeng, W., Liu, T., Xiao, J., Rutherford, S., You, J. & Ma, W. (2016), 'The washout effects of rainfall on atmospheric particulate pollution in two chinese cities', *Environmental Pollution* **215**, 195–202.

He, G., Liu, T. & Zhou, M. (2020), 'Straw burning, pm 2.5 and death: Evidence from china', *Journal of Development Economics* .

He, J., Gouveia, N. & Salvo, A. (2019), 'External effects of diesel trucks circulating inside the são paulo megacity', *Journal of the European Economic Association* **17**(3), 947–989.

Heft-Neal, S., Burney, J., Bendavid, E., Voss, K. K. & Burke, M. (2020), 'Dust pollution from the sahara and african infant mortality', *Nature Sustainability* **3**, 863–871.

Inoue, A. & Solon, G. (2005), Two-sample instrumental variables estimators, Technical report.
URL: *http://www.nber.org/papers/T0311*

ISTAT (2011), 5° censimento generale della popolazione e delle abitazioni, Technical report.

Khomenko, S., Cirach, M., Pereira-Barboza, E., Mueller, N., Barrera-Gómez, J., Rojas-Rueda, D., de Hoogh, K., Hoek, G. & Nieuwenhuijsen, M. (2021), 'Premature mortality due to air pollution in European cities: a health impact assessment', *The Lancet Planetary Health* **5**(3), e121–e134.

Knittel, C., Miller, D. & Sanders, N. (2016), 'Caution, drivers! children present: Traffic, pollution, and infant health', *The Review of Economics and Statistics* **98**(2), 350–366.

Loomis, D., Castillejos, M., Gold, D. R., Mcdonnell, W. & Borja-Aburto, V. H. (1999), Air pollution and infant mortality in mexico city, Technical report.

Margaryan, S. (2021), 'Low emission zones and population health', *Journal of Health Economics* **76**, 102402.
URL: *https://www.sciencedirect.com/science/article/pii/S0167629620310481*

Mavromatis, T. & Voulanas, D. (2021), 'Evaluating era-interim, agri4cast, and e-obs gridded products in reproducing spatiotemporal characteristics of precipitation and drought over a data poor region: The case of greece', *International Journal of Climatology* **41**, 2118–2136.

Neidell, M. J. (2004), 'Air pollution, health, and socio-economic status: the effect of outdoor air quality on childhood asthma', *Journal of Health Economics* **23**, 1209–1236.

Novi, C. D. (2010), 'The influence of traffic-related pollution on individuals' life-style: results from the brfss', *Health Economics* **19**, 1318–1344.
URL: *https://onlinelibrary.wiley.com/doi/full/10.1002/hec.1550*

Orellano, P., Reynoso, J. & Quaranta, N. (2021), 'Short-term exposure to sulphur dioxide (so2) and all-cause and respiratory mortality: A systematic review and meta-analysis', *Environment International* **150**, 106434.

Ortigoza, A., Gouveia, N., Kephart, J., Prado-Galbarro, F., Friche, A., Sanchez, B. & Diez-Roux, A. (2021), 'Association between ambient PM2 · 5 and under-5, infant, and child mortality in Latin America, 2010–15: a longitudinal analysis', *The Lancet Planetary Health* **5**(S16).

Palma, A., Petrunyk, I. & Vuri, D. (2022), 'Prenatal air pollution exposure and neonatal health', *Health Economics* **31**(5), 729–759.

Pandey, J. S., Kumar, R. & Devotta, S. (2005), 'Health risks of no2, spm and so2 in delhi (india)', *Atmospheric Environment* **39**, 6868–6874.

Pope, C. A., Ezzati, M. & Dockery, D. W. (2009), 'Fine-particulate air pollution and life expectancy in the united states', *New England Journal of Medicine* **360**(4), 376–386.
URL: *https://www.nejm.org/doi/full/10.1056/NEJMsa0805646*

Pope, I. C. A. & Dockery, D. W. (2012), 'Journal of the air waste management association health effects of fine particulate air pollution: Lines that connect health effects of fine particulate air pollution: Lines that connect'.
URL: *https://doi.org/10.1080/10473289.2006.10464485*

Pui, D. Y., Chen, S.-C. & Zuo, Z. (2014), 'Pm2.5 in china: Measurements, sources, visibility and health effects, and mitigation', *Particuology* **13**, 1–26.

Rambachan, A. & Roth, J. (2023), 'A more credible approach to parallel trends', *Review of Economic Studies* **90**, 2555–2591.

Sager, L. (2019), 'Estimating the effect of air pollution on road safety using atmospheric temperature inversions', *Journal of Environmental Economics and Management* **98**, 102250. Country/years: -UK 2009-2014 Outcome: Road safety, road traffic accidents, number of vehicles involed in road traffic accidents within 153 NUT3 regions (in log terms) in a day Controls and data unit: -weather conditions,day t and region i, controls are weather conditions, time fixed effects, region fixed effectsMeasure of pollution: -PM2.5Identification: IV atmospheric temperature inversion.

Salva, J., Poništ, J., Rasulov, O., Schwarz, M., Vanek, M. & Sečkár, M. (2023), 'The impact of heating systems scenarios on air pollution at selected residential zone: a case study using aermod dispersion model', *Environmental Sciences Europe* **35**, 1–17.
URL: *https://enveurope.springeropen.com/articles/10.1186/s12302-023-00798-1*

Samoli, E., Aga, E., Touloumi, G., Nisiotis, K., Forsberg, B., Lefranc, A., Pekkanen, J., Wojtyniak, B., Schindler, C., Niciu, E., Brunstein, R., Dodič Fikfak, M., Schwartz, J. & Katsouyanni, K. (2006), 'Short-term effects of nitrogen dioxide on mortality: an analysis within the aphea project', *European Respiratory Journal* **27**(6), 1129–1138.
URL: *http://erj.ersjournals.com/content/erj/27/6/1129*

Schlenker, W. & Walker, W. R. (2016), 'Airports, air pollution, and contemporaneous health', *Review of Economic Studies* **83**, 768–809.

Sexton, K. (1997), 'Sociodemographic aspects of human susceptibility to toxic chemicals:: Do class and race matter for realistic risk assessment?', *Environmental Toxicology and Pharmacology* **4**, 261–269.

Shukla, J. B., Misra, A. K., Sundar, S. & Naresh, R. (2008), 'Effect of rain on removal of a gaseous pollutant and two different particulate matters from the atmosphere of a city', *Mathematical and Computer Modelling* **48**, 832–844.

Sillman, S. (1999), The relation between ozone, no v and hydrocarbons in urban and polluted rural environments, Technical report.

Sundar, S., Mishra, S. N. & Naresh, R. (2020), Modeling the removal of two gaseous pollutants and a mixture of particulate matters formed by these gases in a rain system, Technical report.

Tripathi, A., Misra, A. K. & Shukla, J. B. (2021), 'A mathematical model for the removal of pollutants from the atmosphere through artificial rain', *Stochastic Analysis and Applications* **40**, 379–396.

Virdis, M. R., Gaeta, M., Ciorba, U. & D'elia, I. (2015), Gli impatti energetici e ambientali dei combustibili nel settore residenziale - executive summary, Technical report.

Wang, Y., Wang, Y., Xu, H., Zhao, Y. & Marshall, J. D. (2022), 'Ambient air pollution and socioeconomic status in china', *Environmental Health Perspectives* **130**.
URL: *https://ehp.niehs.nih.gov/doi/10.1289/EHP9872*

WHO (2014), Household fuel combustion who guidelines for indoor air quality, Technical report.
URL: *https://www.who.int/publications/i/item/9789241548885*

Wooldridge, J. M. (2021), 'Two-Way Fixed Effects, the Two-Way Mundlak Regression, and Difference-in-Differences Estimators'. Issue: 3906345 Place: Rochester, NY.

World Health Organization - WHO (2013), 'Newly found health effects of air pollution call for stronger European Union air policies'. Accessed: [Inserisci la data di accesso].
URL: *https://www.who.int/europe/news/item/31-01-2013-newly-found-health-effects-of-air-pollution-call-for-stronger-european-union-air-policies*

World Health Organization - WHO (2021), 'What are the WHO air quality guidelines?'. Feature story.
URL: *https://www.who.int/news-room/feature-stories/detail/what-are-the-who-air-quality-guidelines*

Wu, C., Li, K. & Bai, K. (2020), 'Validation and calibration of cams pm2.5 forecasts using in situ pm2.5 measurements in china and united states', *Remote Sensing 2020, Vol. 12, Page 3813* **12**, 3813.
URL: *https://www.mdpi.com/2072-4292/12/22/3813/htm https://www.mdpi.com/2072-4292/12/22/3813*

Xing, Y. F., Xu, Y. H., Shi, M. H. & Lian, Y. X. (2016), 'The impact of pm2.5 on the human respiratory system'.

Yang, M., Bhatta, R. A., Chou, S.-Y. & Hsieh, C.-I. (2017), 'The impact of prenatal exposure to power plant emissions on birth weight: Evidence from a pennsylvania

power plant located upwind of new jersey', *Journal of Policy Analysis and Management* **36**(3), 557–583.

Yixing, D., Xiaohan, X., Ming, C., Yan, G. & Wang, J. (2016), 'Air particulate matter and cardiovascular disease: the epidemiological, biomedical and clinical evidence', *Journal of Thoracic Disease* **8**(1), e8–e19.

Zauli-Sajani, S., Thunis, P., Pisoni, E., Bessagnet, B., Monforti-Ferrario, F., Meij, A. D., Pekar, F. & Vignati, E. (2024), 'Reducing biomass burning is key to decrease pm2.5 exposure in european cities', *SCIENTIFIC REPORTS* **14**.
URL: *https://publications.jrc.ec.europa.eu/repository/handle/JRC136735*

Zhang, J. & Smith, K. R. (2007), 'Household air pollution from coal and biomass fuels in china: Measurements, health impacts, and interventions', *Environmental Health Perspectives* **115**, 848–855.
URL: *https://ehp.niehs.nih.gov/doi/10.1289/ehp.9479*

Zhao, X., Sun, Y., Zhao, C. & Jiang, H. (2020), 'Impact of precipitation with different intensity on pm2.5 over typical regions of china', *Atmosphere* **11**(9).

Acknowledgments

Această teză este dedicată mamei mele, cu toată dragostea și recunoștința mea profundă, pentru toate sacrificiile și eforturile neobosite făcute ca să-mi ofere o viață mai bună și să-mi deschidă drumul către educație. Curajul, puterea și dedicarea ta au fost și sunt sursa mea de inspirație în fiecare pas.

This thesis is dedicated to my mother, with all my love and deepest gratitude, for all the sacrifices and tireless efforts she made to give me a better life and to open the path to education. Her courage, strength and dedication have been and continue to be my source of inspiration every step of the way.

I would like to express my deepest gratitude to my mother, Maria, for her unwavering support. My sincere thanks go to my Ph.D. Coordinator and Master, Matteo Manera, for providing the necessary guidance and support throughout every stage of this journey.
I am profoundly grateful to my supervisors and mentors - Elena Cottini, Luca Salmasi, Gilberto Turati, and Elena Villar - for their invaluable training, mentorship, and constant encouragement during my academic path.
A special acknowledgment and heartfelt thanks go to Marita Laukkanen, Kimmo Ollikka, Anna Sahari, and all the researchers at VATT, the GSE EE group, and the University of Helsinki for giving me the opportunity to grow in a vibrant and intellectually stimulating environment. Their support has been invaluable in helping me develop my skills and explore new research topics.
I extend my gratitude to the NCDC Climate Services Branch (CSB) for providing access to weather data. My sincere thanks go to Cinzia Di Novi for her insightful remarks as discussant at the workshop "Understanding Inequalities: New Evidence and Open Questions" (held at the Catholic University of Milan on 20 February 2023). I am also deeply appreciative of the workshop participants for their constructive feedback, which has been instrumental in enhancing this research. Additionally, I wish to acknowledge Fabio Berton, Domenico Depalo, Ludovica Gazzè, Joanna Kopinska, and Alessandro Palma for their valuable comments and support in refining this work.
Finallly, I extend my appreciation to my colleagues for making challenging moments more manageable and to my partner and his family for standing by my side, ensuring that I could find joy in both my work and life.

To all the challenges overcome, to the unwavering support of those who stood by me, and to the strength drawn from self-belief and confidence in my abilities, all dedicated to the pursuit of a better life.